Universitetet
i Stavanger

FACULTY OF SCIENCE AND TECHNOLOGY

MASTER'S THESIS

Study programme/specialisation: Biological Chemistry	Spring / Autumn semester, 20..18 Open/Confidential
Author: Bjørn-Christian Ormhaug	Bjørn-Christian Ormhaug (signature of author)
Programme coordinator: Peter Ruoff Supervisor(s): Oddmund Nordgård and Kjersti Tjensvoll	
Title of master's thesis: Isolation and Characterization of Exosomes from cell culture Medium and Human Plasma in Relation to Cancer Diagnostics	
Credits: 60	
Keywords: Biological Chemistry, Molecular Biology, Extracellular vesicles, EV isolation, Exosomes, Biomarkers, dsDNA, KRAS, Pancreatic Cancer	Number of pages: 91 + supplemental material/other: 138 Stavanger, 15.06.18 date/year

University of Stavanger - Faculty of Science and Technology

MASTER'S THESIS

Biological Chemistry Master's Programme

Isolation and Characterization of Exosomes from Cell Culture Medium and Human Plasma in Relation to Cancer Diagnostics

Main supervisor: Oddmund Nordgård

Co-supervisor: Kjersti Tjensvoll

by

Bjørn-Christian Ørnholt

223795

[date here, ex: 15.05.2018]

ACKNOWLEDGEMENTS

The work done for this thesis was performed at the laboratory for molecular biology by Stavanger University Hospital (SuS).

I would like to extend my most sincere thanks to my main supervisor Oddmund Nordgård for his stellar guidance throughout this project: his wealth of scientific knowledge is surely only rivalled by his fierce dedication to his students. I would also like to thank my co-supervisor Kjersti Tjensvoll, not only for her guidance with this thesis, but for her guidance on the mind-set of a scientist.

I would like to thank Satu Oltedal and Morten Lapin, who have both contributed their skill and expertise to the work in this thesis. I would also like to thank Siri Lunde for her cheerful aid in collecting the necessary blood.

My most heartfelt thanks go out to everyone at the laboratory for molecular biology: your sharp minds and wonderful humour have made this last year one I will always remember fondly.

ABSTRACT

The interest in exosomes and other extracellular vesicles (EVs) has been steadily increasing for the past several years, as a growing body of evidence for their potential use as non-invasive biomarkers for disease such as cancer has emerged. Evidence indicates that these EVs may contain high quantities of tumour specific proteins and nucleic acids (including DNA), and their ubiquity in bodily fluids make them ideal candidates for novel liquid biopsy methods.

Four different methods for EV isolation was used on conditioned cell culture media from the PANC-1 cell line and their performance was compared to that of traditional differential centrifugation (UC) for exosome isolation. The methods tested were qEV Size Exclusion Chromatography (SEC, Izon Science), ExoEasy affinity chromatography (Qiagen), as well as the Total Exosome Isolation (TEI, Thermo Fisher) and ExoQuick (System Biosciences) polymer precipitation reactions. Isolated EVs were characterized according to size, concentration and relative vesicle fraction by Tuneable Resistive Pulse Sensing (TRPS) analysis. Their relative content of exosome marker proteins was measured by bead-assisted flow cytometry (BAFC) analysis and their dsDNA content was isolated and then measured by fluorometry. The three best methods according to exosome content, purity and DNA content were selected for further validation by isolating exosomes from human plasma. EV isolation by TEI, qEV and ExoEasy techniques were validated on plasma from healthy control persons and patients with pancreatic cancer by the same analyses as described above. In addition, the level of tumour DNA in the EV fractions were estimated by KRAS Peptide Nucleic Acid (PNA) Clamp PCR assay.

It was shown that traditional EV isolation method of differential centrifugation is ineffective with regards to EV yield, specificity and purity from contaminants, when compared to newly available EV isolation methods. All tested techniques performed as well or better than UC in every aspect investigated. It was demonstrated that the qEV technique provides the purest, least contaminated exosome isolates, and the most highly concentrated tumour DNA of all the tested techniques, but at a low overall EV concentration. TEI yielded the by far greatest dsDNA concentrations from both CCM and plasma, but co-isolated many non-target biomolecules. ExoEasy was shown to isolate some exosome-like vesicles and some dsDNA, but with a generally heterogeneous and non-specific EV population. Tumour DNA, identified by mutated KRAS alleles, were detected in EV isolate samples of ExoEasy, TEI and qEV, and with the highest overall yield detected in samples from the qEV technique.

Table of Contents

ABBREVIATIONS

exoDNA = Exosomal DNA

cfDNA = Cell-free DNA

dsDNA = Double stranded DNA

ctDNA =circulating tumor DNA

EV = Extracellular Vesicle

MV = Microvesicle

MVB = Multivesicular Body

IEV = Intraluminal Endosomal Vesicle

ApoBDs = Apoptotic Bodies

ROS = Reactive Oxygen species

DDR = DNA Damage Response

SEC = Size Exclusion Chromatography

qEV7 = qEV (Izon Science) SEC-column eluate fraction #7 (first 500µL fraction after void volume)

qEV8 = qEV (Izon Science) SEC-column eluate fraction #8 (second 500µL fraction after void volume)

qEV9 = qEV (Izon Science) SEC-column eluate fraction #9 (third 500µL fraction after void volume)

TEI = Total Exosome Isolation (EV precipitation reagent)

UC = Ultracentrifugation

BAFC = Bead-assisted flow cytometry

RCF = relative centrifugal force

PC = Pancreatic cancer

TR = Technical replicate

BR = Biological replicate

AChE = Acetylcholinesterase

LO = Large Oncosome

CCM = Conditioned cell culture media

HDL = High density lipoproteins

PEGS = Polyethylene Glycols

TRPS = Tuneable Resitive Pulse Sensing

NTA = Nanoparticle tracking analysis

ELISA = Enzyme linked immunosorbent assay

PBS = Phosphate buffered saline

DMEM = Dulbecco's modified eagle medium

FBS = Foetal bovine serum

1. INTRODUCTION

1.1 Pancreatic cancer and liquid biopsies

Pancreatic cancer (PC) is a lethal malignancy which is notoriously difficult to diagnose, and carries a very poor prognosis [1, 2]. Typical symptoms of PC are very similar to many other, less serious diseases, and due to the placement of the pancreas behind the peritoneum, no diagnostic examination has proven clinically practical [2]. Additionally, high tumour content of stromal tissue may lead to inconclusive results [1]. This is despite early detection being one of the most reliable factors for an improved diagnosis [2]. Because of the challenging nature of diagnosing pancreatic cancer, liquid biopsies have attracted much interest in recent years [1]. By collecting circulating tumour cells and circulating tumour DNA, it is hoped that non-invasive methods of diagnosis with high prognostic value can be developed based on ctDNA mutation detection [1, 3]. Low quantities of DNA, low mutation frequencies and background noise has however posed major roadblocks on the way to developing such liquid biopsy methods [3]. Ways of isolating sufficiently concentrated amounts of tumour DNA are therefore highly sought-after, and the subject of much research.

In recent years, an increasing body of evidence has building for a close relation between certain extracellular vesicle (EV) subtypes, and cancer [4, 5]. One aspect of this relationship is their reported specific enrichment in tumour DNA [6]. This has marked EVs as a promising candidate biomolecule for use in liquid biopsies and rapid diagnosis of challenging diseases such as PC [5]

1.2 Extracellular vesicles

1.2.1 Overview

The term EV encompasses a wide range of membrane bound bodies, all of which are currently the subjects of intense study [7, 8]. Broadly divided into the three main categories of apoptotic bodies (ApoBDs), microvesicles/ectosomes (MVs) and exosomes, EVs can vary greatly in both biological origin and function [9, 10]. As their name suggests, all EVs share the common trait of being located outside the plasma membrane of their parent cell (hence extracellular), and have been detected in biofluids as diverse as blood [11] (circulating EVs), urine [12] and even saliva [13]. These EVs span a large range of sizes, from the very small exosomes (50-150nm) [6, 14] to microvesicles (MVs, 100-1000nm)[15] very large apoptotic bodies (ApoBDs, 1-5µm) [16]. In between these ranges are the fairly newly coined “oncosomes” (100-400nm), a group of EVs proposed to be specifically released by cancer cells and, like exosomes [17], to carry potentially transforming mutant macromolecules [18]. The lipid bilayer structure of the EV membrane typically consists of material once part of the cell plasma membrane (figure 1), which has undergone a varying amount of intermediary stages depending on the type of EV. Even so, their contents, associated proteins and membrane structures are reported to vary widely depending on factors such as environmental conditions and cellular source [9].

1.2.2 Discriminating between EV subpopulations

In the literature, the terminology surrounding EVs is not in all cases strictly defined, and many terms are used differently by different authors [19]. One of the earliest popular definitions of exosomes was

based on what relative centrifugation force (RCF) at which they were found to sediment, and another as “secreted vesicles that may serve a physiologic function”[19]. Similar confusion surrounding definitions also exist for MVs [19]. Broad definitions make claims regarding having isolated a certain type of EV less contentious. However, considering the likeness in external physical properties of EVs coupled with the large variability in cargo even within defined groups of EVs [9], there are many proponents of their definition not by size and density, but rather by biogenesis [9]. This, as well as the specific borders of the size ranges in which each type of EV is found, is still a topic of debate. This is of particular relevance, as many methods for isolation of exosomes and specific MVs rely on their relative sizes and densities to a very large extent [20]. Additionally, also in part because of the rapid development within the in the field, accurately classifying isolated EVs within a specific category according to biogenesis can be a time-consuming and expensive endeavour, as no single biomarker to guarantee a specific biogenesis is generally agreed upon [21]. It is however possible to become increasingly confident in characterizing the EVs in a sample by identifying more than one marker such as different proteins known to be enriched in the MV in question. Examples of such marker proteins for exosomes include ALIX and the tetraspanins CD9, CD63, among others [22]. Other intraluminal markers such as RNAs enriched in specific motifs have additionally been proposed [23]

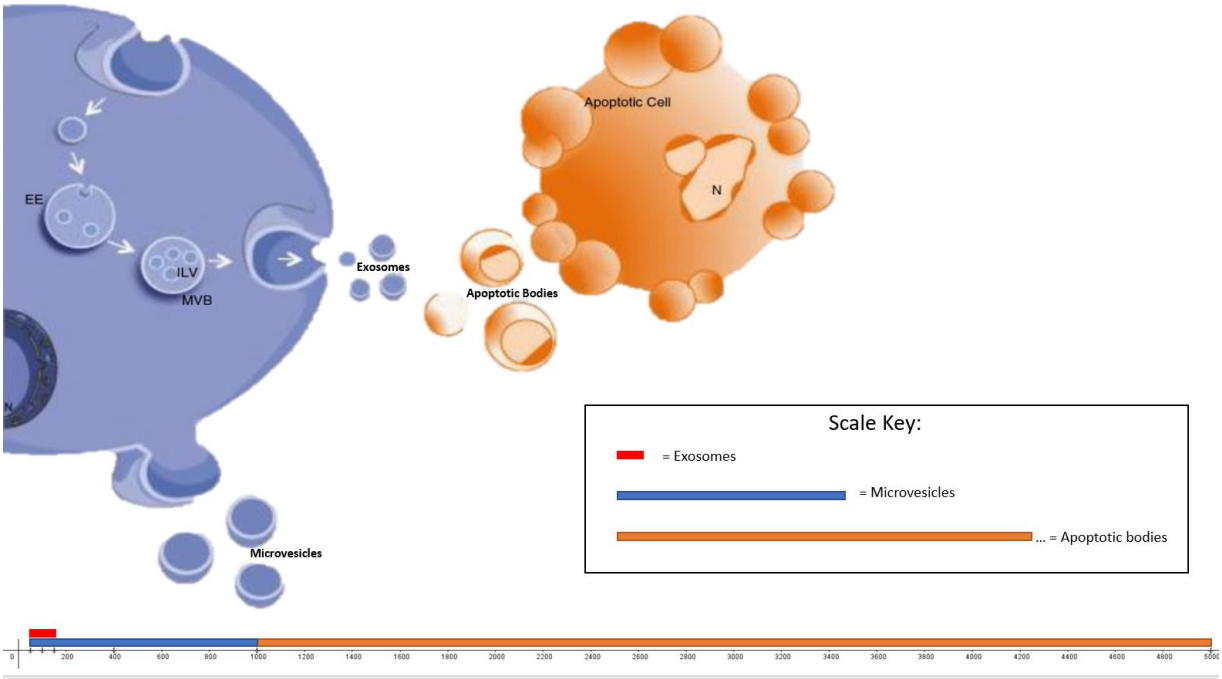

Figure 1: The biogenesis, release and relative scale of the three main classes of Extracellular vesicles. The top left part of the image illustrates how an early endosome (EE) matures to a multi-vesicluar body (MVB) filled with intraluminal vesicles (ILV), which upon release are known as exosomes. To the bottom left it is illustrated how micorvesicles (MVs) may form by outward budding of the plasma membrane. In the top right corner apoptotic bodies are shown “blebbing” (Zeiosis) off a cell undergoing apoptosis. The diameter range of each type of nanoparticle is given by the scale at the bottom of the image, the key for which is found in black box. This Illustration is reproduced with some modifications under the creative commons licence, © 2015 María Yáñez-Mo et al [9]

1.3 Extracellular vesicle subtypes

EVs have been reported to carry out several different roles in eukaryotes. These functions include tasks as diverse as functioning as cellular recycling bins and stretch all the way to novel EV-mediated cell signalling pathways, in which they allow for the transfer of macromolecules such as lipids, sugars and nucleic acids [9]. Discoveries leading up to a connection between tumours and EV's were being made as early as the 1980's, with discovery of "membrane fragments" rich in antigenic sites typical of certain tumour tissue membranes [24]. This connection has been bolstered as research has progressed, and EVs have in recent years been proposed to play important and direct roles in aspects as fundamental as maintaining tumour cell homeostasis [25], and metastasis and angiogenesis [26]

1.3.1 Apoptotic Bodies

1.3.1.1 Apoptotic Body Biogenesis

ApoBDs are large EVs which originate as buds om the plasma membrane of the apoptotic cell[27]. In general, as the apoptotic cell moves through the stages of programmed cell death it shrinks and chromatin condenses (pyknosis). This is followed by plasma membrane blebbing and the breakdown of the nucleus (karyorrhexis). Cell fragments eventually separate into apoptotic bodies as the formed "blebs" transition into the process of budding [27]. Notably, while ApoBDs are created as an apoptotic cell is breaking down, they are not formed randomly, but follow distinct steps regulated by molecular factors. This process is generally known as cell disassembly [28].

1.3.1.2 Apoptotic Body Function and relation to cancer

ApoBDs are traditionally known for performing the function of a cell component recycling bin, providing safe containers for the macromolecule components of an apoptotic cell as they are readied for clearance by a phagocyte [27, 28]. Their contents are diverse, and can contain entire organelles such as the Endoplasmic reticulum or Golgi apparatus, or large collections of macromolecules such as condensed chromatin [28]. The packaging of various cellular contents in this manner is believed to be involved in regulating immune response and tissue repair [29]. ApoBDs have additionally been suggested as vehicles for the horizontal transfer of biomolecules and oncogenes [30], and to be important regulators in the onco-regenerative niche [31]

1.3.2 Exosomes

1.3.2.1 Exosome Biogenesis

A very different type of EV which has garnered a large amount of interest in the last few decades since their discovery, are the Exosomes. Descriptions of vesicles increasingly matching that of the modern definition of exosomes were being made throughout the 1980's, with an outline of exosomes and their biogenesis being well formulated as early as 1987. Exosomes were at this time identified as part of a pathway for the expulsion of certain proteins from maturing reticulocytes, as a part of their normal maturation process [32]. The proteins found, included among others acetylcholinesterase (AChE) enzyme. What was particularly interesting, was that when following the fate of these proteins, it was discovered that the process first involved endocytosis, forming an endosome, which in turn also were subject to inward budding. This resulted in a so called multivesicular body (MVB), 0.5-1µm in length. The MVB was in turn found to fuse with the plasma membrane, releasing its very small internally held vesicles into the cell exterior (figure 1). These small vesicles, or exosomes, were found to be the vehicles for the further transport of the reticulocyte proteins in question. When viewed under the

electron microscope, exosomes were observed to have a cup-like morphology. This was later revealed to be an artefact of the microscopy fixation process [19, 33].

1.3.2.2 Exosome Function and relation to cancer

In addition to their function in the maturation process of reticulocytes, exosomes have been shown to carry a plethora of biologically interesting proteins, including Rab proteins (Ras-like small GTPase superfamily), ALIX, Major histocompatibility complexes I and II and many more [10] (figure 2). In the course of the 2000's, further discoveries were made, demonstrating many exciting potential functions of exosomes in the body, with potential future medical applications [5, 34]. Among the most exciting recently reported findings is the potential role of exosomes in preventing the accumulation of chromosomal DNA in the cytosol of cells, as an important part of the cell's DNA damage response [25]. This would be done by targeted collection and export of cytosolic DNA out through plasma membrane by exosomes [25]. The rapid removal of generated cytosolic DNA may in this case be a critical feature of tumour cells in order to avoid natural senescence-associated tumour suppression, and produce exosomes loaded with tumour DNA cargo [25]. Others report that as much as 93% of amplifiable cell free DNA (cfDNA) in blood plasma is located in exosomes, while also asserting a connection between exosomes and double stranded DNA (dsDNA) [35]. Further finds link genomic dsDNA featuring mutated KRAS and p53 genes to exosomes from pancreatic cancer (PC) cell lines and PC patient serum [6]. Finally, exosomes may play an important role in tumour growth and angiogenesis [36]. Tumour-derived exosomes have further been found to be involved in metastasis by inducing pre-metastatic niche formation in distant organs [4] and for all these reasons provide a promising candidate for future use in liquid biopsies and diagnosis of cancer [5].

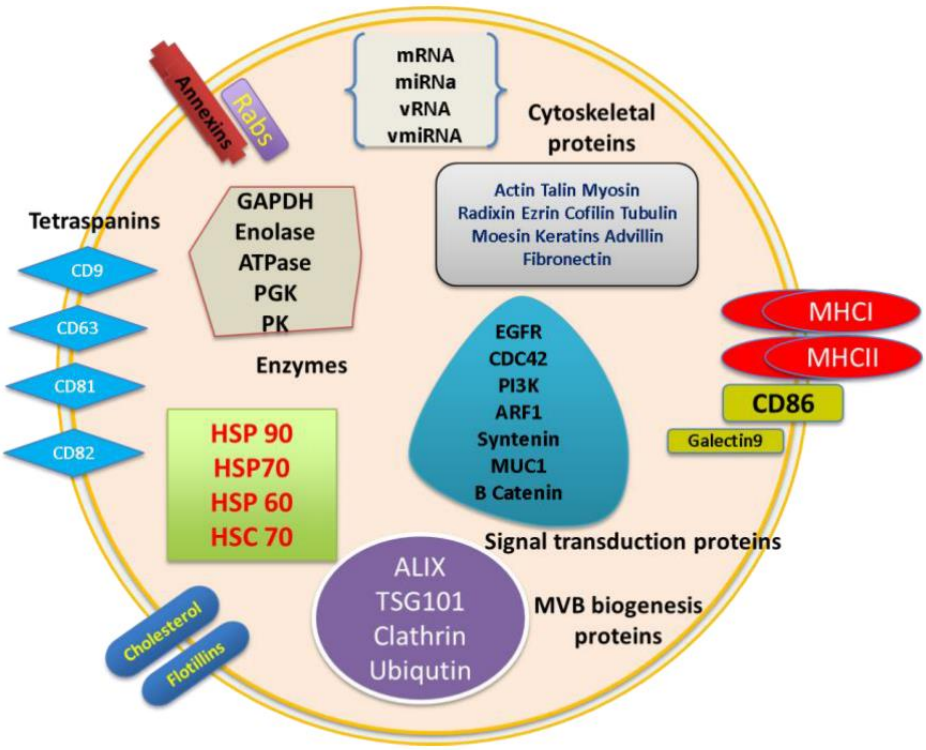

Figure 2: Structure and composition of an exosome (not all components shown). The lipid bilayer membrane holds many proteins characteristic to exosomes such as the tetraspannins CD9 and CD63, whereas the internal cargo typically includes

nucleic acids such as various RNAs. This Illustration is reproduced under the creative commons licence, ©Chahar HS et.al. 2015 [37]

1.3.3 Oncosomes and large oncosomes

1.3.3.1 Oncosome and Large oncosome Biogenesis

Oncosomes are a relatively newly coined group of EVs (2008) [18], characterized in part by being released exclusively by tumour cells. In this way the 100-400nm oncosomes differentiate themselves from EVs also produced by non-transformed cells, such as exosomes and ApoBDs.

1.3.3.2 Oncosome and large oncosome function and relation to cancer

Oncosomes were upon first discovery described as carrying phosphatidylserine on their surface and mediating the release of mutant macromolecules and oncogenes from tumour cells [18]. A year later in 2009, a different type of EV was discovered and coined "Large Oncosomes" (LOs) due to their massive diameter of 1000 – 10 000nm [38]. It should be noted that while the two share similar names and are both produced exclusively by tumour cells, oncosomes and LOs have different size, contents, origins, and criteria for formation, and so the terms should not be used interchangeably [18]. The study of LOs is very young, and much has yet to be determined specifically with regards to their contents. Currently accepted marker proteins for LOs however include HSPA5 and HSPD1, and they have been reported to contain nucleic acids such as miRNA [39]

1.3.4 Microvesicles

1.3.4.1 Microvesicle Biogenesis

Also known as ectosomes, MVs are EVs 100-1000nm in diameter formed thorough outward budding or "shedding" of the plasma membrane. MVs were previously known only as pro-coagulant platelet dust [40] generated by human blood platelets [15].They are today known to be produced by virtually all eukaryotic cells [41]. Due to their biogenesis, MVs have plasma membrane similar in composition to that of the cell membrane, but have been reported to lack the asymmetric distribution of lipids, such as phosphatidyl-serine and ethanolamine, across the two plasma membrane leaflets [21]

1.3.4.2 Microvesicle function and relation to cancer

MVs have been found to be abundant in various biofluids [9] and have been suggested as important paracrine messengers [42]. Among their cargo there has been reports of biologically active proteins [43] and circulating miRNAs[44] and various other nucleic acids [41]. MVs have been reported to have pro-metastatic functions in malignancies such breast cancer [15]

1.4 Common substrates for EV isolation

Per definition, EVs are exuded from their parent cell and into the external environment [9]. For cells in a culture, this corresponds to the cell culture media, which after hosting cells and exchanging biomaterials with the culture often is called conditioned cell culture media (CCM). CCM was in a 2016 worldwide survey determined to be the most commonly used material for EV isolation, with 83% of respondents using it as their only or primary material for EV isolation [25]. When isolating EVs from CCM, it is important not to introduce external exosomes by ways of additives to the medium, such as for instance regular foetal bovine serum (FBS) or other supplements [45]. Additionally, as discussed

previously, cell death will lead to the formation of ApoBDs. It is therefore important to avoid undue stress on the cells or culturing past full confluence. In the case of excessive cell death, there is no way to guarantee the quality of the later measured exosomes. Cell live count should therefore be measured prior to proceeding with exosome isolation from a given batch of CCM. It is also essential to avoid any and all disruption of cells, so the collection process must be gentle [46]. After collection, CCM should be clarified by removal of cellular debris, ApoBDs and shedded vesicles through careful centrifugation and/or filtration steps [25]

When it comes to liquid biopsy samples, EVs can be found in most body fluids, including blood [5, 35]. Therefore, when selecting material for the study of EVs for use in liquid biopsy, a natural choice would be blood plasma, as blood is a routinely collected and easily accessible bodily fluid rich in circulating EVs [20]. The plasma fraction in particular is not subject to the factors released by leukocytes during coagulation as is serum, and can be rapidly isolated from whole blood and used for EV isolation [20]. Even so, careful clarification should be performed by introducing centrifugation and filtration steps prior to exosome isolation in order to avoid contamination by platelets [20]

1.5 Technologies for EV isolation

1.5.1 Traditional EV isolation- Ultracentrifugation

Ultracentrifugation (UC) was determined to be the most common technique for EV isolation in the same 2016 worldwide survey mentioned above, with 81% of respondents reporting to use ultracentrifugation (including differential centrifugation) as their primary EV isolation technique. This was coupled with a reported 64% using an ultracentrifugation washing step for clean-up/purification. [47]. EV isolation by centrifugation relies on the density, size and shape of the EVs to deposited, where the most dense and/or biggest particles deposit out of solution first [33]. In differential centrifugation, successive centrifugations at steadily increasing RCFs are therefore performed in order to deposit and discard large particles which are not wanted in the final EV isolate [20]. The full process of going from heterogeneous suspension to EV isolate using only centrifugation steps and ending with ultracentrifugation, is known as differential centrifugation[20]. The typical differential centrifugation protocol in this manner involves discarding the formed pellet at each step and further centrifuging the supernatant (figure 3). Large EVs (MVs, oncosomes) are generally considered to isolate out at 10 000 – 20 000x g, whereas small EVs (exosomes) require RCFs of 100 000 – 200 000x g [20]. Isolation of EVs thorough differential centrifugation does however not discriminate against EV subpopulations or other particles of similar size and/or density to the target [48]. Ultracentrifugation has further been found to cause EV aggregation [49] as well as to co-isolate a various non-vesicular materials not easily removed by normal washing of the pellet [50]. Common contamination co-isolates include proteins, protein aggregates, lipoproteins, cell organelles and viruses [20]. Reports of the total recovery of EVs by differential centrifugation varies widely, from 2%-80%[20], and a typical protocol may take from one to two days to complete [51].

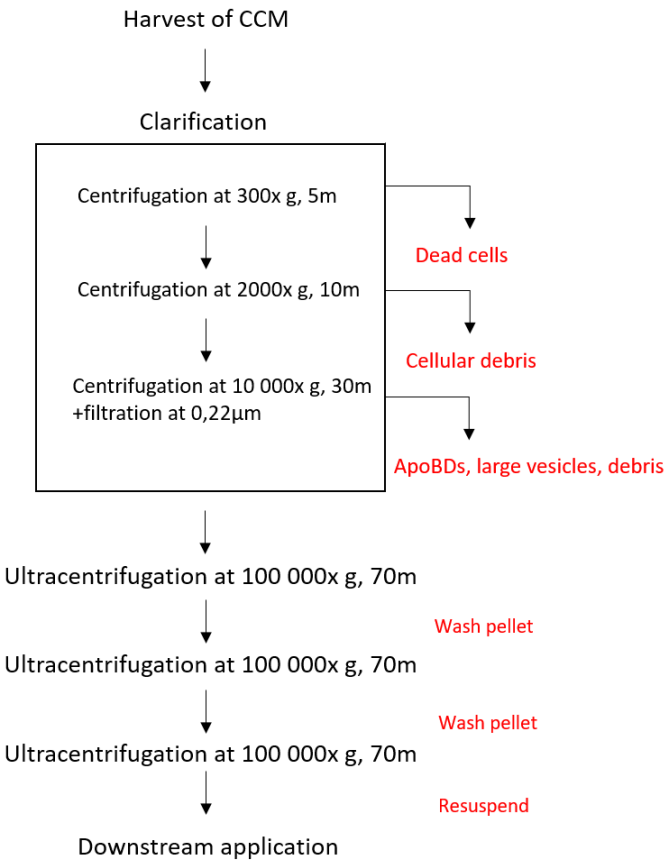

Figure 3: An example of a typical differential centrifugation workflow for isolation of small EVs like exosomes from CCM. After multiple steps of clarification of the CCM follow several long ultracentrifugation steps in order to deposit and wash the very small EVs. Example times and speeds for this particular workflow follow that of Takahashi et.al. 2016 [25]

An alternative UC-based technique for EV isolation to differential centrifugation, is density gradient centrifugation [20]. In this technique the relative density of each EV subpopulation is further emphasized, allowing for more specific isolation [33]. It works on the principle of placing a density gradient medium in a centrifugation tube, where the medium has a progressively increasing density moving from the top of the tube to the bottom (sorting EVs by size and mass) or from the bottom to the top (mass density only) [20]. By placing the sample material on the top of the density gradient medium, the different suspended EVs will sediment at different rates during UC [33]. This causes distinct zones of EVs in the density gradient medium from which a specific fraction can be recovered. This method is particularly useful for isolating very small yet low density EVs such as exosomes, but is typically even more labour intensive than even differential centrifugation [51]

1.5.2 Size Exclusion Chromatography

In size Exclusion Chromatography (SEC), a specialized porous material such as CL-2B Sepharose in a column is used as a stationary phase, and the material from which EVs are to be isolated constitutes a mobile phase to be passed through the column. Particles with a small hydrodynamic radius are able to interact with the pores of the stationary phase, and are therefore hindered as they travel through the column. As radius increases, particles interact less with pores of the stationary phase, and therefore

pass through the column more quickly [52]. In this manner, nanoparticles of a very specific diameter may be isolated by collecting only the fractions of the mobile phase in which they are contained, as it passes through the column [33]. SEC is considered a gentle method of EV isolation, as it typically relies on gravity-flow elution and involves no potentially aggregating, deforming or disrupting centrifugal forces [52]. This is generally considered ideal for the purposes of maintaining the integrity of the isolated EVs, and the technique is also considered to be particularly concise and reproducible [52]. While SEC effectively removes contaminating high density lipoproteins (HDL) and plasma proteins, isolates may contain very low density lipoproteins (30-80nm) and chylomicrons (100-600nm) in small amounts. Overall, SEC has been reported as capable of removing more than as 95% of all non-vesicular proteins from a sample [53]. Overall vesicle yields have however been reported as low [54], and attempts at concentrating steps post-SEC may result in lowering both vesicle recovery and sample purity depending on the methods used [53].

1.5.3 Polymer precipitation

A third option for EV isolation, are polymer precipitation reactions. Before isolation by such technologies, the sample must first be clarified from cells and cellular debris [33]. By adding a reactant to the material from which EVs are to be isolated which reduces their solubility, EVs can be precipitated from solution and at relatively low centrifugation speeds [33]. Water molecules are tied up by the addition of high-solubility polymers such as polyethylene glycols (PEGS), forcing the less soluble EVs out of solution [51]. However, in principle any solute less soluble than the added polymer is precipitated. Depending on the specific methodology used, polymer precipitation has been shown to co-precipitate contaminants such as lipo-proteins and other non-vesicular material [52].

1.5.4 Affinity spin-column purification

Not unlike SEC, Affinity chromatography works on the principle of differences in interaction strength between a mobile phase and its different solute biomolecules, and a stationary phase. In the stationary phase of affinity chromatography however, there are immobilized ligands [55] specially designed to bind to the target, for instance EV's. The crude sample (heterogonous mixture of target EVs and non-target biomolecules) is mixed with a buffer changing the pH or other factors necessary to allow for binding to occur between EVs and the immobilized ligand. When the sample is passed through the stationary phase, the EVs bind to the ligand-enriched membrane, and non-target biomolecules can be washed away. The EVs can then be eluted by the addition of a buffer which releases them from the immobilized ligands [55].

By making the stationary phase a permeable membrane and placing it in centrifuge-compatible column, a single pass of the sample thorough the column can achieve more than a 1000-fold increase in purity of for example a protein target [55]. This however, comes coupled with warnings of the affinity spin technology resulting in a more heterogeneous mix of isolated EVs with a wider size-range than what can be obtained through SEC, more contaminating proteins of various types including lipoproteins and plasma proteins [54].

1.6 Characterization of EVs and nucleic acid cargo

As described above, all EV isolation techniques have the potential to co-isolate proteins or other non-target vesicles. In order to determine the yield and homogeneity of the isolate from any given technique, the resultant nanoparticles must therefore be characterized. Because no single biomarker can sufficiently characterize a nanoparticle as a given EV, several characteristics must be used simultaneously. Several technologies are available today which may allow one to narrow down what nanoparticles have been isolated

1.6.1 Tuneable resistive pulse sensing (TRPS)

The size of isolated nanoparticles as well as their concentration can be determined by TRPS analysis. The concentration of isolated nanoparticles within the size range of your target EVs is an important indicator for the success of the isolation. TRPS works on the principle of applying a voltage across a small pore (nanopore) filled with an electrolyte, and continuously measuring the electrical resistance. By placing a liquid sample containing suspended nanoparticles of a suitable size on top of the nanopore and applying a pressure, nanoparticles will start to migrate thorough the nanopore. As each nanoparticle travels through the pore, it increases the measured electrical resistance, resulting in a "dip" in the current, also known as a "blockade event". The length and magnitude of the dip can be used to calculate the dimensions of the nanoparticle [56]. By applying different pressures and measuring the difference in rate of blockade events, the concentration of nanoparticles in the detection range can be calculated. As data is collected on the size of each individual nanoparticle which passes through the nanopore, a very detailed size distribution of nanoparticles can also be measured. The "tuneable" part of the TRPS name, comes from each nanopore being stretchable, allowing for the user to move the detection range of a given nanopore up or down to some extent. The nanopores are also user replaceable, so that pores of different diameters entirely can be used[56]. One of the very few commercially available solutions using this technology is the qNano Gold instrument, by Izon Science [57].

Additionally, a study has shown that exosomes and larger EVs can be lysed effectively at 0,075% (v/v) of the non-ionic detergent Triton X-100, and that the use of the detergent is compatible with TRPS analysis on the qNano Gold [58]. This can therefore be used to estimate the relative fraction of vesicles in the sample, by comparing identical samples with and without triton x-100

1.6.2 Enzyme linked colorimetric assay

Exosomes have been found to be enriched in the enzyme acetylcholinesterase [32]. Based on this principle, a commercial colorimetric assay named the ExoCet exosome quantitation assay has been developed by System Biosciences (SBI). The assay works on the change in OD405nm caused by the action of the exosomal AChE enzyme on a substrate in the assay. SBI provides a standard solution of AChE as well as instructions for a dilution series in the kit. This is used to create a standard curve for the assay which SBI claims to be accurately calibrated to correspond to a given number of exosomes using Nanoparticle Tracking Analysis (NTA) [59].

1.6.3 Bead-assisted flow cytometry analysis

In order to classify isolated EVs as exosomes, ideally more than one protein known to be enriched in the EV should be identified in the sample. In a Bead-assisted flow cytometry (BAFC) analysis of EVs, EV isolate samples to be analysed are incubated with and bound to aldehyde/sulfate-latex beads. After binding, unbound sites on the beads can be blocked, the EV-linked beads washed from unbound contaminants. EV marker protein antibodies can then be added before the protein-coupled beads are stained with fluorescent dye [60]. By running the sample of dyed EV-linked beads through a flow cytometer, the presence of the proteins in question, as well as their relative concentrations can be determined. The technique is in many ways similar to Enzyme Linked Immunosorbent Assay (ELISA), but can be used effectively on as little as 1/5 of the required sample volume (20µl), and can easily assay for several proteins simultaneously. Due to the nature of each bead being able to bind several EVs however, the method cannot be used for absolute quantitation, but rather only for direct comparisons of samples in the same assay [61].

1.6.4 EV associated nucleic acid analysis

When isolating EVs in the range of exosomes, dsDNA cargo can be expected [35]. Detection of internal dsDNA cargo in isolated EVs can therefore be seen as an indication that the isolated nanoparticles are indeed EVs, like for instance exosomes. In addition to this comes the potential detection of tumour DNA, in the case of isolations from cancer patient samples. Somatic mutations to the KRAS gene has been shown to be present in 80-90% of pancreatic cancers [62]. It is therefore reasonable to expect MVs such exosomes which are reported to carry tumour DNA, to have DNA testing positive for mutation in this gene in the case that they themselves have been isolated from the blood of a person with pancreatic cancer (PC). A very sensitive method for detection would be preferable however, in order to avoid false negatives.

1.7 Aims of the thesis

The aim of the thesis was to compare four new methods for EV isolation from CCM and plasma to the traditional gold standard of EV isolation: ultracentrifugation. EVs including exosomes show great promise in delivering high concentration tumour DNA suitable for use in novel liquid biopsies. The criteria for evaluation of each isolation technique was therefore weighted towards their ability to isolate EVs showing typical exosome characteristics and a content of dsDNA. We further aimed to evaluate the best three techniques in terms of the relative content of tumour DNA in the vesicle isolates from plasma samples from pancreatic cancer patients, with the perspective of potential future use in cancer diagnostics by assay of EV associated nucleic acids.

2. MATERIALS AND METHODS

2.1 Materials

2.1.1 Cell lines

- PANC-1 (ECACC # 87092802):

2.1.2 medium formulations:

Growth medium (standard):

- DMEM, high glucose (500mL)
- 10% FBS (50mL)
- 2mM Glutamine (5mL)
- Pen/strep antibiotics (5mL)

Growth medium (exosome free):

- DMEM, high glucose (500mL)
- 10% Exosome Depleted FBS (50mL)
- 2mM Glutamine (5mL)
- Pen/strep antibiotics (5mL)

2.1.3 Prepared solutions

Acetylcholinesterase (AChE,1mg/mL, 8.2mL)

- Lyophilized AChE enzyme (8.2mg)
- Tris-HCL, pH= 7.5 (20mM, 8.2mL)

1x PBS (200mL)

- 1 PBS tablet
- 200mL Milli-Q water (Milli –Q® Integral 5 water purification system)

1x PBS, 20% ethanol (v/v)

- 1PBS tablet
- 160mL Milli-Q water
- 40mL Ethanol (99.9%)

qNano Gold Stock PBS

- 1 PBS tablet
- 200mL Milli-Q water
- 0.6mL wetting solution (Izon)

qNano Gold Measurement Electrolyte

- 12ml qNano Gold stock PBS
- 3mL coating solution (Izon)

2.1.3 Kits used

Table 1: Kits used during experimentation.

Kit	Manufacturer	Catalogue number	Use
AllPrep DNA/RNA/miRNA	Qiagen	80224	DNA isolation (CCM)
QiAmp Circulating Nucleic	Qiagen	55114	DNA isolation (Plasma)
Qubit™ dsDNA HS Assay kit	Thermo Fisher	Q32851	dsDNA quantitation
TRPS Reagent Kit	Izon Science	N/A	qNano Gold reagents
TRPS Training Kit	Izon Science	N/A	qNano Gold training
ExoEasy Maxi Kit	Qiagen	76064	EV isolation
ExoQuick-TC™	SBI	EXOTC10A-1	EV isolation
qEVoriginal	Izon	N/A	EV isolation
TEI (from plasma)	Thermo Fisher	4484450	EV isolation
TEI (from CCM)	Thermo Fisher	4478359	EV isolation
EXOCET	SBI	EXOCET96A-1	Exosome quantitation

2.1.4 Reagents

Table 2: Reagents used during experimentation

Material	Manufacturer	Catalogue number	Use
DMEM, high glucose	Sigma	D5671	Cell culture
DPBS	Sigma	D8537	Cell culture
L-Glutamine 200mM	Sigma	G7513	Cell culture
Pen/strep antibiotics	Sigma	P4333	Cell culture
FBS	Sigma	F7524	Cell culture
Exosome depleted FBS	Thermo Fisher	A2720803	Cell culture
Trypsin-EDTA	Sigma	T4049	Cell culture
Trypan Blue (0.4%)	Thermo Fisher	T10282	Cell culture
RQ1 DNase	Promega	M610A	EV external DNA
RQ1 10x Rxn buffer	Promega	M198A	EV external DNA
RQ1 Stop Solution	Promega	M199A	EV external DNA
PBS tablets	Sigma	P4417-100TAB	EV suspension
Buffer XBP	Qiagen	76204	EV isolation
Absolute alcohol prima	Antibac	600068	Bacteriostatic

2.2 Methods

2.2.1 Cultivation of PANC-1 cell line and preparation of Conditioned Cell Culture Media (CCM) samples for exosome isolation

2.2.1.1 Resuscitation and of the PANC-1 cell line

An ampulla of PANC-1 cells was collected from storage (LN_2) and thawed briefly in a water bath (37°C) until only a small amount of ice remained. Resuscitation was completed by transfer of the cells to 10ml pre-heated (37°C) normal Dulbecco's Modified Eagle's Medium- high glucose growth medium (DMEM) with glutamine (2mM), Sterile Filtered Foetal Bovine Serum (10%, Sigma Aldrich, "FBS"), 1x sterile filtered Penicillin-Streptomycin (Sigma, P4333) in a T75 Nunc™ EasYFlask™ (Thermo Fisher, No.156499) cell culture flask in a Laminar Airflow (LAF) cabinet while observing good sterile technique. The newly resuscitated PANC-1 cell culture was incubated at 37°C, 5% CO_2 for two days before sub culturing.

2.2.1.2 Maintenance and sub culturing of the PANC-1 cell line

The PANC-1 cell line was maintained in high glucose DMEM growth medium with all additives (described above). Cell confluence was estimated qualitatively each day by light microscopy. At around 70% confluence, cells were sub cultured by first discarding conditioned cell culture media (CCM) and washing the adherent cell monolayer three times using pre-heated (37°C) Ca^{2+}/Mg^{2+}-free Dulbecco's Phosphate Buffered Saline (10ml, "DPBS"). Cells were incubated in Trypsin/EDTA (2ml, Sigma Aldrich) at 37°C for 3 minutes. Growth medium (3mL) was added in order to neutralize the Trypsin. Based on the visual estimation of the cell density, a fresh T75 Nunc™ EasYFlask™ (Thermo Fisher) containing pre-heated (37°C, water bath) high-glucose DMEM (20mL) with all additives was inoculated with a volume of the cell suspension appropriate for achieving a seeded cell density of roughly 20 000- 30 000cells/cm^2 and incubated at 37°C, 5% CO_2. All open work with open cell lines was carried out in the LAF cabinet while observing good sterile technique. Subcultures were incubated at 37°C, 5% CO_2.

2.2.1.3 Cell enumeration

For sub culturing of cells used in exosome isolation experiments, cells were seeded to 15000 cells/cm^2. After suspension of adherent cells using Trypsin/EDTA (described above) a small aliquot of the suspension (50µL) was transferred to a 1.5mL microcentrifuge tube. The remainder of the suspended cell culture was placed under incubation (37°C, 5% CO_2) for the duration of the cell enumeration process. The cell suspension aliquot was mixed with Trypan Blue Stain (0.4%) for use with the Countess™ Automated Cell counter (50µL, Thermo Fischer Scientific) by pipetting, and 10µL of the mixture was transferred to the chamber on a Countess™ Cell Counting Chamber Slide (Thermo Fischer Scientific). The slide was incubated at room temperature (RT) for 10 seconds before it was loaded into the Countess® II Automated Cell Counter (Thermo Fisher Scientific). Cells were enumerated by the instrument and reported as number of live cells, dead cells and the percentage of dead cells relative to the total. The cell concentration in the suspension was calculated automatically by the instrument.

2.2.1.4 Sub culturing for production of CCM as a raw material for exosome isolation

Exosome-free DMEM was prepared by replacement of the normal FBS additive with Gibco™ Exosome-Depleted FBS, One-Shot™ format (50mL, Cat. A2720803 Thermo Fisher).

PANC-1 cell culture was sub cultured simultaneously to two T75 flasks as previously described, but using exclusively exosome-free high glucose DMEM. Subcultures were incubated at 37°C 5% CO_2 until 70% confluence. Cells were washed and trypsinated as previously described and enumerated using the Countess® II automated cell counter (Thermo Fisher Scientific). An appropriate volume of cell suspension (equation 1) was transferred to fresh pre-heated (37°C) exosome-free high glucose DMEM (50mL, all additives), for a seeded density of 15 000 cells/cm^2 in four fresh T175 Nunc™ EasYFlask™ (Thermo Fisher, No.159910). PANC-1 cultures were subsequently incubated at 37°C, 5% CO_2 until 95-100% confluence before harvesting the CCM into conical base tubes (50mL, Sarstedt No. 62.547.004). Cell monolayer was washed and trypsinated as previously described. An aliquot (0.5mL) of the cell suspension was used to enumerate cells and verify a live-cell fraction of ≥95% using the Countess® II automated cell counter.

$$Inoculation\ volume\ (mL) = \frac{Target\ \#cells}{Live\frac{cells}{ml}counted} \quad (1)$$

2.2.1.5 Clarification of collected CCM for use in exosome isolation

Collected CCM was clarified by serial centrifugation for 10 minutes at RT at 300x g, 1500x g and 3000x g using the Allegra x-30R centrifuge (Beckman Coulter) with a swinging bucket rotor (Beckman Coulter SX 4400). The supernatant was aspirated and transferred to a fresh 50mL tube between each centrifugation, and the old tube was discarded along with the debris pellet. Supernatant was filtered using a 0,8µm Millex® AA Filter Unit (MF-Millipore, SLAA033SB) into a sterile container and mixed by gentle agitation. Clarified CCM was immediately used in the various protocols for exosome isolation (described below).

2.2.2 Preparation of plasma samples for exosome isolation from whole blood

Samples of whole blood (2x 9mL) were drawn from 3 presumed healthy control group donors into BD Vacutainer® EDTA haematology tubes (Becton, Dickinson and Company) and plasma isolated by centrifugation at RT, 2000x g for 20 minutes using a Kubota 2800 table centrifuge with a swinging bucket rotor (Kubota RS240). Plasma (approx. 4mL/vacutainer) was carefully transferred to sterile microcentrifuge tubes (2mL) and clarified by centrifugation at 10 000x g for 20 minutes at RT using the Eppendorf MiniSpin® Plus table centrifuge with a fixed angle rotor (Eppendorf F-45-12-11). While avoiding to disturb the debris pellet, clarified supernatant plasma was aspirated and filtered using a 0.8µm Millex® AA Filter Unit (MF-Millipore, SLAA033SB) and stored on ice for a maximum of 3 hours before use in exosome isolation.

Samples of isolated plasma (3x 1.5mL) previously prepared from whole blood as described above from late-stage pancreatic cancer (PC) patients was collected from storage (-80°C) and thawed on ice. Tubes were inverted several times before clarification by centrifugation and filtration as described above. All subjects gave written informed consent prior to donating the blood used during experiments.

2.2.3 Techniques for exosome isolation

2.2.3.1 ExoEasy Maxi Kit (Qiagen), membrane affinity spin columns for CCM

Fresh clarified CCM (16mL) and ExoEasy Maxi Kit (Qiagen) buffer XBP (16mL, Qiagen) was mixed in each of two 50mL sterile conical base tubes (Sarstedt) by inverting the tubes 5 times. The mix from each tube was passed through separate ExoEasy spin columns in aliquots of 16mL by centrifugation at 500x g, 1 minutes at RT using the Allegra x-30R centrifuge (Beckman Coulter) with a swinging bucket rotor (Beckman Coulter SX 4400). Flow-through was collected and discarded between centrifugations. Residual liquids were cleared from spin columns by centrifugation at 4000x g for 1 minute at RT. Buffer XWP (Qiagen) was added to each spin-column and subsequently centrifuged at 4000x g for 5 minutes at RT. The flow through was collected and discarded before transfer of the spin column to a fresh collection tube (Qiagen). Elution buffer (500µL, Qiagen buffer XE) was added directly to the spin-column membrane and incubated for 1 minute at RT before centrifugation at 500x g for 5 minutes at RT. The eluate was collected and re-applied to the column and incubation repeated. Final centrifugation of the eluate was performed at 5000x g for 5 minutes at room temperature, before transferring the exosome isolate (500µL) in aliquots to 5 x 1.5 mL Protein LoBind micro centrifuge tubes (Eppendorf) and stored at -80°C.

2.2.3.2 ExoEasy Maxi Kit (Qiagen), membrane affinity spin columns for plasma

Clarified plasma samples (1mL) mixed with 1mL buffer XBP in 2mL sterile micro centrifuge tubes and homogenized by inverting the tubes 5 times. Tubes were incubated for 15 minutes at RT in order to ensure equilibration to room temperature, before proceeding with the ExoEasy protocol as described above for CCM.

2.2.3.3 ExoQuick (System Biosciences), precipitation reaction

Fresh clarified CCM (16mL) was transferred to conical base tubes (50mL, Sarstedt) and ExoQuick-TC™ precipitation reagent (3.2mL, System Biosciences) added before mixing by inverting the tubes several times. The mixed solution was incubated in an upright position at 4°C for 12 hours before centrifugation at 1500x g for 30 minutes at 4°C using an Allegra x-30R centrifuge (Beckman Coulter) with a swinging bucket rotor (Beckman Coulter SX 4400). While carefully avoiding to disturb the pellet, the supernatant was aspirated and discarded before centrifuging the tubes at 1500x g for 5 minutes at 4°C and carefully aspirating the remaining supernatant. The pellet was suspended in 500µL 1xPBS and transferred to 1.5 mL Protein LoBind micro centrifuge tubes (Eppendorf) in aliquots for storage at -80°C.

2.2.3.4 Total Exosome Isolation (Invitrogen), precipitation reaction for CCM

Fresh clarified CCM (16mL) was transferred to 100mL rounded bottom centrifuge tubes (Kubota) and mixed with Total Exosome Isolation (from cell culture media) (8mL, Invitrogen “TEI”) by pipetting and briefly vortexing the tubes until homogeneous. The mixtures were incubated at 4°C overnight in an upright position. Precipitate was pelleted by centrifugation at 10 000x g for 1 hour at 4°C using the Model 7780 High Speed Refrigerated Centrifuge (Kubota) with a fixed angle rotor (AG 1008A 8x 100mL) and the supernatant carefully aspirated and discarded. EV-containing pellets were suspended in 500µL 1xPBS by pipetting, and transferred to 1,5mL protein LoBind micro centrifuge tubes (Eppendorf) in aliquots for storage at -80°C.

2.2.3.5 Total Exosome Isolation (Invitrogen), precipitation reaction for plasma

Clarified plasma samples (1mL) were individually diluted with 500µL filtered (0.2µm, Millex®-MP 0,22µm filter unit, Merck Millipore Ltd) 1x PBS and thoroughly mixed by vortexing. Total Exosome Isolation Kit (from plasma) precipitation reagent (300µL, Invitrogen™) was added to each sample, and the mixture vortexed briefly. Samples were incubated at RT for 10 minutes before the precipitate was pelleted by centrifugation at 10 000x g for 5 minutes at room temperature using the Eppendorf MiniSpin® Plus table centrifuge with a fixed angle rotor (Eppendorf F-45-12-11). The supernatant was carefully aspirated and discarded and the pellet submerged in 500µL of filtered (0.2µm) 1xPBS, and incubated at RT for 1 hour until partially resuspended. The partial suspension was homogenized by vigorous pipetting, and vortexed until apparent complete suspension was achieved. All TEI precipitates from plasma suspensions were observed to have an opaque yellow or white appearance, depending on the donor sample. EV isolates were subsequently pipetted into aliquots in 1.5mL protein LoBind tubes (Eppendorf) for storage at -80°C.

2.2.3.6 qEV original columns (IZON science), Size Exclusion Chromatography (SEC) for CCM

Fresh clarified CCM (16mL) was concentrated using Amicon® Ultra-15 Centrifugal Filter Device (10K Nominal Molecular Weight (NMWL), Merck Millipore Ltd.) and centrifugation at 4000x g for 30 minutes at RT using the Allegra x-30R centrifuge (Beckman Coulter) with a swinging bucket rotor (Beckman Coulter SX 4400). CCM concentrate for was collected from the filter device and diluted to 500µL total volume with filtered (Millex®-MP 0.22µm filter unit, Merck Millipore Ltd.) 1x PBS and stored on ice for a maximum of 30 minutes before use with the qEV columns.

One fresh qEVoriginal Size Exclusion Column (IZON science, “qEV”) for each biological replicate to be processed was equilibrated to room temperature and rinsed by passing 10mL filtered (0,22µm) 1xPBS through each column. The bottom luer-slip was replaced in order to prevent the column from running dry. Remaining buffer over the column top filter was pipetted off immediately before loading of CCM concentrate sample (500µL) into each column, and the bottom luer-slip removed. The first 3mL of flow-through was collected and discarded (500µl fractions 1-6, equating to the column void volume) before the three subsequent eluate fractions of 500µL (fractions 7-9) was collected and each divided into aliquots in 1,5mL protein LoBind tubes (Eppendorf) for storage at -80°C.

2.2.3.7 qEV original columns (Izon science) SEC for plasma

Clarified plasma samples (1mL) were concentrated by centrifugation at 4000x g, 20 minutes at RT using the Allegra x-30R centrifuge (Beckman Coulter) with a swinging bucket rotor (Beckman Coulter SX 4400) using separate Amicon® Ultra -4 Centrifugal Filter Units (10K NMWL, Merck Millipore Ltd.). Concentrate was collected by pipetting from the filter to a 1,5mL microcentrifuge tube, rinsing the Amicon Ultra-4 filter with 30µL filtered (0,22µm) 1x PBS and adding to the transferred concentrate. The total collected concentrate was then diluted to 500µL using additional filtered (0,22µm) 1x PBS, and stored on ice for a maximum of 1 hour while qEVoriginal columns (Izon Science) were being equilibrated for use. Concentrated clarified plasma samples were subsequently equilibrated to RT before EVs were isolated using fresh qEVoriginal columns (Izon Science) as described above for CCM. EV isolates were stored at -80°C as aliquots suitable for downstream application.

2.2.3.8 EV isolation by differential centrifugation with ultracentrifugation (UC).

Freshly clarified CCM (see chapter 2.1.5) was transferred to a 100mL round bottom centrifuge tube (Kubota) and centrifuged at 10 000x g for 30 minutes at 4°C using the Model 7780 High Speed

Refrigerated Centrifuge (Kubota) with a fixed angle rotor (AG 1008A 8x 100mL). The supernatant CCM was aspirated and transferred to a sterile 50mL tube and stored at -80°C until ready for use.

Before ultracentrifugation, the frozen CCM sample was moved to a separate laboratory and stored on ice overnight in a cold-storage chamber (4°C). The sample was then fully thawed by holding the tube in hand, and inverting several times. CCM supernatant (16,5mL) was transferred to a thickwall polycarbonate 32mL ultracentrifuge tube (Beckman Coulter, No.355631). A second ultracentrifuge tube was filled to the same level, within a margin of ±0.0015g using the tare function of a laboratory scale. The accuracy of the weight measurement was verified by repeating measurement of the first tube. A marker was used on the exterior of each tube for simplifying localization of pellet after centrifugation.

The ultracentrifuge tubes containing the CCM (16,5mL) were then placed into a pre-chilled (4°C) rotor (Beckman Coulter No. 337922, Type 70 Ti) and centrifuged at 118 000x g_{avg} (acceleration =2, Deceleration =4) for 2 hours at 4°C using the Optima™ XPN-100 ultracentrifuge (Beckman Coulter). The supernatant was aspirated and discarded before dissolving and washing the pellet in 16.5mL 1x PBS and repeating the ultracentrifugation as described above. The supernatant was again aspirated and discarded before resuspending pellet in 500µL 1x PBS. EV isolates were stored at -80°C as aliquots according to downstream application.

2.3 Quantitation and characterization of isolated EVs

2.3.1 qNano Gold (Izon Science) TRPS nanoparticle analysis

A TRPS reagent kit (Izon Science) were used in order to prepare coating solution and measurement electrolyte for all measurements using the qNano Gold (Izon Science). Measurements were conducted using 3 recordings at varying pressures of each sample as per recommendation by the manufacturer. Each recording was set to a 90 seconds of recording time. Each EV isolate sample was measured using both Nano Pore (NP) 100 and NP200, paired with appropriate calibration particles (CPC). CPC100 and CPC200 (Izon Science) were used with NP100 and NP200 respectively. CPC100 was diluted in measurement electrolyte (Izon Science) to a concentration of $1{,}0*10^{10}$ particles/mL and CPC200 to a concentration of $2{,}0*10^{9}$ particles/mL prior to use in calibrations, according to the manufacturer's recommendations. EV isolate samples were similarly diluted to an appropriate concentration for measurement using freshly made filtered (Millex®-MP 0,22µm filter unit, Merck Millipore Ltd.) measurement electrolyte. The appropriate dilution factor was determined experimentally for each individual sample using concentration estimates previously collected using the ExoCet EV Quantitation Assay (SBI) (chapter 2.4.2) and fine-tuned using the qNano Gold. Low concentration samples were diluted as little as 2x, whereas high concentration samples were diluted as much as 40x, in order to achieve a suitable balance between number of recorded particles and measurement stability.

All NP100 were tuned to the size interval 50nm-200nm, and NP200 to the interval 85nm-340nm. Calibration using the appropriate CPC was performed twice for each set of measurements, prior to- and after recording samples. To reduce the risk of errors due to pore blockages and other changing conditions, no more than 4 measurements were attempted for any given session, excluding calibrations. Measurements on the qNano Gold were carried out using the measurement assistant

function of the Izon control suite (v. 3.3.2.2001) for Microsoft Windows. The qNano Gold instrument and fitted nanopores were prepared according to the instructions provided in the Izon Control suite measurement assistant protocol for use with reagent kit, immediately prior to all recording sessions. Parameters for measurements such as current, drift and noise (RMS) were monitored and kept within margins specified in the Izon training manual for the qNano Gold (Izon science).

The qNano gold instrument reports concentration EV sample (nanoparticles/mL). These were normalized to correspond to particles/mL starting material used during EV isolation. The concentration value reported by the qNano Gold was multiplied by 0,5mL (the total volume of EV isolate sample) to estimate the total number nanoparticles in the full sample volume. qEV fractions were pooled at this point by addition of the total measured nanoparticles of fractions 7, 8 and 9. The calculated nanoparticle values were then divided by the volume of starting material used during EV isolation. The final calculated value corresponds to the estimated nanoparticle yield per mL of starting material.

2.3.2 qNano Gold analysis of triton x-100 treated samples

An equal aliquot of EV isolate sample stock was transferred to each of two 1,5mL microcentrifuge tubes. Both samples were diluted to a concentration previously verified as appropriate for the sample stock using fresh filtered (0,22µm) measurement electrolyte, and one of the samples modified by the addition of Triton x-100 (10%) to lyse vesicles, and subtraction of an equal volume of diluent, to a final Triton x-100 concentration of 0,1% (v/v). Both samples were vortexed briefly and allowed to incubate at RT for 20 minutes prior to measurement using the qNano Gold.

2.3.3 Making Combined Size Distribution Histograms (CSDHs)

The data collected by measuring the diameter and concentration of the same EV isolate samples using NP100 and NP200 were used to create histograms showing the overall size distribution of nanoparticles by their concentration (CSDHs) for each EV isolation techniques. Each CSDH was based on data obtained in the size interval 50-340nm. Particle diameter data from qNano Gold measurement pressures 1 and 2 were considered technical replicates, and both included in the datasets. Data from pressure 3 in some cases suffered from low overall particle counts, resulting in less statistical power and increased chance of non-representative average particle diameters. The third pressure measurement data were therefore not included in the making of CSDHs. Data of measured nanoparticles from the NP100 and NP200 with a bin size of 10nm was exported from the Izon software suite and processed using a specially made script in the R software environment [63]. Data on the concentrations of nanoparticles of 50-120nm in diameter were used from the NP100 datasets, and from 121 to 340+ nm in diameter from the corresponding NP200 datasets. In EV isolates from CCM, all samples were measured in two TRs using the qNano Gold. Each CCM based CSDH is therefore based on a total of 4 NP100 and 4 NP200 datasets. Each plasma derived sample was measured in one TR. Each plasma based CSDH is therefore based on 2 NP100 and 2 NP200 datasets.

2.3.4 ExoCet Exosome Quantitation Assay (SBI)

EV isolate samples from the TEI isolation technique were collected from storage (-80°C) and incubated for 20m on ice. They were then vortexed briefly, and incubated at RT for 3 hours prior to the ExoCet assay. Frozen samples were thawed completely by holding in the hand. ExoCet buffer A, PBS-B and lysis buffer were collected from storage (4°C) and placed on the benchtop 2 hours prior to the assay in order to equilibrate to RT. EV isolate samples of qEV 7, qEV 8, qEV 9, and ExoEasy were incubated on

ice 20 minutes prior to ExoCet Exosome Quantitation Assay (System Biosciences, "SBI"). Samples were thawed completely by holding in the hand and homogenized by vortexing briefly. A positive control sample of Acetylcholinesterase (1µg/mL, Sigma Aldrich, "AChE") was prepared by three steps of serial tenfold dilution in Tris-HCl (20mM, pH= 7,5) stock solution (1mg/mL, Sigma Aldrich, "AChE") with Tris-HCl (20mM, pH= 7,5). Negative controls consisting of the elution buffers of the various EV isolation techniques (Qiagen buffer-XE for ExoEasy samples, 1xPBS for all other samples) were additionally prepared. These were additionally used as blanks during calculations for the various samples.

ExoCet lysis buffer (60µl) was added to 1,5mL one 1.5mL microcentrifuge tube for each planned reaction. Each EV isolate sample (60µl) was then added and mixed by briefly vortexing the tubes before incubation at 37°C for 5 minutes (dry block) in order to lyse EVs. Debris was removed by centrifugation at RT 1500x g for 10 minutes using the Eppendorf Mini Spin Plus table centrifuge, and the supernatant of each sample (110µl) was carefully transferred to a fresh set of 1,5mL tubes. Samples were stored on ice until completion of assay preparation (< 15 minutes), and then equilibrated to RT before assay.

Double ExoCet standard curves were prepared by serial dilution by twice performing the dilution series described below (table 3).

Table 3: The dilution series for the ExoCet Exosome Quantitation Assay (SBI) standard curve. A total of 8 points of data was prepared for each curve, with the last being a blank (column 1 from the left). The number of exosomes corresponding to the levels of AChE enzyme in each dilution (as estimated by the manufacturer) is shown in column 2. Column 3 gives the dilution factor of each data point relative to the stock solution, and the last two columns shows the required volumes to mixed for each dilution in the series.

Tube	**# of exosomes**	**Dilution factor**	**Standard soln. (Stock)**	**PBS-B**
1	$1.28*10^{10}$	1	128µL	0
2	$6.40*10^{9}$	1:2	60µL (from tube 1)	60µL
3	$3.20*10^{9}$	1:4	60µL (from tube 2)	60µL
4	$1.60*10^{9}$	1:8	60µL (from tube 3)	60µL
5	$8.00*10^{8}$	1:16	60µL (from tube 4)	60µL
6	$4.00*10^{8}$	1:32	60µL (from tube 5)	60µL
7	$2.00*10^{8}$	1:64	60µL (from tube 6)	60µL
Blank	0	Blank	0	60µL

ExoCet reaction buffer was prepared by mixing ExoCet buffer B (0.5µL/rxn) with ExoCet buffer A (50µL/rxn) and vortexing briefly. The reaction buffer (50µL/rxn) was then immediately loaded into each well of the ExoCet-kit included 96-well microtiter plate. In order to minimize time mixed with reaction buffer prior to measurement, each sample (50µl) was loaded into a separate 96-well staging microtiter plate in accordance with the planned loading order (see appendix section 7.4). While carefully avoiding making bubbles, a Pipet-lite 20-200µL 8-channel multichannel pipette (Rainin) was used in order to quickly transfer all samples from the staging plate to the ExoCet microtiter plate pre-loaded with reaction buffer in each well. The plate containing the sample-reaction mix was then transferred to a Model 680 XR Microplate reader (BioRad) set with plate shake option enabled for gentle mixing of reagents. The optical density (OD) at 405nm was measured at 5 minute intervals from 0 minutes to 40 minutes.

The EV isolate samples were observed to have some variance in their apparent opacity (judging by eye), and as such, a series of further specialized blanks were designed for the ExoCet in an effort to

account for any sample opacity caused by colloid particles in the various samples. Material from each individual EV isolate sample from control group donor 2 (for the control group assay) and PC patient donor number (PC patient group assay) was used to prepare an additional set of ExoCet assay samples (2 ExoCet technical replicates), as described previously. The wells of the 96-well microtiter plate designated for these samples, were loaded with ExoCet buffer A (50µL/rxn), but buffer B was not mixed in, rendering the reaction mix inert. Samples were loaded in accordance with the loading order, and measured alongside the other samples as described previously.

An estimation of the combined OD405nm in each microtiter plate well stemming from ExoCet reaction mix, sample buffer and individual innate sample opacity (OD405nm unrelated to enzymatic action) was achieved by adding together the OD405nm of a given samples normal blank +specialized blank. The resultant value was subtracted from the given sample as a new specialized blanking value. It was against using the values of these blanks during calculation of final ExoCet assay results (see discussion).

2.3.5 Characterization of EVs by bead-assisted flow cytometry analysis

EV isolates from CCM were analysed for the presence and relative concentration of CD9 and CD63 protein by BAFC in 2 TR. Each TR consisted of one sample fraction (50µL) of stained sample assay mix (sample) and one fraction (50µL) of unstained sample assay mix (negative control).

A volume of 0.91µL aldehyde/sulfate latex Beads (4% w/v, 4µm diameter, Molecular Probes) was added to Tris-buffered saline (1mL, 0.9% w/v NaCl, 5mM Tris-HCl "TBS") in a protein LoBind (Eppendorf) microcentrifuge tube, for an overall bead-count of 10^5 beads/tube. The number of beads was determined so as to be large enough to prevent over saturation of EVs on each bead, yet small enough to allow for detection of EVs in small sample volumes. EV isolate samples (50µL) was added and mixed by pipetting, before overnight incubation at 4°C with agitation in a hula shaker. Bead-coupled EVs were then pelleted by centrifugation at 3000x g for 10m at RT (swinging bucket rotor). Unbound sites on beads were blocked by the addition of Glycine (1mL, 100mM in TBS) and incubation for 30 minutes at RT. Bead-coupled EVs were again pelleted by centrifugation at 3000x g for 10 minutes at RT, before washing with 1mL TBS. Pellets were Then resuspended in staining buffer (100µL, PBS, 0.5% Bovine Serum Albumin, 2mM EDTA). BAFCR Blocking reagent (25µL, Miltenyi Biotech) was added to each sample, before staining with either:

a. CD9 phycoerythrin (10µL, "PE", Methylene Blue "MB", Clone: SN4 C33A2, Miltenyi Biotech) or isotype control (2µL, IgG1 PE, Miltenyi Biotech)
b. CD63 Allophycocyanin ("APC", 10µL, MB, clone HBC6, Miltenyi Biotech) or isotype control (2µL, IgG1 APC, Miltenyi Biotech)

Samples were then incubated for 20 minutes at RT, shielded from light. Samples were washed with staining buffer (1mL) and beads re-pelleted by centrifugation at 3000x g for 10m at RT. Pellet was then resuspended in staining buffer (500µl) before analysis on the CytoFLEX Flow Cytometer Platform (Beckman Coulter). For analyses, the CytExpert software (Beckman Coulter) was used. Gating of EV coupled beads was tuned so as to include only single beads, using the SSD/FSC parameters, and the CD9 and CD63 expression was calculated as the median fluorescence intensity (MFI) of 5000 single beads.

The work for the BAFC analysis fort CD9 and CD63 protein was done by another member of the research group, Morten Lapin (Ph.D.).

2.4 Isolation, quantitation and characterization of EV DNA

2.4.1 Elimination of non-EV DNA by RQ1 DNase treatment of EV samples

2.4.1.1 EV isolates from CCM

EV isolate samples from CCM were collected from storage (-80°C) and thawed on ice. Each sample was homogenized by vortexing briefly, and 70µL transferred to fresh 1,5mL micro centrifuge tubes before the addition of 7.5µl RQ1 RNase-Free DNase 10x reaction buffer and 1µL RNase-Free DNase (Promega). Samples were mixed carefully by pipetting before incubation at 37°C for 30 minutes (water bath). The reaction was terminated by the addition of 7.5µL RQ1 DNase stop solution (Promega). Sample and stop solution was mixed by briefly vortexing the tube, which was then incubated at 65°C for 10 minutes (dryblock).

2.4.1.2 EV isolate from plasma

EV isolate aliquots (from plasma) were collected from storage (-80°C) and thawed on ice in the same manner as described above. No more than 15 samples were processed at a time. Each sample was homogenized by vortexing briefly, and 100µL transferred to fresh 1.5mL micro centrifuge tubes before the addition of 11µl RQ1 RNase-Free DNase 10x reaction buffer and 1µL RNase-Free DNase (Promega). Samples were mixed carefully by pipetting before incubation in water bath at 37°C for 30 minutes. The reactions were terminated by the addition of 11µL RQ1 DNase stop solution (Promega), mixing by brief vortex and incubation at 65°C for 10 minutes (dryblock). DNase treatment was carried out immediately prior to DNA isolation, without delay.

2.4.2 EV DNA isolation

2.4.2.1 DNA isolation from EV isolate samples from CCM (Qiagen Allprep)

DNase treated EV isolate samples from CCM (70µL, diluted to 86µL with RQ1 DNase reagents during treatment, (section 2.4.1.1) were diluted to a total volume of 700µL with lysis buffer (Qiagen Allprep buffer RLT plus) and EVs lysed and homogenized by vortexing for 1 minute. All sample tubes were spun down briefly and the lysate transferred to AllPrep DNA mini spin columns in 2mL collection tubes. The continued isolation of DNA was performed directly in accordance with protocol for AllPrep® DNA/RNA/miRNA Universal Handbook provided by manufacturer (Qiagen). The final elution of isolated DNA was performed using 2x 50µL of elution buffer EB (Qiagen) in two centrifugation steps of 9000x g for 1 minutes at RT, for a total elution volume of 100µL. DNA isolate (20µL) was in all cases immediately analysed for concentration of dsDNA using the Qubit dsDNA HS assay the same day. Remainder DNA-isolate (80µL) was stored at -20°C. The process was repeated for an additional isolation of DNA from samples of non-DNAse treated EV isolates (100µl).

2.4.2.2 DNA isolation from EV isolate samples from plasma (Qiagen QiAmp circulating nucleic acid kit)

DNA was extracted from DNase treated samples (100µL EV isolate solution diluted to 123µL with RQ1 DNase reagents during treatment) according to protocol provided by the manufacturer (Qiagen) for

QiaAmp Circulating Nucleic Acid Kit for isolating of free-circulating DNA and RNA from human plasma or serum (1mL or less starting volume). No carrier RNA was used. The final elution of isolated DNA was performed using 50µL of elution buffer AVE (Qiagen) and centrifugation at 16 000x g for 1 minute.

2.4.3 Quantitation of dsDNA by Qubit® dsDNA HS assay

Samples of isolated nucleic acids (see Allprep and QiaAmp above) were thawed on ice for dsDNA quantitation using the Qubit™ dsDNA HS assay kit (Thermo Fisher Scientific) and Qubit™ 2.0 fluorometer (Invitrogen, Life technologies).

Qubit Workings Solution (200µL,"WS") was prepared for each reaction by mixing of Qubit reagent with Qubit™ dsDNA HS buffer (1:200). The Qubit™ 2.0 fluorometer uses two standard solutions in order to automatically generate a standard curve for measurements of concentrations. These were prepared by adding WS (190µL) to each of two Qubit™ Assay Tubes (Thermo Fisher Scientific) and adding a volume of 10µL of either Qubit™ dsDNA HS Standard solution 1 or 2. WS (180µL) was then added to one Qubit™ Assay for each sample to be measured, and sample (20µL) was added to each tube. All standard and sample reaction mixes were homogenized by vortexing for 3 seconds before spinning down briefly using a table centrifuge. The reaction mix was incubated for 2 minutes at RT before measuring the standard solutions on the Qubit™ 2.0 fluorometer (Invitrogen, Life technologies, dsDNA HS setting). Samples were subsequently analysed, and the dsDNA concentration of the DNA isolate samples determined using the Qubit™ 2.0 fluorometer calculator function.

2.4.4 Identification of KRAS mutation by PNA clamp qPCR assay

Isolated exoDNA (20µL, see Allprep, QiaAmp above) was amplified and screened for KRAS mutations by PNA Clamp quantitative real-time PCR (qPCR) Assay for KRAS mutation. Each sample was tested in two TRs, each consisting of PNA positive (+PNA) and PNA negative (-PNA) assay sample (each original DNA isolate divided into 4 sample aliquots in total). A negative control consisting of WT isolated plasma DNA (5µL) from a healthy individual was used along with a positive control (5µL, 10ng/µL) consisting of a 1:100 diluted mixed LS174T (heterozygous GGT > GAT codon 12 KRAS mutation ([c.35G > A]) in Caco-2 (KRAS WT) cell line DNA isolate.

PNA (sequence 5'-CCTACGCCACCAGCTCC-3') and PCR forward (5'-GCCTGCTGAAAATGACTGAATATAA-3' KRAS-PNA-FB, Oligodatabase ID 85) and reverse (5'-CGTCAAGGCACTCTTGCCTAC-3' KRAS-PNA-RB, Oligodatabase ID 88) primers were acquired and prepared as in Tjensvoll *et.al.* 2015 [64]

Reagents and DNA samples were thawed on ice in separate LAF benches, and mastermix sufficient for all reactions in accordance with table 4 below. Before the addition of PNA, the mastermix was separated into two tubes, and PNA added to one (+PNA) and Milli-Q water to the other (-PNA, see table 4). Mastermix (20µL) was then added into wells on a 96-well PCR plate meant for samples/controls. The PCR plate with master mix was moved to the LAF bench with the DNA samples, and sample (5µL) was added to each well in accordance with the planned loading order. The PCR-plate was covered in adhesive foil, and spun down briefly before loading into the Mx3000P qPCR System (Agilent Technologies).

Table 4: Reagents and volumes for the PNA Clamp PCR Assay for KRAS mutation. The order in which reagents were added follows the table from top to bottom.

PNA-clamping	**PCR**	**Phusion**		***20 µl***	***mastermix***
				+PNA	-PNA
Number of rxn:	112			56	56
Reagent	**Conc.**	**Volume/rxn**	**Mastermix**	**+PNA**	**-PNA**
Vann		12,987	1454,5		
5x Phusion HF buffer	1x	5	560		
25 mM dNTP	0,2 mM	0,2	22,4		
KRAS-FB primer	0,15	0,375	42		
KRAS-RB primer	0,15	0,375	42		
SYBR Gr. I 1:200		0,75	84		
2 U/µl Phusion pol.	0,02 U/µl	0,25	28		
Final		19,937	2232,9	**1116,47**	**1116,47**
100 µM PNA	0.25 µM	0,063		**3,500**	0
MQ-H_2O				0	**3,500**
Final		20,000		1120	1120

The PCR program was then run using the following program:

- 98°C, 30 seconds (activation of enzyme)
- 45 cycles:
    - 98°C, 20 seconds (denaturing)
    - 76°C, 10 seconds (PNA annealing)
    - 60°C, 20 seconds (primer annealing)
    - 72°C, 72 seconds (elongation), with measurement of fluorescence

The work for the PNA Clamp qPCR assay for KRAS mutation was done by another member of the research group, Satu Snikka Oltedal (Ph.D.).

3. RESULTS

An overview of the overall workflow for the experimentation in this study is shown below (figure 4). The main phases of EV isolation and characterization is shown for samples form CCM and plasma. More in-depth descriptions will be given under each individual section.

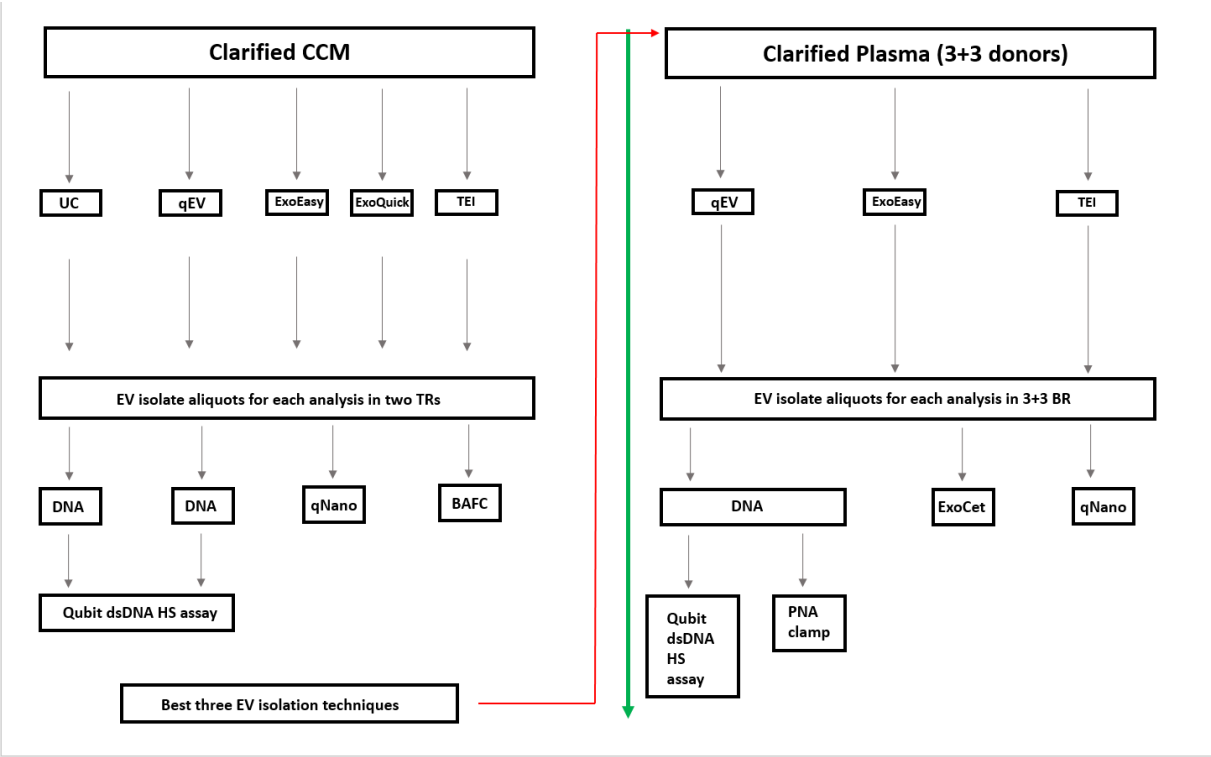

Figure 4: Outline of the workflow for EV isolation and characterization with samples from CCM shown to the left, and samples from plasma shown to the right. In each case the general workflow goes from raw material to isolated EVs. These are then divided into aliquots which are used for the various analyses. TR = technical replicate. BR = biological replicate

3.1 Overview

3.1.1 EV isolations using CCM as starting material

For EV isolations using CCM as a starting material, PANC-1 CCM was produced (section 2.2.1.4) and clarified (section 2.2.1.5) and a volume of 16ml CCM was used for each technique in two TR (section 2.2.3). The only exception to this was the UC technique, for which some additional steps were taken (section 2.2.3.8). EV isolation on CCM was carried out using differential centrifugation (UC), SEC (qEV), affinity chromatography (ExoEasy) and polymer precipitation (ExoQuick, TEI). After EV isolation using each technique, EVs were resuspended/eluted to a volume of 500µL. The suspended EVs were then stored in aliquots at -80°C until use in the various analyses (table 5).

Table 5: Sample aliquots prepared from EV isolate from CCM (2x 16mL). The 500µL of EV isolate from each of the two EV isolate technical replicates (column 1 from the left) was divided into aliquots according to intended downstream application (column 2). The volumes of each aliquot is shown in column 4.

# TR	Downstream application	Abbreviation	Aliquot volume (µL)
2	qNano Gold	qNan	180
2	DNA analysis (+DNase)	DNA+	70
2	DNA analysis (- DNase)	DNA-	100
2	BAFC	BAFC	100
2	Other	N/A	50

Two replicate samples of each EV isolation technique was later thawed and used for each of the planned analyses (sections 2.3, 2.4) by TRPS (Size, concentration, vesicle fraction), BAFC (exosome marker proteins), and Qubit dsDNA HS assay (dsDNA cargo, effect of DNase). The dsDNA for the Qubit dsDNA assay was isolated using the Allprep DNA/RNA/miRNA kit.

The goals of these experiments were to establish good methodology and get a general overview of the efficacy of each individual technique, was well as identifying the three most promising EV isolation techniques. Only the three best techniques would be used for the next phase of experimentation using human plasma as starting material.

3.1.2 EV isolations from human plasma samples

After establishing the methodology and testing results from CCM were reviewed, the three EV isolation techniques showing the best performance in relation to our criteria were advanced to the next stage of testing, using human plasma as starting material for EV isolation. The techniques selected were ExoEasy, TEI and qEV (section 3.3).

Here, plasma was collected from control and PC patient donors, clarified (section 2.2.2), and used for EV isolation using the ExoEasy, TEI and qEV techniques. Samples were then used for determination of dsDNA content (Qubit dsDNA HS assay), levels of tumour DNA (PNA clamp), exosome concentration (ExoCet), nanoparticle concentration, size distribution and vesicle fraction (TRPS). DNA for the Qubit and PNA-clamp assays was isolated using the QiAmp Circulating Nucleic Acid Kit (Qiagen)

3.2 Comparison of methods of EV isolation from cell culture medium

For EV isolations using CCM as a starting material, 200mL of PANC-1 CCM (passage 35) was produced (section 2.2.1.4) and clarified (section 2.2.1.5) and used to carry out exosome isolation on 16mL of CCM using each exosome isolation technique (section 2.4) in two TR. The only exception to this was the UC technique (section 2.4.8). In this case, an aliquot of 40mL freshly clarified CCM was first used for the preparatory centrifugation stage (10 000xg, 30m). This step was unique to the UC technique, and the larger volume was to allow for some shrinkage. Out of the supernatant from this centrifugation, two aliquots of 16.5mL were used during ultracentrifugation. This volume had to be used due to a particularity of the ultracentrifuge tubes, which required a filling level of 16.5mL. This difference in starting volume between the UC technique and the other EV isolation techniques (16.5mL versus 16.0mL) was corrected for mathematically in all results.

Exosome isolation on CCM was carried out using differential centrifugation (UC), SEC (qEV), affinity chromatography (ExoEasy) and polymer precipitation (ExoQuick, TEI), the results are shown in section 3.2 below.

After exosome isolation using each technique, exosomes were resuspended/eluted to a volume of 500µL. In the case of ExoEasy (Qiagen), the eluent used was the proprietary buffer XE, which was part of the ExoEasy maxi kit. For all other EV isolations, 1xPBS was used. The suspended EVs were then stored in aliquots at -80°C until use in the various analyses (table 5).

Two replicate samples of each EV isolation technique was then used for each of the planned analyses (sections 3.2.1 – 3.2.4). The nanoparticle concentration and size distribution was determined for each EV isolation technique using the qNano Gold TRPS analysis (section 3.2.1). Additionally, the relative vesicle fraction in for each sample was estimated by treatment with Triton x-100 (0.1% v/v) and TRPS concentration measurements (section 3.2.2). The relative levels of the exosome marker proteins CD9 and CD63 was measured using BAFC assay (section 3.2.3) and the relative concentrations of EV dsDNA cargo achieved through each EV isolation technique was measured using the Qubit dsDNA HS assay (section 3.2.4). Here the relative amount of dsDNA contained within EVs was also estimated by DNase treatment of the raw EV isolate sample prior to DNA isolation.

A schematic illustration of the workflow from clarified starting material to the various analyses is shown below (figure 5).

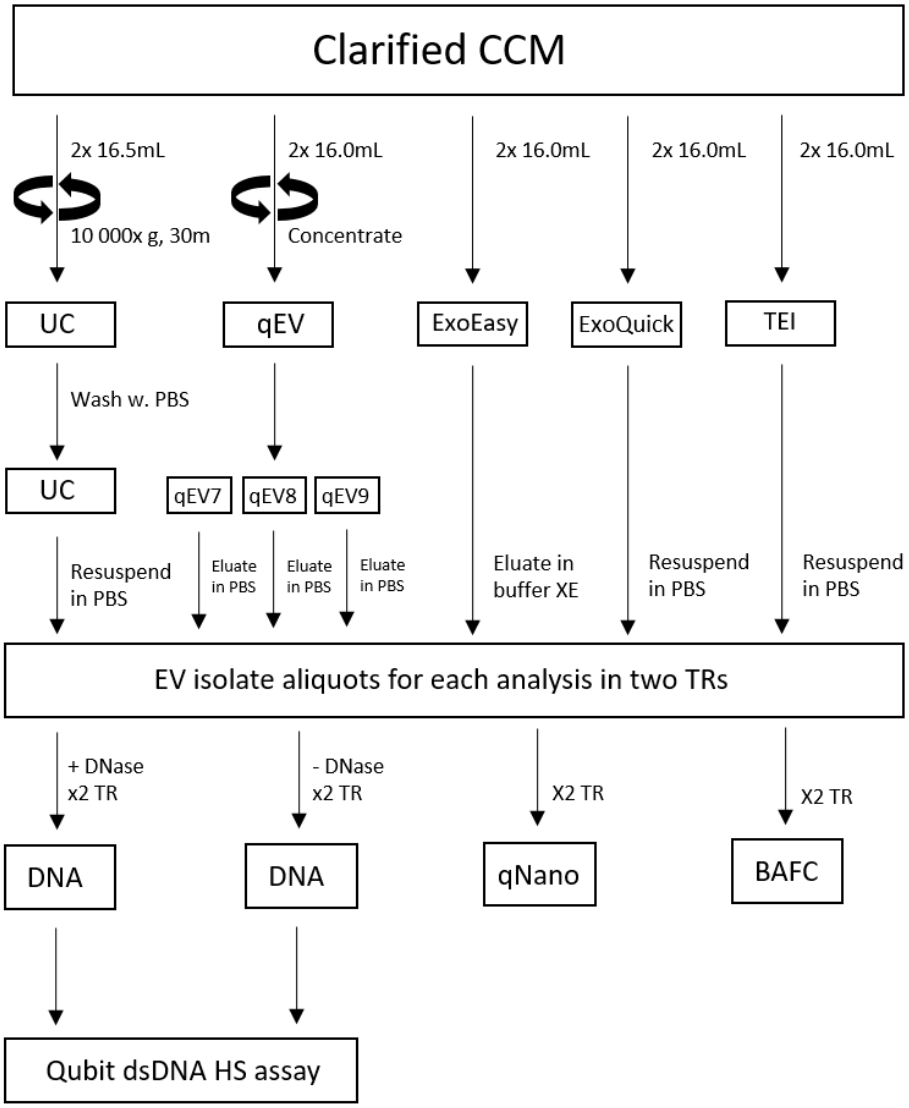

Figure 5: General workflow for EV isolate samples using CCM as starting material. The paths between various stages (black boxes) in the process from raw material to EV analysis is indicated by the black arrows. Next to each arrow is additional information pertaining to the particular step in question. BR = biological replicate. TR = technical replicate

3.2.1 Determination of particle concentration and size

In order to assess the yield and types of EV primarily isolated by each individual technique, nanoparticle diameter and concentration was determined by TRPS analysis using the qNano Gold (section 2.3.1). The instrument could not distinguish vesicles from other nanoparticles. Samples of ExoEasy, TEI, ExoQuick, qEV7, qEV8, qEV9 and UC were measured in two TR. Each sample was measured at the manufacturer-recommended three pressures, in order to achieve high quality concentration measurements. The qNano Gold instrument reported nanoparticles/mL were normalized so as to correspond to nanoparticles/mL CCM used during EV isolation (16mL in the case of CCM samples, 16.5mL for UC samples).

Nanoparticle concentrations

The average nanoparticle concentration and standard deviation in the range of each nanopore was calculated based on the two TRs measured of each sample. A figure illustrating the measured CCM derived EV isolate nanoparticle concentrations is shown below (figure 6). The full collected data can be found in the appendix (Section 7.5)

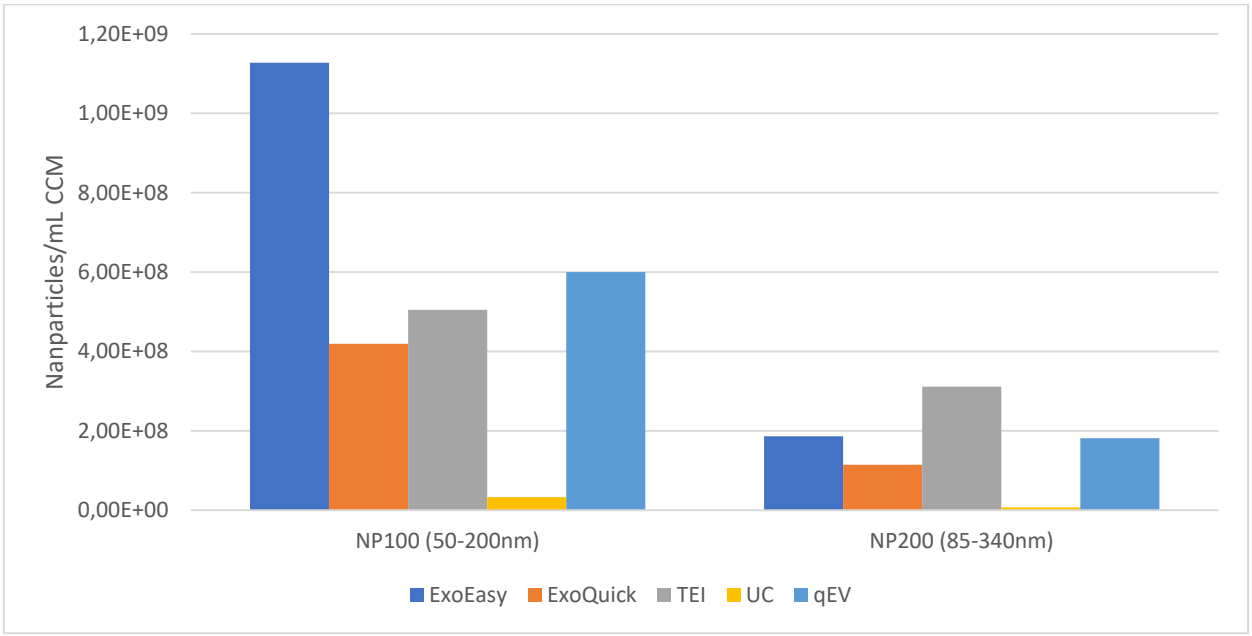

Figure 6: TRPS measurements on samples of EV isolates using CCM as raw material. NP100 (particle diameter 50-200nm) measurements are shown on the left, and NP200 (particle diameter 85-340nm) on the right. Fractions of qEV were measured individually and have been pooled mathematically.

The qNano Gold measurements on samples from CCM indicated an overall concentration of nanoparticles much higher in the 50-200nm range than in the 85-340nm range. Interestingly, the observed reduction in nanoparticles between seize was variable between EV isolation techniques, indicating variance in nanoparticle size distribution. While the ExoEasy EV isolate yielded by far the highest measured concentration in the NP100 range (1,13E+09 P/mL vs. 5,05E+08 P/mL respectively), TEI gave the highest concentration in the NP200 range (TEI at 3,11E+08 P/mL vs ExoEasy at 1,86 E08 P/mL). The pooled qEV yield proved to do well in both ranges, yielding the second highest nanoparticle

concentration in the NP100 range (6,0E+08 P/mL) and very nearly coming second also in the NP200 range (1,81E+08 P/mL). ExoQuick, while not far behind, had the third highest yield in both particle size-ranges, with NP100 and NP200 concentrations of 4.19E+08 P/mL and 1,14E+08 P/mL respectively. The UC samples provided the lowest nanoparticle concentrations of all the techniques by far, in both NP100 and NP200 ranges.

Nanoparticle average size distributions

The qNano gold, in addition to collecting concentration data, collects size data on each individual particle which passes through the nanopore, and is within the detection limit size range of the pore. An average particle diameter can therefore be calculated, and correlated with sample concentration as done for EV isolate samples from CCM below (figure 7).

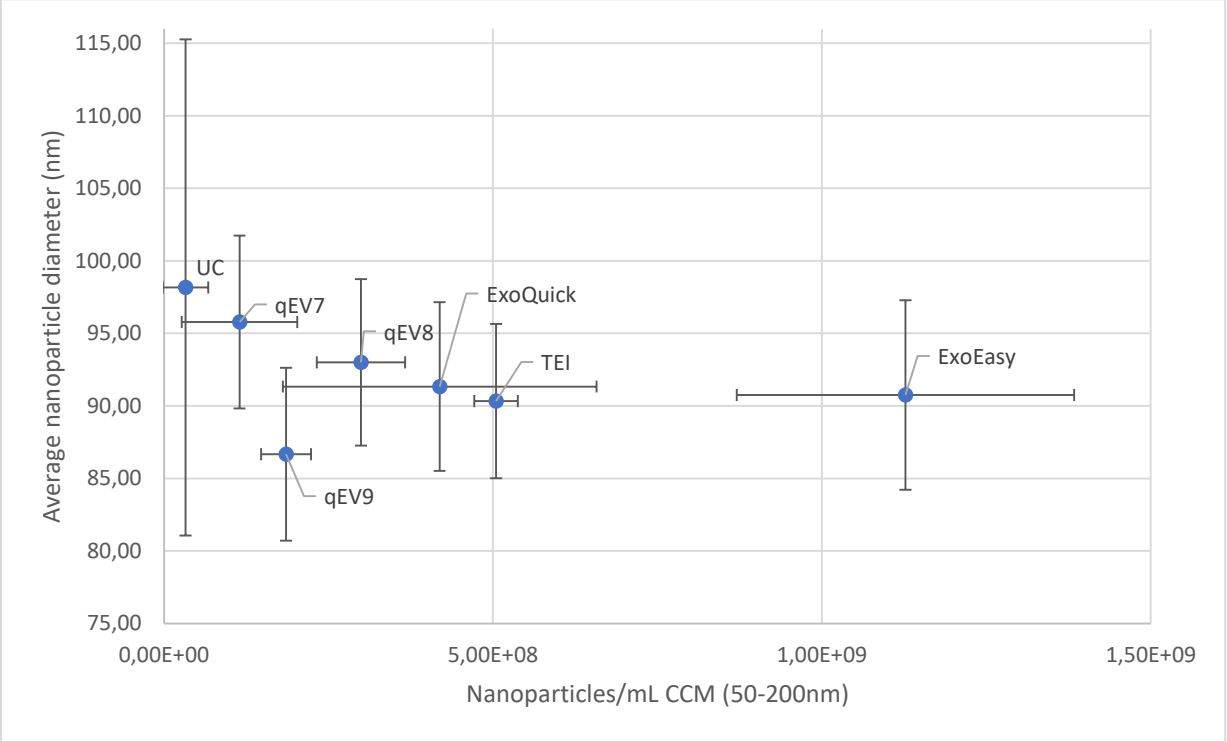

Figure 7: Average nanoparticle diameter as a function of concentration, by EV isolation technique. Values shown are calculated across all qNano Gold NP100 (50-200nm) measured particles from CCM. In the chart, movement to the right signifies increasing concentration, whereas movement upwards means increasing average particle diameter. Error bars on the y-axis are based on the standard deviation associated with average particle diameter as reported by the qNano gold. The error bars on the x-axis are based on technical replicate measurements of the concentration of each sample.

On average, in EV isolates from CCM, the particles isolated by the UC technique gave the largest overall particles, combined with the lowest particle concentration (figure 7). Progressively smaller nanoparticle average diameters were achieved for the qEV fractions 7, 8 and 9, with the latter having the smallest average diameter of all the EV isolates using CCM as raw material. The TEI and ExoEasy techniques gave very similar average particle diameters.

Combined Size Distribution Histograms

We combined the size information obtained from the NP100 and NP200 pores for each of the EV isolates (figures 8,9, 10 and 11).

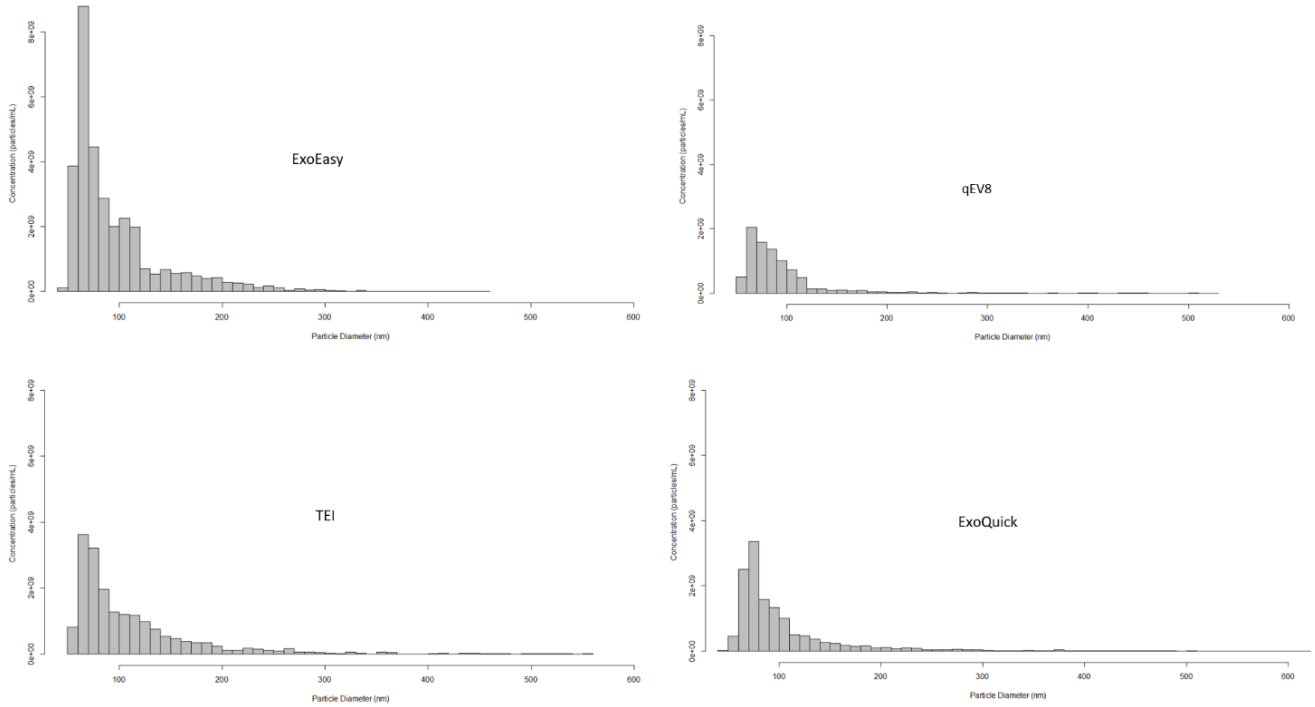

Figure 8: Combined Size Distribution Histograms (CSDH) for samples of ExoEasy, TEI, qEV 8 and ExoQuick from CCM. Each bin spans 10nm in particle diameter. All CSDHs are modelled based on size distribution data collected using the qNano Gold, and are a combination of data from nanopores NP100 (50-120nm) and NP200 (121nm+). The y-axis has for all histograms been set to 8E+09 particles/mL, and the x-axis to 600nm, for ease of comparison between EV isolation techniques.

The combined size histograms (CSDHs) of ExoEasy, TEI, qEV8 and ExoQuick (figure 8) revealed a roughly similar size distribution of nanoparticles in the 4 samples. The smallest nanoparticles were in all cases most frequent, with modes around 60nm, and then rapidly declining as nanoparticle diameter approached 200nm. This substantiated the already reported findings of the particle concentration differences between the NP100 (50-200nm) and NP200 (85-340nm) for qNano gold NP100 measurements on samples from CCM (figure 6). There were however some differences visible in how concentration decreased, as particle diameter increased from 70-200nm. TEI and ExoQuick were very similar in this regard, both showing many particles in the 70-100nm range, and then showing a smooth gradual decline of concentrations, continuing throughout the entire measured interval. TEI however appeared to have the overall greatest concentration in the interval from 100-150nm, the interval in which exosomes would fall. qEV 8 appeared to have a somewhat more rapid decline in concentration, as diameters exceeded 110nm, than did the other techniques compared here. ExoEasy appeared to have a very large number of particles in a plateau from 90-120nm. Concentrations then rapidly dropped off, to nearly half of that observed in TEI in the 120-130nm interval.

It should be noted, that the sensitivity cut-off for all measurements was at 50nm. It is therefore possible that concentrations even higher than what is shown in the diagrams, is present in the diameter range from 50nm and below. It should further be noted that the histogram data reflects particles/mL measured sample, and has as such not been normalized so as to reflect particles/mL starting material during EV isolation.

The qEV fractions and the UC sample yielded much lower absolute concentrations, than did TEI, ExoQ and ExoEasy. As such, they can better be compared using a slightly smaller scale (figure 9). Out of the qEV fractions, qEV 8 had the greatest overall concentration by far, with a very large amount of particles

measured in the 60-120nm range. Concentrations then dropped off sharply, for higher particle diameters. qEV 7 conversely, showed a much more gradual decline in concentrations as particle diameter increased, with overall low particle concentrations. qEV 9 showed a particle distribution in the 60-100nm range reminiscent to that of qEV 8, but with a much less sharp cut-off at higher particle diameters. The ultracentrifugation CSDH indicated a very flat distribution, somewhat favouring particles in the 60-110nm range. Larger standalone versions of each CSDH shown in figures 8 and 9 can be found in the appendix (section 7.5.2)

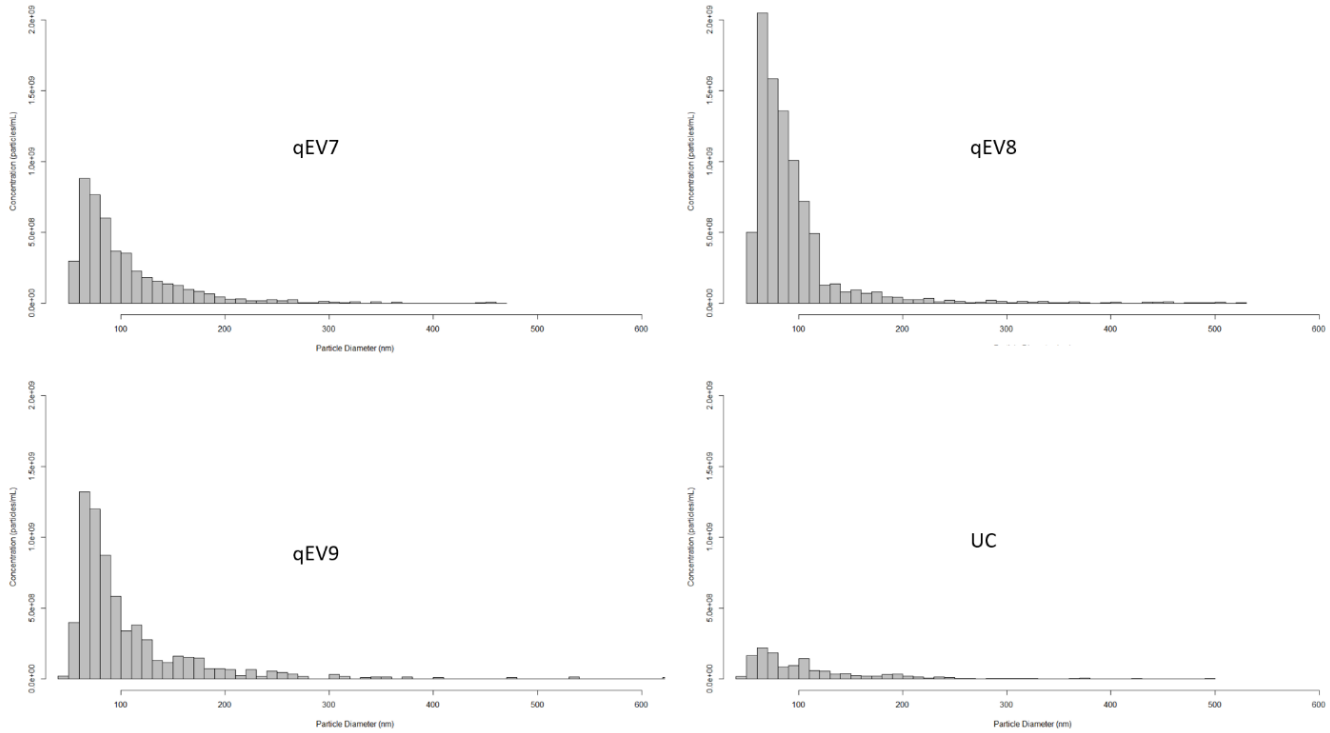

Figure 9: Combined Size Distribution histograms (CSDH) for samples of qEV 7, qEV 8, qEV 9 and UC from CCM. Each bin spans 10nm in particle diameter. All CSDHs are modelled based on size distribution data collected using the qNano Gold, and are a combination of data from nanopores NP100 (50-120nm) and NP200 (121nm+). Note that the scale of the y-axis has been reduced relative to figure 8. The y-axis has for all histograms been set to 2E+09 particles/mL, and the x-axis to 600nm, for ease of comparison between EV isolation techniques

Relative presence of large EVs (200nm+)

In addition to nanoparticles in the general size-range for exosomes (50-150), also the relative concentrations of potential EVs of greater dimension, such as MVs and oncosomes, are of interest. In order to better assess the concentrations of these nanoparticles, the scales of the y-axis of each CSDH was changed to better show the distributions of larger nanoparticles (200nm+, figures 10, 11)

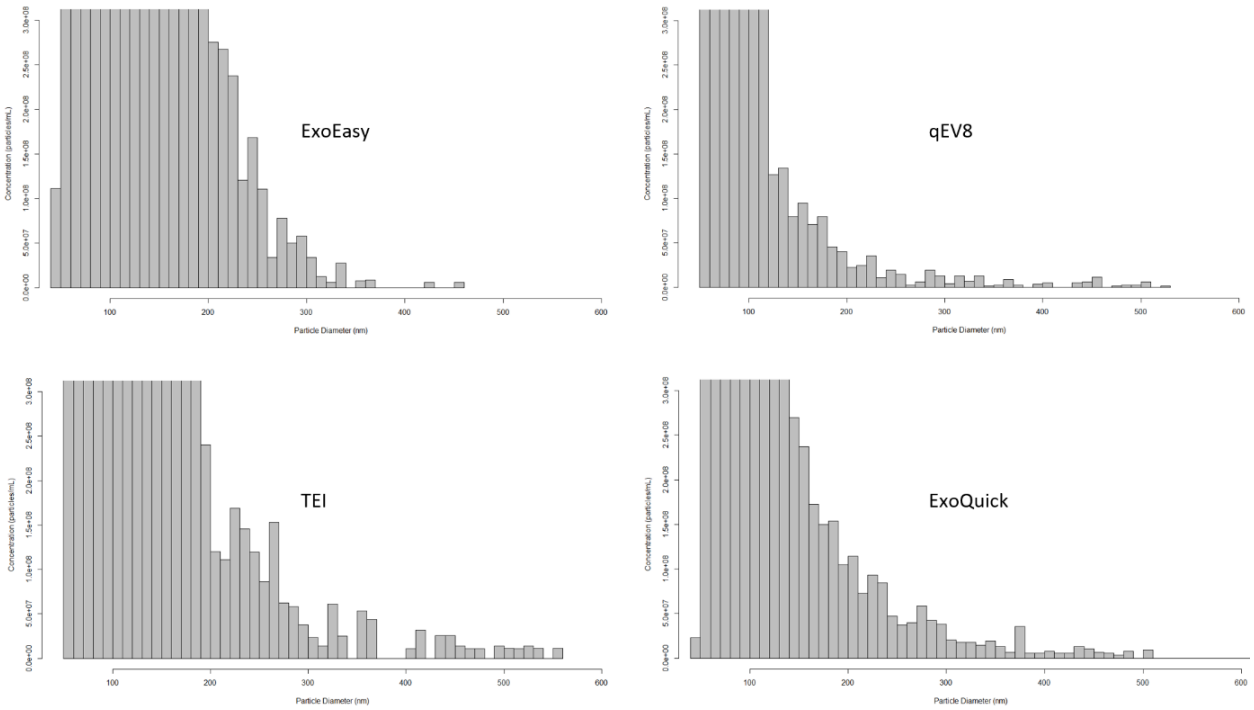

Figure 10: Combined Size Distribution Histograms (CSDH) for samples of ExoEasy, TEI, qEV 8 and ExoQuick from CCM. Each bin spans 10nm in particle diameter. All CSDHs are modelled based on size distribution data collected using the qNano Gold, and are a combination of data from nanopores NP100 (50-120nm) and NP200 (121nm+). Note that the scale of the y-axis has been reduced even further relative to figure 8, in order to better allow comparisons of size distributions of particles with diameter >200nm. The y-axis has for all histograms been set to 3E+08 particles/mL and the x-axis to 600nm.

Focusing on these nanoparticles with diameters exceeding 200nm (figure 10), TEI showed the overall most diverse concentrations of particles, with a relatively large amount found in the 200-300nm range, as well as a trail of particles of even larger diameters. ExoEasy conversely, had the largest amount of particles in the 200-300nm range, but very few particles exceeding 300nm in diameter. ExoQuick and qEV 8 showed very similar distributions in the 200-500nm range, with a gentle slope from 200nm and out. ExoQuick did, however, display the overall larger amount of particles in this range, when compared to qEV8.

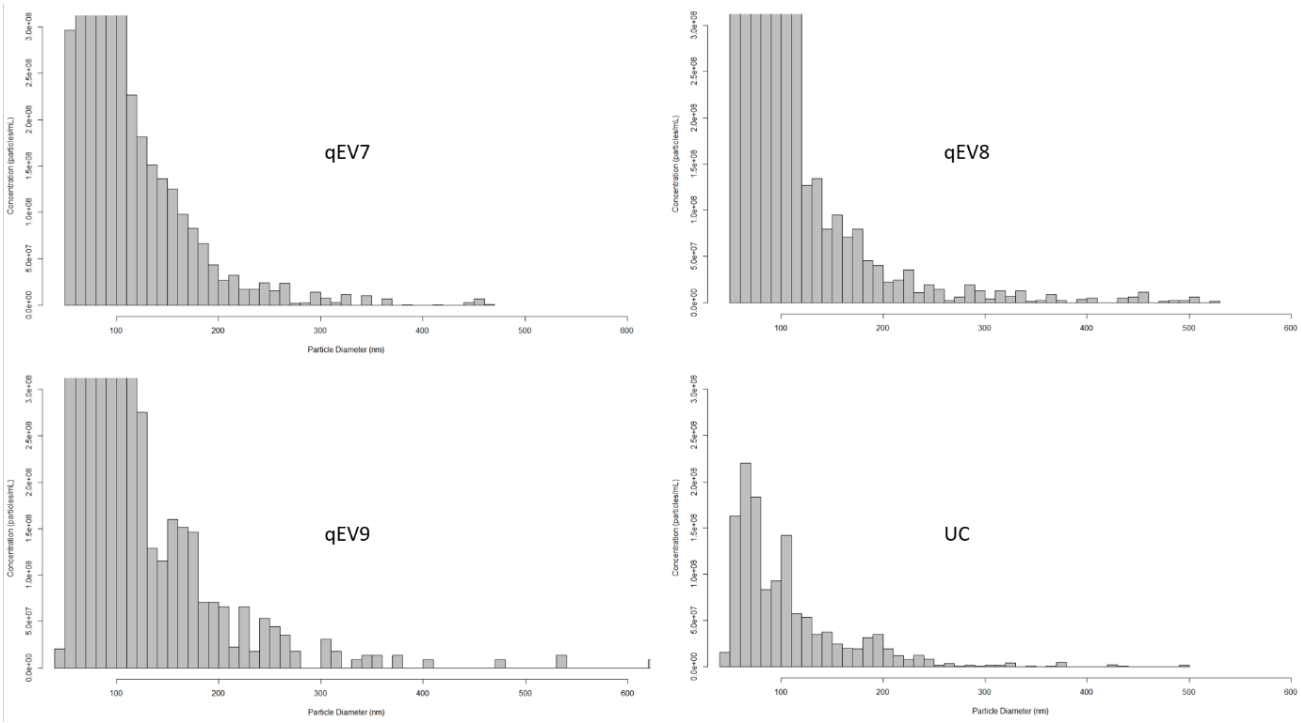

Figure 11: Combined Size Distribution Histograms (CSDH) for samples of ExoEasy, TEI, qEV 8 and ExoQuick from CCM. Each bin spans 10nm in particle diameter. All CSDHs are modelled based on size distribution data collected using the qNano Gold, and are a combination of data from nanopores NP100 (50-120nm) and NP200 (121nm+). Note that the scale of the y-axis has been reduced even further relative to figure 9, in order to better allow comparisons of size distributions of particles with diameter >200nm. The y-axis has for all histograms been set to 3E+08 particles/mL and the x-axis to 600nm

Also when comparing particles above 200nm, qEV7 and qEV8 displayed very similar distributions (figure 11), with a gentle slope stretching until about 500nm. qEV9 appeared somewhat different, with a very sparse and discontinuous particle population above 200nm. The UC sample showed a sloping distribution similar to that described for qEV7, qEV8, ExoQuick and TEI previously, although with much lower overall concentrations.

3.2.2 Estimation of vesicle fraction by sample treatment with Triton x-100

In order to estimate the fraction of EVs in the measured nanoparticle population (as opposed to protein aggregates and other contaminants), a set of TRPS measurements of EV samples from ExoEasy, TEI, ExoQuick, qEV7, qEV8, qEV9 and UC was performed with and without treatment with Triton x-100 (0.1% v/v). By adding a non-ionic detergent such as Triton x-100, membrane bound bodies such as EVs will dissolve, and only non-membranous nanoparticles will remain. The difference in measured nanoparticles before and after treatment should therefore equate to the number of vesicles in the sample.

In this set of measurements, two equal aliquots of EV isolate sample from each of the EV isolation techniques were diluted in fresh filtered (0.2µm) measurement electrolyte to the concentrations previously determined to be ideal for measurement of the that particular sample (section 3.2.1). One of the samples was treated with Triton x-100 (0.1% v/v, section 2.3.2). For a full list of all measured concentrations in this experiment, see the appendix (section 7.5.1).

Based on the two measured nanoparticle concentrations, the change (Δ) following treatment with Triton x-100 (0,1% v/v), corresponding to the vesicle fraction, was calculated and is show below figure 12). Additionally, the Δ in mean nanoparticle diameters was calculated (figure 13)

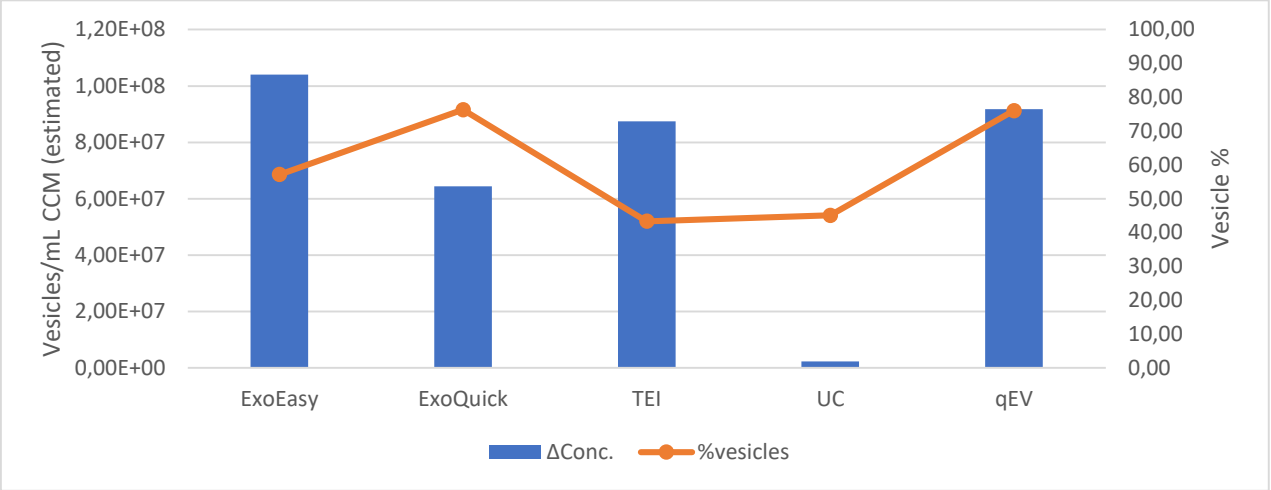

Figure 12: The vesicle fraction of the NP200 nanoparticle measurements in EV isolate samples from CCM, estimated by treatment with Triton x-100 shown in vesicle concentration (blue bars, left y-axis). Calculated vesicle fraction (%) of each individual EV isolate sample is shown in the same diagram (orange line, right y-axis). The height of each bar relative to the left y-axis corresponds to the estimated concentration of vesicles or other membrane-bound bodies per mL of CCM, within the measurement interval (85-340nm). The height of each point indicates the relative percentage of nanoparticles in the sample determined to be vesicles.

When considering only the total vesicle yield (figure 12), ExoEasy gave the highest estimated number of vesicles, at 1.04E+08 vesicles/mL CCM. While none of the qEV fractions alone came close to this number, their combined contribution came out to be 9.18E+07 vesicles/ml CCM, and thus placing qEV at second best in this respect. Third was TEI at 8.75E+07 vesicles/mL CCM, followed by ExoQuick and UC respectively, with UC yielding the fewest overall vesicles by a wide margin.

Conversely, when considering the vesicle fraction (figure 12), The qEV7 EV isolation fraction was determined to be of the greatest purity, with 86.73% of all measured NP200 particles being vesicles and other membrane-bound bodies. TEI was conversely determined the least pure, at only 43,34% of particles estimated to be vesicles. ExoQuick appeared to yield the second purest vesicle fraction, at 73.3% vesicles. qEV fractions 8 and 9 were estimated to similar purities, with 56.56 and 59.48% vesicles respectively. Ultracentrifugation gave a marginally better purity than TEI, at 45,09%. This however has to be weighed up against the very significant difference in overall nanoparticle yield between the techniques.

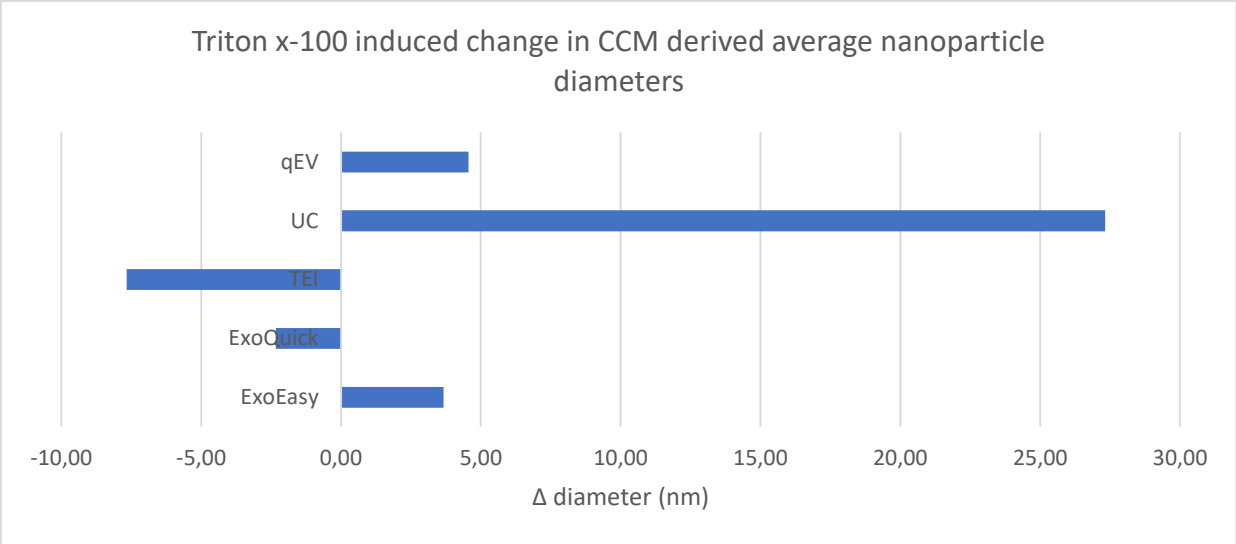

Figure 13: The Triton x-100 (0.1% v/v) induced change in mean particle diameter (nm) in the 85-340nm range. Change is calculated as diameter after treatment with Triton x-100, subtracted from diameter before treatment. Movement to the left in the figure indicates a measured overall decrease in nanoparticle diameter resulting from the treatment, whereas movement to the right signifies an increase in particle diameter.

The overall largest change in particle diameter was observed in the UC sample, with a large increase in mean particle diameter (figure 13). The UC EV isolate was also the one with the largest starting average particle diameter, indicating the dissolution of many small particles during the treatment. While qEV and ExoEasy experienced moderate increases in mean particle diameter, the TEI and ExoQuick samples displayed the opposite, with small to moderate reductions in nanoparticle diameters. A reduction would indicate that the particles dissolved by the treatment was of an on average larger diameter than the remaining ones.

3.2.3 Characterization of CD9 and CD63 protein levels in EV isolates

As a means of characterizing the isolated EVs, a bead-assisted flow cytometry (BAFC) assay was used to measure the levels of CD9 and CD63 proteins of each sample. These are proteins known to be enriched in exosomes, but are not unique to them (section 1.2.2.). For this assay, samples of ExoEasy, TEI, qEV7, qEV8, qEV9 and UC in two TR were adsorbed to latex beads (4µm diameter) and stained using a phycoerythrin (PE)-conjugated CD9 antibody or a allophycocyanin (APC)-conjugated antibody against CD63 (section 2.5.6). Results were quantitated based on relative interaction between EVs bound to latex beads and CD9 as well as CD63 antibodies. The interaction when stained resulted in a median fluorescence intensity (MFI) fold change, relative to a negative sample stained with isotype control. A greater fold change meant greater relative levels of the target protein in the sample.

In the BAFC assay for the presence of CD9, all qEV-fractions scored particularly well, with qEV9 displaying the largest measured MFI of any sample at 4,69 (figure 14). The second largest MFI was very closely contested between the ExoEasy sample and the qEV 8 fraction, with values of 3,06 and 2,97 respectively. The third highest detected MFI for CD9-antibody interaction, was the last qEV-fraction,

qEV7, at 2,19, handily exceeding the values measured for TEI, ExoQuick and UC (1.43, 1.33, 1.23 respectively).

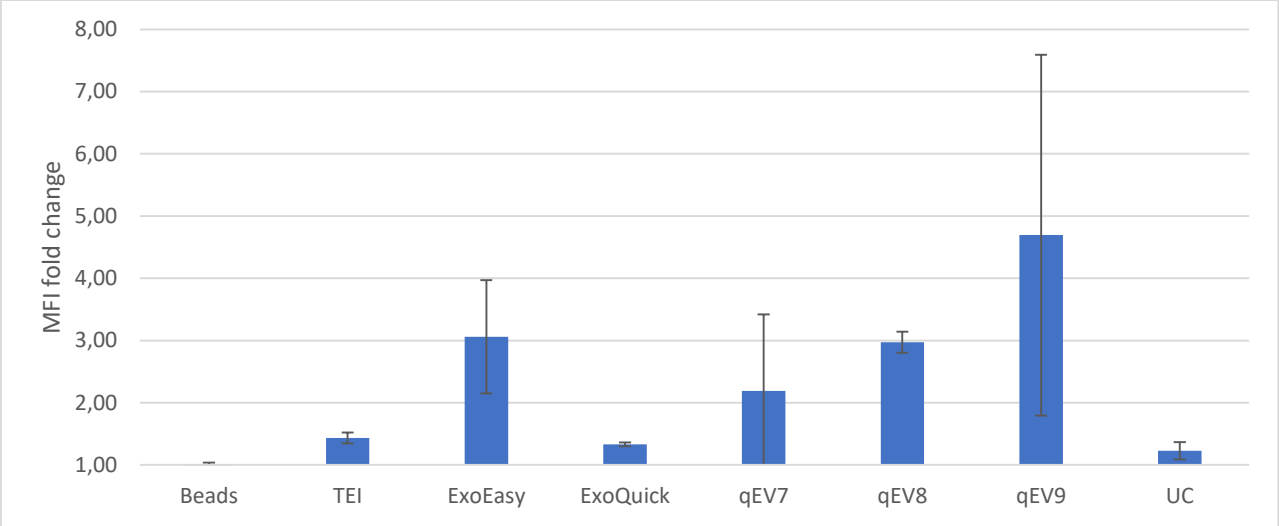

Figure 14: CD9 BAFC measured relative MFI fold change between EV isolate samples from CCM. The y-axis shows the relative MFI fold-change for each individual EV isolate sample.

Using the CD63 antibody and APC stain resulted in a much higher overall signal strength, yet with overall similar relationships between samples as detected using CD9 (figure 15). All qEV fractions gave clear MFI fold change values also in the case of CD63. In contrast to the CD9-based measurements however, ExoEasy provided the single highest MFI fold change in this case, at a value of 20,15. In second, third and fourth place came qEV 9 (18.95), qEV8 (10.76) and qEV7 (7.48) respectively. Notably, while TEI, ExoQuick and UC samples all gave very low MFI fold change results relative to the ExoEasy and qEV samples, the UC sample here in fact scored marginally higher than TEI and ExoQuick.

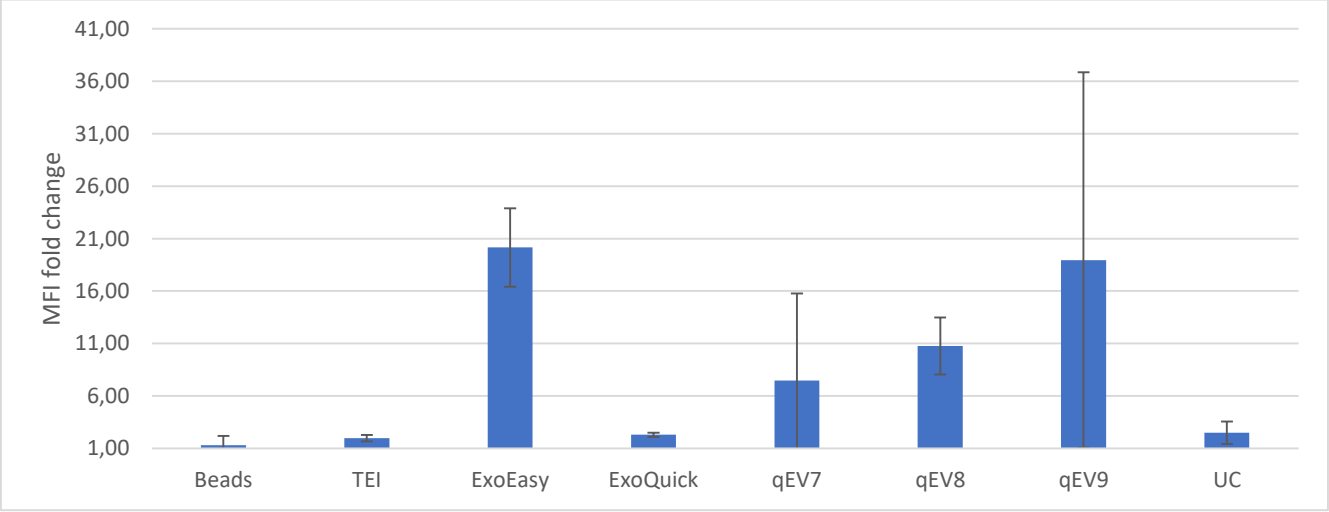

Figure 15: CD63 BAFC measured relative MFI fold change between EV isolate samples from CCM. The y-axis shows the relative MFI fold-change for each individual EV isolate sample.

3.2.4 Determination of isolated EV dsDNA content

Samples of ExoEasy, TEI, qEV7, qEV8, qEV9 and UC EV isolates (100µL) in two TR were treated with RQ1 DNase (Promega) prior to DNA isolation using the Allprep kit (Qiagen), and compared with DNA isolated from untreated samples. In this manner, the dsDNA concentration measured in the samples treated with DNase would represent the DNA internal to EVs (and therefore protected from the action of the enzyme) and the untreated samples represented the total DNA. After correcting fort starting volumes, the difference between the samples corresponded to the DNA which was exterior to EVs, and therefore vulnerable to the DNase treatment. All data were normalized to reflect the dsDNA content per mL of CCM used during EV isolation. For a breakdown of the calculations used in order to calculate the dsDNA/mL starting material see the appendix (section 7.1)

The data showed a clear trend of exome isolate treatment prior to DNA isolation resulting in a slight reduction in the measured dsDNA. The TEI EV isolation technique provided the highest measured levels of dsDNA with 45.36 ng/mL CCM. This constituted nearly double that of the second highest yielding technique, ExoEasy (Qiagen) with its 23.18 ng/mL CCM. When the yields of the qEV fractions were pooled, the total dsDNA/mL without DNase treatment was 12.43ng/mL, and the yield from the DNase treated samples 5,47ng/mL (figure 16)

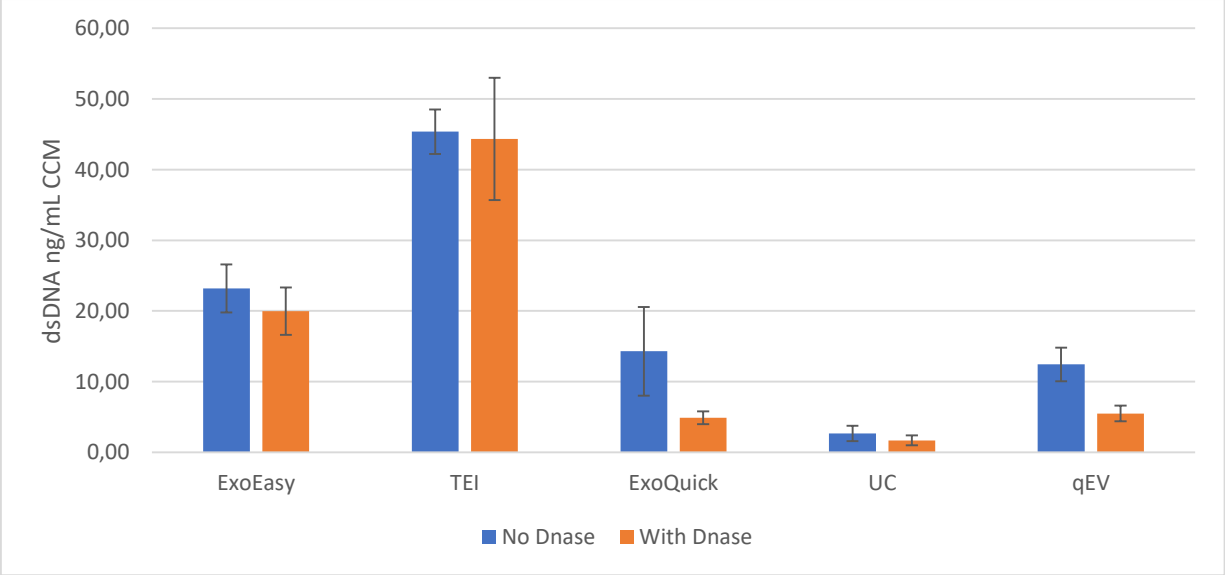

Figure 16: dsDNA /mL CCM by EV isolation technique, with and without DNase treatment. Non-DNase treated samples are shown in blue, whereas DNase treated samples are show in orange. qEV fractions have been pooled mathematically (see appendix, section 7.1). Error bars are based on the calculated standard deviation of the two technical replicates of each sample.

ExoQuick (SBI) proved to be the technique most greatly impacted by the DNase treatment, with a reduction in measured dsDNA by more than 34% from 14,29ng/mL in the untreated samples, and a mere 4,88 ng/mL in the treated sample. As such, the ExoQuick technique could be said to the lowest dsDNA yield internal to its isolated EVs with the exception only of UC. With the very lowest yield in dsDNA was the UC technique, with a calculated dsDNA/ml of only 2,65ng for the non-DNase treated sample, and 1,69ng for the DNase treated sample.

3.2.5 Comparison between measured dsDNA and nanoparticle concentrations

3.2.5.1 dsDNA per nanoparticle

The measured dsDNA concentrations for DNase treated EV isolates from CCM (section 3.2.4) were divided by the corresponding TRPS measured nanoparticle concentrations for the same samples. This resulted in a "dsDNA/nanoparticle" value, indicating what technique on aggregate isolated the EVs richest in dsDNA. The calculated numbers were multiplied by 1.0E+08 for a more intuitive scale (figure 17).

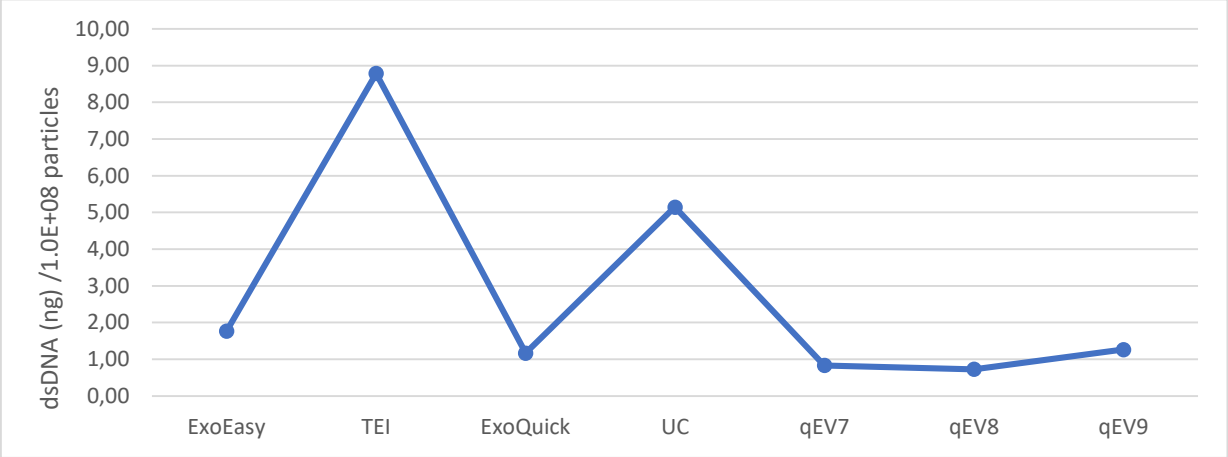

Figure 17: Calculated dsDNA (ng) per 1.0E+08 TRPS measured nanoparticle (50-200nm diameter) in EV isolates from CCM. dsDNA data is collected from EV isolate samples treated with DNase prior to DNA isolation using the Allprep kit (Qiagen).

The division of dsDNA per nanoparticle calculation (figure 17) illustrated how the TEI technique isolated the most dsDNA enriched EVs, relative to its total amount of isolated nanoparticles. In the qEV fractions, an upwards trend could be observed in the relative dsDNA content per nanoparticle as the qEV fraction number increases. Interestingly, the UC technique, despite a generally very low yield in bot isolated nanoparticles and dsDNA, in fact isolated more dsDNA/nanoparticle than did any other technique apart from TEI,

3.2.5.2 Correlation between 50-200nm diameter nanoparticles and dsDNA concentrations

Additionally, in an effort to estimate the correlation between increasing yields of nanoparticles and measured dsDNA, a scatterplot comparting the two was constructed (figure 18).

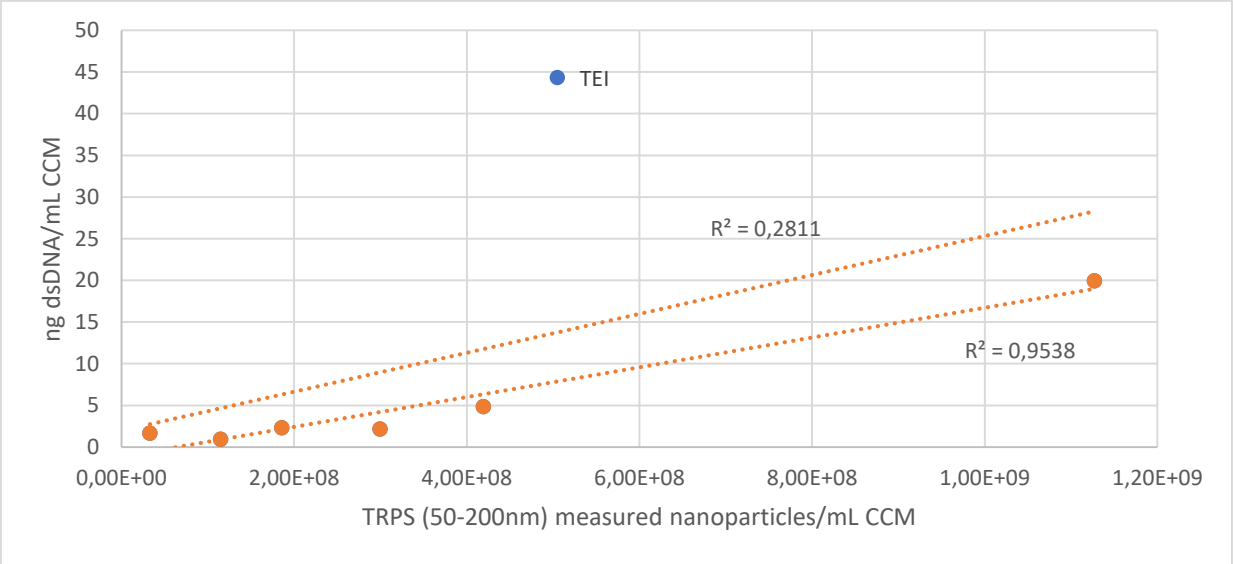

Figure 18: Correlation between TRPS measured nanoparticles (50-200nm) and dsDNA yield. The outlier (blue point) at approximately 45ng/mL dsDNA (y-axis) represents the TEI sample (marked "TEI"). When the outlier is included (top trend line) the R^2 of the trend (shown above the trend lines) becomes very low (0.2811). When the outlier is removed (bottom trend line) the R^2 value increases dramatically to 0,9538 (shown below the trend lines).

The plot for correlation between 50-200nm TRPS measured nanoparticle and dsDNA concentrations was at first observed to yield a fairly low R^2-value, due to an outlier data point with a drastically higher dsDNA concentration than would be expected based on the precedence set by the other samples. The outlier was determined to correspond to the TEI sample. By removing the TEI data point as an outlier, the fit of the trend line increased significantly, to an R^2- value of 0.9538.

3.2.5.3 Correlation between 85340nm diameter nanoparticles and dsDNA concentrations

In the same manner as done previously (figure 18), the 85-340nm diameter nanoparticle concentrations were plotted against the same dsDNA data as previously (section 3.2.5.2) in order to estimate the correlation (figure 19).

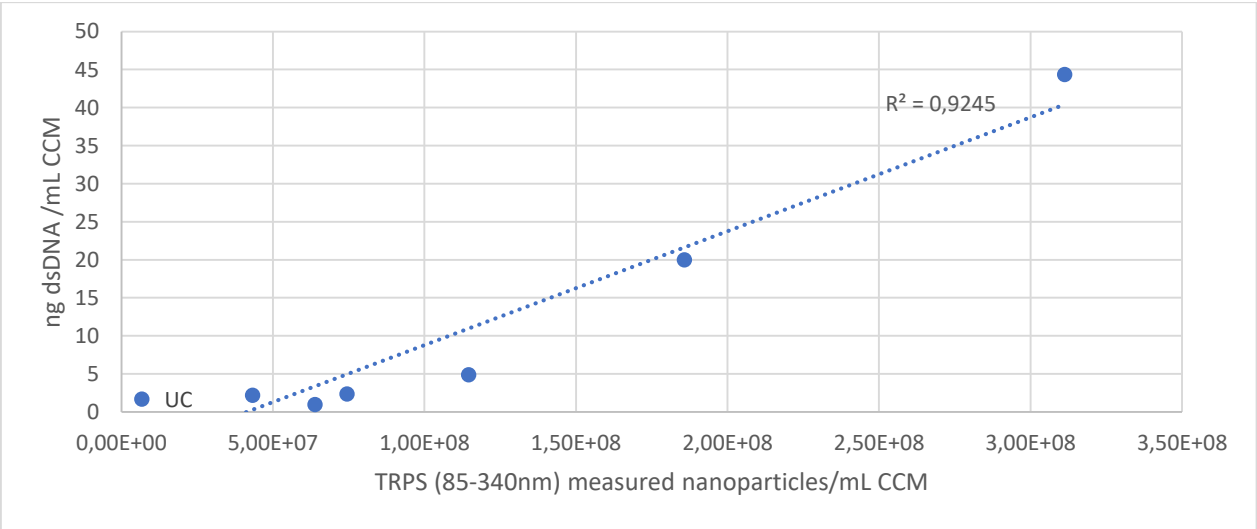

Figure 19: Correlation between the measured number of qNano Gold NP200 nanoparticles (85-340nm), and dsDNA yield. The R^2 value for the correlation is shown at the right-most ends of the trend line.

Interestingly, by plotting not the 50-200nm diameter particles against DNA concentrations, but choosing instead the 85-340nm size interval, a very well fitting trend line was immediately obtained (figure 19). In this case, TEI fit in on the trend collectively set by all samples, whereas the UC sample turned out to fit the least well into the established trend.

3.2.5.4 measured dsDNA concentration vs CD9 and CD63 content

Finally, a plot was constructed superimposing the measured dsDNA concentrations of each EV isolate sample from CCM with their corresponding measured CD9 and CD63 content (figure 20). The goal was to look for any trends between the two separate factors.

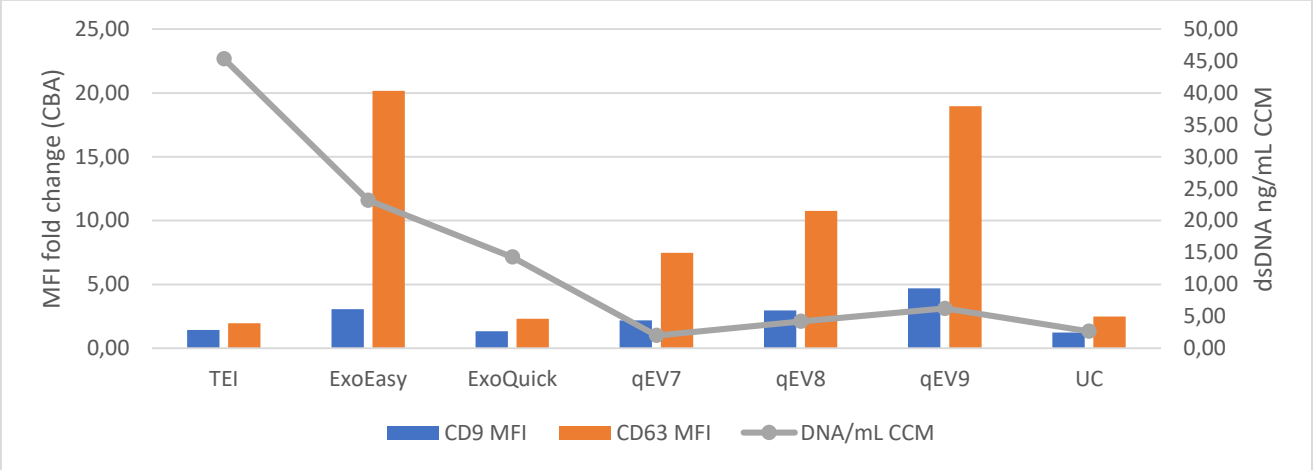

Figure 20: The BAFC measured MFI fold change (left y-axis) of CD9 (blue bars) and CD63 (orange bars) vs. the Qubit measured dsDNA (ng/mL CCM, right y-axis, grey line). Note that the line and bars use different absolute scales.

The comparison revealed a tendency of dsDNA concentration to increase as exosome marker protein increased in the ExoEasy and qEV samples. Notably, this trend did not hold true for either of the precipitation reactions (ExoQuick and TEI) which both showed disproportionately high dsDNA concentrations relative to their measured CD9 and CD63 content.

3.3 Comparison of EV isolation methods for plasma

After the initial phase of experiments using CCM as a raw material was completed, a second phase of plasma based tests were begun. Based on the data collected on all the EV isolation techniques during the initial testing phase, The ExoEasy, TEI and qEV techniques were deemed to show the most overall promise with regards to ability to isolate large quantities of vesicles, high dsDNA yields and EVs featuring exosome marker proteins (see discussion). ExoEasy, TEI and qEV were therefore selected for further testing using human plasma as starting material, in the search for the technique best suited for isolated tumour DNA.

Blood from 3 healthy control donors was used to isolate plasma (section 2.2.2) and each used to generate two EV isolation (2 TR) using each of the three EV isolation techniques. This constituted the control group, with a total of 3 BR each in two TR of each of the three isolation techniques. Similarly, plasma samples previously isolated from three PC patients were collected from storage (-80°C) and used for EV isolation. In the same manner as the control group, plasma from each PC patient donor was used to generate one EV isolation using each of the three selected EV isolation techniques. Due to the limited amount and valuable nature of the PC patient sample material however, no technical replicates were created in this case. This constituted the PC patient group, with a total of three BR for each EV isolation technique. As for samples using CCM as starting material, the plasma derived EV isolates were divided into aliquots before storage (-80°C) according to their planned downstream application.

One sample from the control group and one from the PC patient group were used for determination of the nanoparticle concentration and size distribution of each EV isolation technique (section 2.3.1). Additionally, control group samples (3BR x 2TR) and PC-patient group samples (3BR) were used to measure the concentration of exosomes achieved through each EV isolation technique by ExoCet Exosome quantitation assay (section 2.3.4). The same set of samples as were used for determination of the nanoparticle concentrations were additionally used for estimation of the relative fraction of vesicles in each sample through treatment with Triton x-100 (0.1% v/v) by TRPS (section 2.3.2). Control group samples (3BR x 2TR) and PC-patient group samples (3BR) were used determine the EV cargo dsDNA yield was using Qubit dsDNA assay (section 2.4.3). The remainder of DNA isolate from the PC patient group was used to determine the relative amount of KRAS mutated alleles in EVs isolated by each EV isolation technique (section 2.4.4). An overview of the general workflow of EV isolation from plasma is shown below (figure 21).

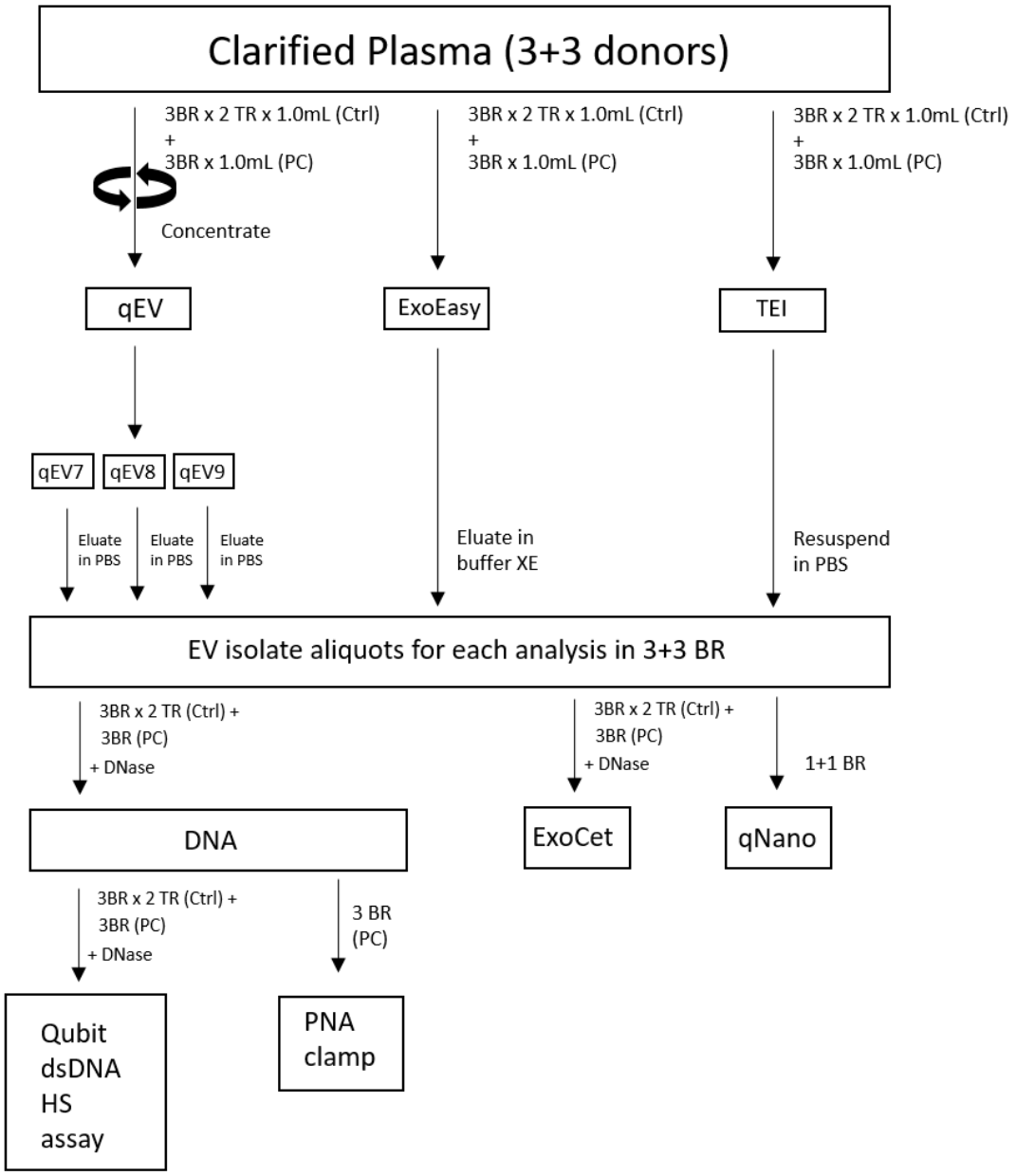

Figure 21: General workflow for EV isolate samples using plasma as starting material. 3 control group and 3 PC patient (3+3) donors contributed the plasma used for EV isolation. The paths between various stages (black boxes) in the process from starting material to EV analysis is indicated by the black arrows. Next to each arrow is additional information pertaining to the particular step in question. TR= Technical Replicate. BR = biological replicate.

3.3.1 Determination of particle concentration and size

Similarly, to what was done with EV isolates from CCM, Nanoparticle concentrations and diameters from EV isolate samples plasma were determined using the qNano Gold (IZON science). Measurement results were normalized to reflect nanoparticles/mL starting material during EV isolation (here, 1mL plasma), as described previously (section 3.2.1)

3.3.1.1 Nanoparticle concentrations

EV isolate samples from plasma (1TR) of one PC-patient and one control group donor was selected for measurement with the qNano Gold. The samples to be measured from each of the two donors was ExoEasy, TEI, qEV7, qEV8 and qEV9. As before, sample was measured at the manufacturer recommended three pressures. Each sample was measured using both NP100 and NP200 nanopores. Data was normalized to correspond to nanoparticles/mL plasma (as previously described) can be seen shown below (figure 22). A summary of the full collected data can be found in the appendix (Section 7.5)

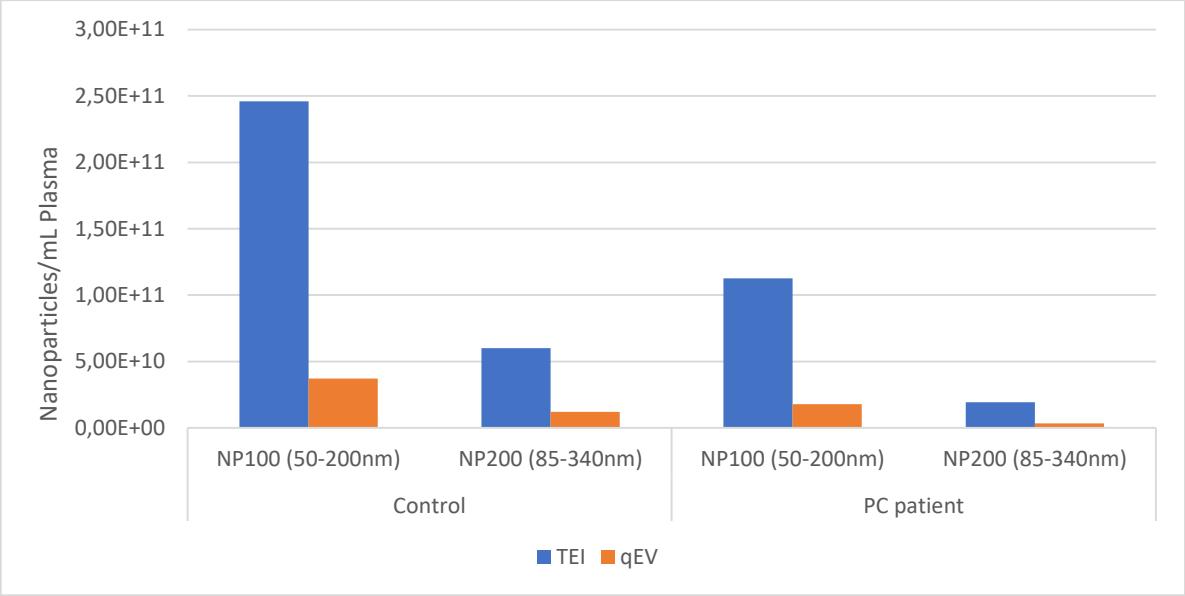

Figure 22: TEI and qEV (pooled) nanoparticles/mL plasma, measured using qNano Gold with nanopores NP100 (particle diameter 50-200nm) and NP200 (particle diameter 85-340nm). Control group measured concentrations can be seen to the left of the chart, and PC patient group measured concentrations to the right. ExoEasy concentrations are not included in the diagram in this case, due to low qNano Gold measurement quality of these samples.

During measurements however, it was discovered that no measurements could be made using the qNano Gold on samples of ExoEasy from plasma in all but two instances where poor quality measurements were obtained (see discussion). Various dilutions of the two separate ExoEasy samples ranging from a factor of 1:2 to 1:60 were attempted, as well as measuring using nanopores NP100, NP200 and NP250. While the exact reason for this apparent incompatibility is not known, some speculation may be done (discussion section 4.1.3). The only EV isolation techniques from plasma available for comparisons by TRPS were therefore TEI and qEV.

Interestingly measured nanoparticle concentrations were higher for the selected control group donor than for the PC patient samples. This was true for both NP100 and NP200 measurements of both TEI and qEV (figure 22). In the NP100 range for both donors, the TEI isolation technique proved to yield a much higher concentration of particles/mL, than did even the pooled qEV fractions. In this range (50-200nm particle diameter) the pooled qEV fractions nanoparticle yield for the control donor constituted only 15,1% of the corresponding TEI nanoparticle concentration. In the case of the PC patient samples, qEV similarly constituted only 15,8% of the corresponding TEI concentration in the same range. This trend was observable also in the NP200 range, although to a somewhat lesser extent.

3.3.1.2 Comparing EV isolates from plasma and CCM nanoparticle concentrations

The TRPS measured nanoparticle concentrations for TEI and qEV in the 50-200 and 85-340nm ranges were compared in order to assess the relative difference in isolated nanoparticles between the two starting materials (figure 23)

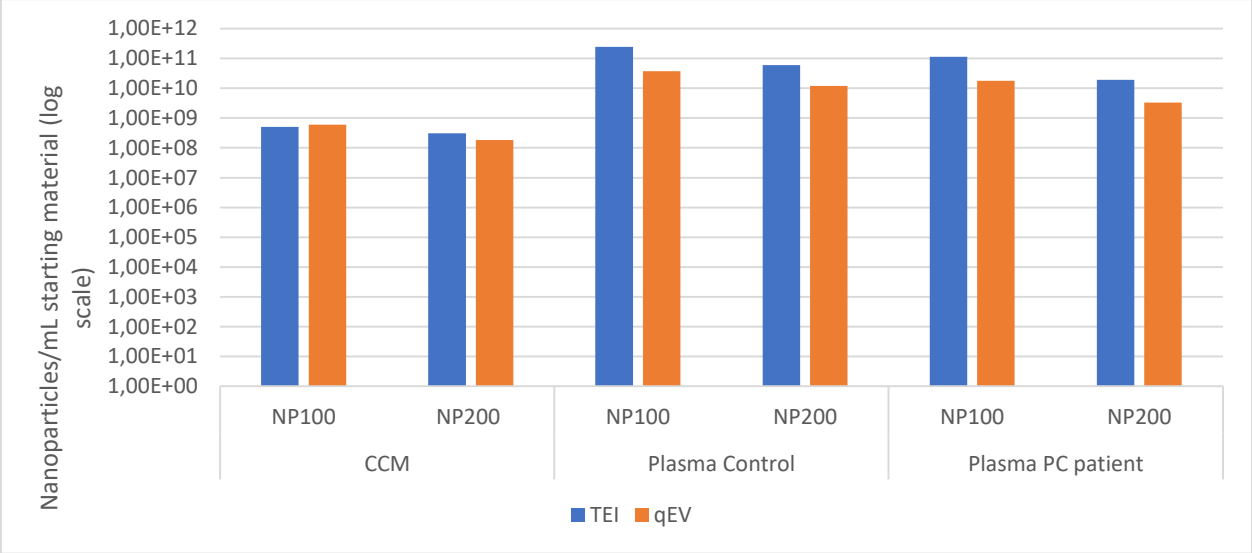

Figure 23: Comparison of TRPS measured nanoparticles/mL starting material (CCM/Plasma), from TEI and qEV EV isolation techniques. Blue bars represent TEI data, whereas orange bars represent qEV. Both NP100 and NP200 measured concentrations are shown. The y-axis is in logarithmic scale, due to the difference in concentration between CCM and plasma derived samples.

The comparison revealed that the plasma derived EV isolated had yielded up to several orders of magnitude more overall nanoparticles in both measured size intervals.

3.3.1.3 Nanoparticle size distributions

As with the EV isolates from CCM, the average nanoparticle diameters of isolates from plasma were determined. A plot giving an overview over their average size distribution was created (figure 24).

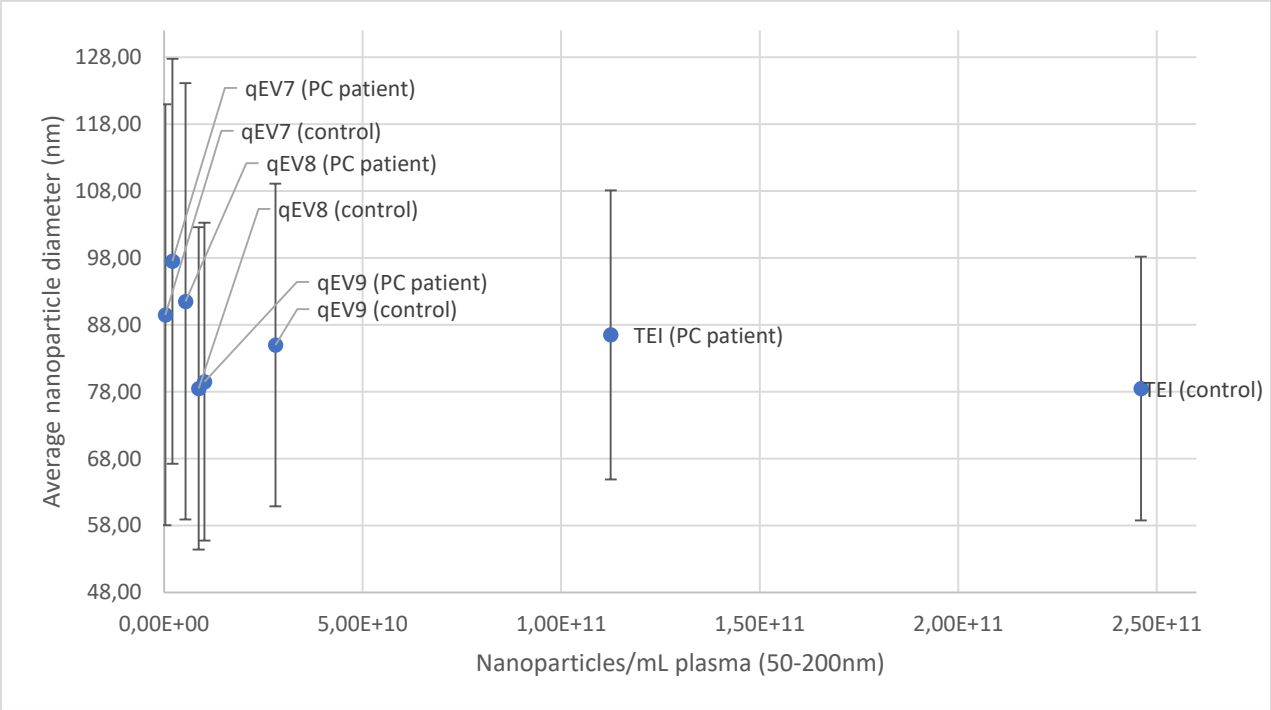

Figure 24: The average nanoparticle diameter calculated across all qNano Gold NP100 (50-200nm) measured particles from plasma. In the chart, movement to the right signifies increasing concentration, whereas movement upwards means increasing average particle diameter. Error bars on the y-axis are based on the standard deviation in average particle diameter reported by the qNano gold.

In the plasma derived EV samples, again a general trend of decreasing average particle diameter could be observed as qEV fraction number increased from qEV 7 to 9 (figure 24). This applied roughly for both PC patient and the plasma control samples, with the plasma control sample in general giving somewhat lesser averages than the PC patient donor isolates. The TEI technique gave averages on the low end of the overall distribution, but with much higher overall particle concentrations than the various qEV fractions.

CSDHs were constructed also for the EV isolate samples from plasma, and are displayed below (figures 25 and 26).

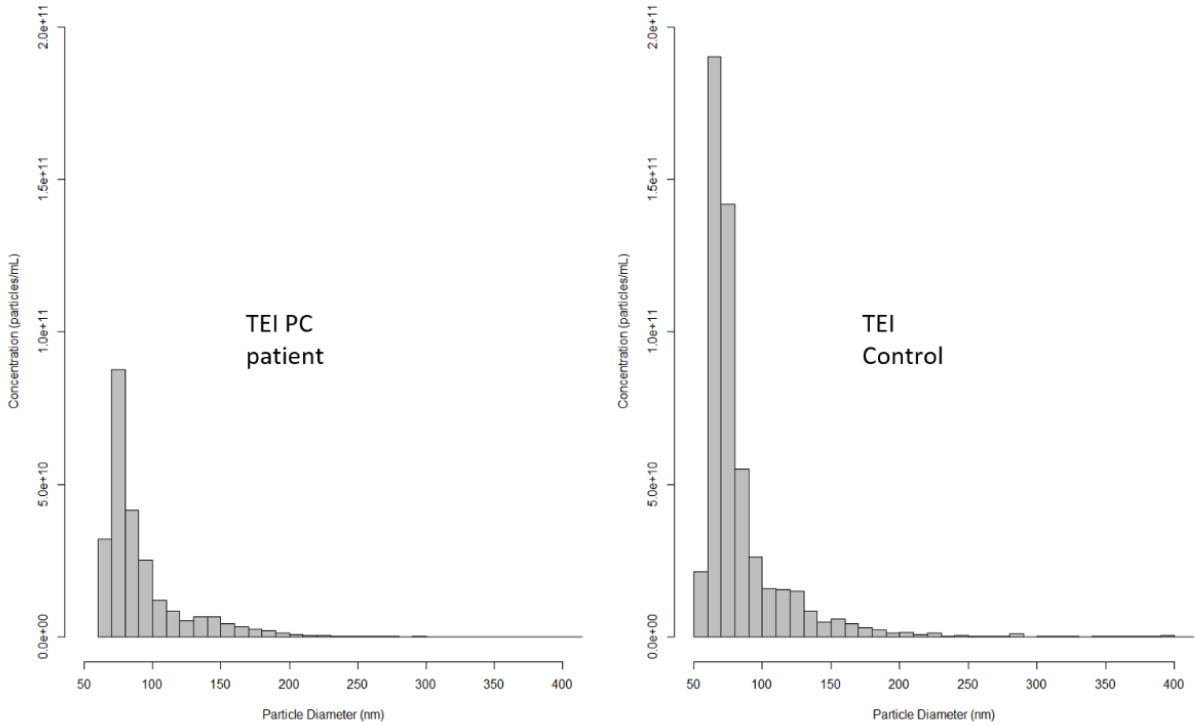

Figure 25: Combined Size Distribution Histograms (CSDH) for samples of TEI for the selected PC patient (to the left) and control (to the right) from plasma. Each bin spans 10nm in particle diameter. CSDHs are modelled based on size distribution data collected using the qNano Gold, and are a combination of data from nanopores NP100 (50-120nm) and NP200 (121nm+). The y-axis has for both histograms been set to 2.0E+11 particles/mL and the x-axis to 400nm

Overall, the CDSHs for the plasma samples showed a very narrow distribution, with no appreciable amount of nanoparticles beyond 300nm in diameter (see figure 25). The previously observed tendency towards smaller nanoparticles was even more pronounced in the plasma samples, with particle concentration peaking dramatically around 60nm in diameter, and rapidly declining so that only a minute fraction remains past 200nm in diameter. This was true for all qEV fractions (example figure 26) as well as for TEI. Additionally, the plasma samples peaked much higher in the y-axis than the corresponding CCM samples. All CSDHs from plasma can be found in the appendix section 7.5.3

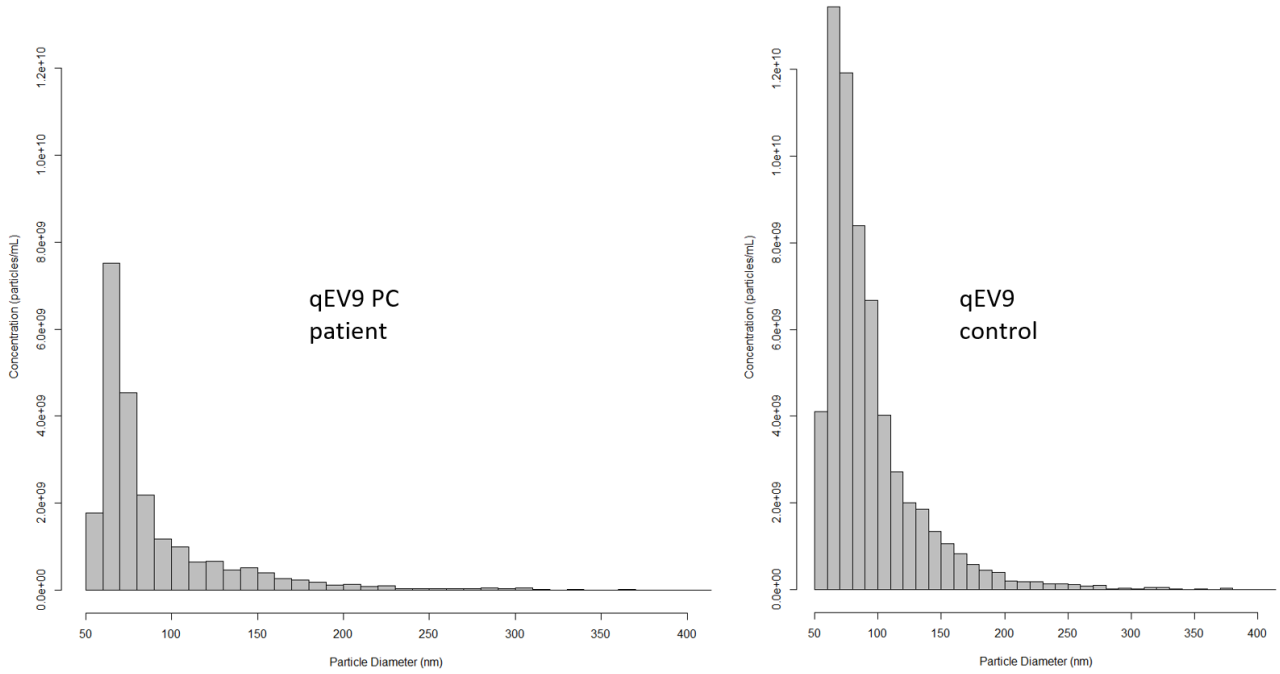

Figure 26: Combined Size Distribution Histograms (CSDH) for samples of qEV9 for the selected PC patient (to the left) and control (to the right) from plasma. Each bin spans 10nm in particle diameter. CSDHs are modelled based on size distribution data collected using the qNano Gold, and are a combination of data from nanopores NP100 (50-120nm) and NP200 (121nm+). The y-axis has for both histograms been set to 1.2E+10 particles/mL and the x-axis to 400nm

3.3.1.4 Comparative size distribution between CCM and Plasma derived EV isolates

A comparison was made between the CSDHs of qEV9 and TEI EV isolates from plasma and CCM (figure 27). The scale was set to be equal for all CSDHs, and set to have a low x-axis max value, so as to better illustrate the differences in large nanoparticles (200nm+).

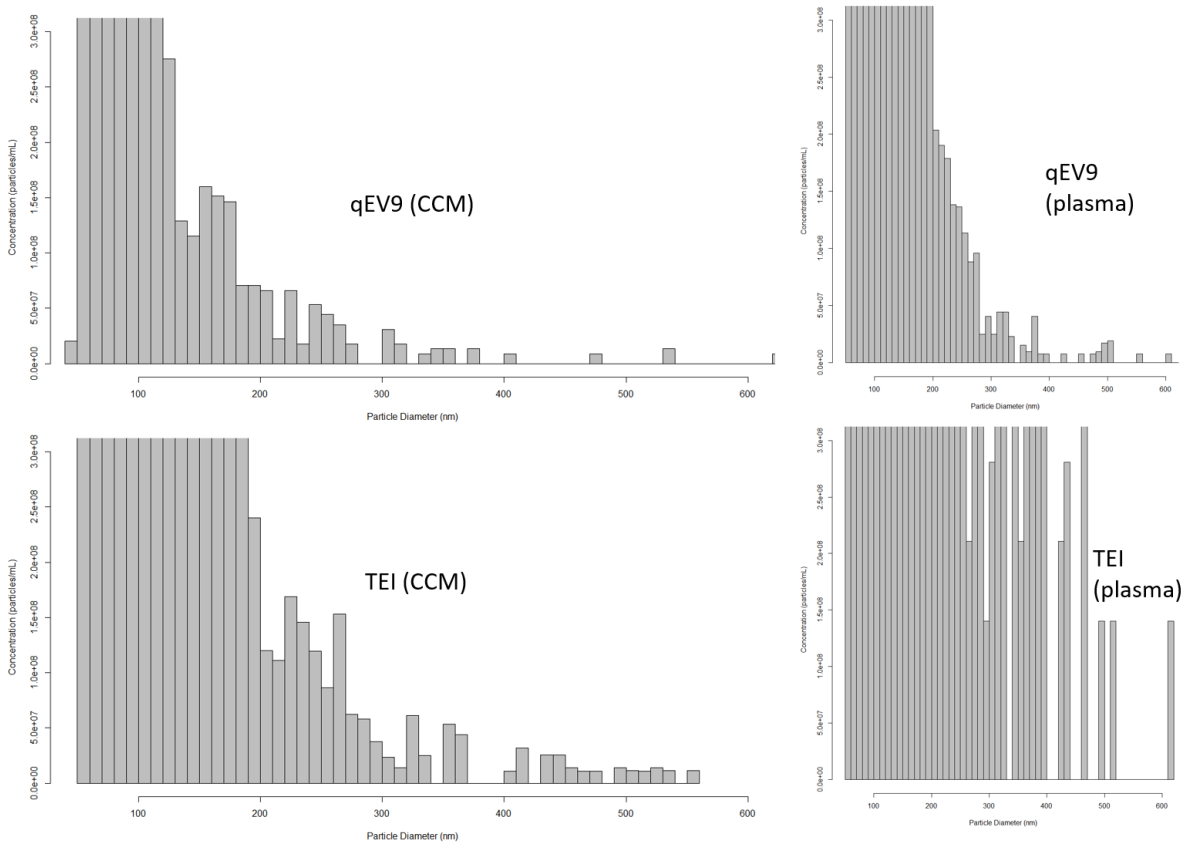

Figure 27: qEV9 and TEI from CCM (to the left) and from plasma (to the right) CDSHs set to the same scale for comparisons of large (>200nm) nanoparticles. While there are fewer large particles relative to small ones in the EV isolate sample from plasma, the absolute concentration of large particles is in fact greater. It appears to be a change in the relative fraction of small particles to larger ones which affects the average distributions.

The comparison showed that while overall the size distributions of EV isolate samples from plasma may appear sharp and highly focused, the plasma samples in fact have more overall nanoparticles of a diameter greater than 200nm, than do the corresponding EV isolates from CCM.

3.3.2 Estimation of vesicle fraction from plasma by sample treatment with Triton x-100

3.3.2.1 Vesicle fraction of plasma control group samples

In order to estimate the relative vesicle yield from each EV isolation technique, the samples of from plasma were measured with and without treatment with 0.1% triton x-100 (v/v). Samples of ExoEasy, TEI, qEV7, qEV8 and qEV9 were each measured in one biological replicate from one PC patient donor and one Control group donor in the manner described above (section 2.3.2). For EV isolates from blood plasma, 0.1% v/v Triton x-100 samples were measured using both NP100 and NP200 nanopores. As previously mentioned, no TRPS measurements of acceptable quality could be made of the ExoEasy samples from plasma. The vesicle fraction could only be estimated for TEI samples and qEV fractions. For a full list of measurements, see the appendix section 7.5.1.

For plasma derived EV isolates from the control group, the calculated change (Δ) in concentration following treatment with Triton x-100 (0,1% v/v), corresponding to the vesicle fraction, is illustrated in figure 28. The corresponding change in mean and mode particle diameters can be seen below (figure 29).

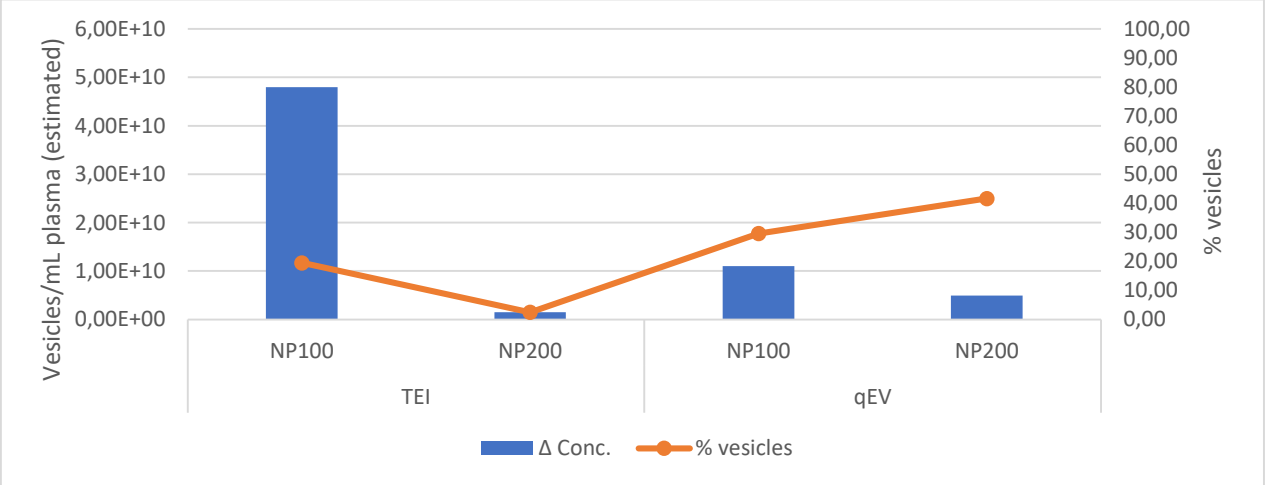

Figure 28: Vesicle concentrations in EV isolates from the plasma control group. Estimated by TRPS and sample treatment with Triton x-100. The height of each bar (left y-axis) corresponds to the estimated concentration of vesicles or other membrane-bound bodies within the measurement intervals. The orange line corresponds to the relative vesicle fraction (right y-axis) of each sample. ExoEasy concentrations are not included in the diagram in this case, due to low qNano Gold measurement quality of these samples.

In the case of the estimated overall vesicle purities for the same samples, a large drop was observed, compared to that of the corresponding samples from CCM. This was especially true in the NP100 range, where qEV proved to yield the overall greatest purity, with an average of 29.57% vesicles across all fractions (figure 28). In the same range, TEI, although only 19,51% vesicles by particles/mL plasma, still gave the overall highest total number of vesicles. This was with an overall concentration of 4,80E+10 vesicles/mL as opposed to qEV with a pooled fraction yield of 1,1E+10 vesicles/mL plasma. Interestingly, the roles appeared to be reversed in the NP200 range, where qEV yielded the overall greatest number of vesicles, with an average of 3.7E+09 vesicles/mL. This likely is due to a very low TEI

purity in the NP200 range, with only 2,5% of measured nanoparticles estimated to be vesicles. It should again be noted that the overall vesicle yield appears to be largest by far in the NP100 size range

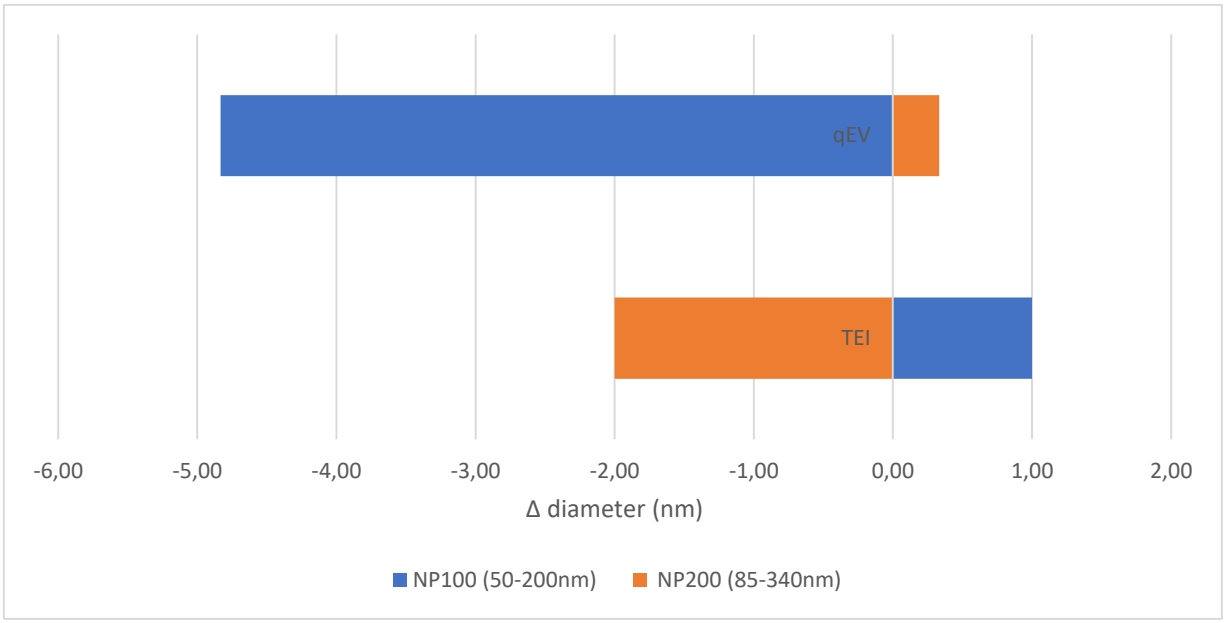

Figure 29: The measured change in mean particle diameter (nm) in the NP100 (50-200nm) and NP200 (85-340) range as a result of treatment with Triton x-100 (0,1%) in EV isolate sample from plasma (control donor). Change is calculated as diameter after treatment with Triton x-100, subtracted from diameter before treatment. Movement to the left in the figure indicates a measured overall decrease in nanoparticle diameter resulting from the treatment, whereas movement to the right signifies an increase in particle diameter

Following treatment with Triton x-100 (0.1% v/v) on the EV isolate samples from the plasma control group donor, the direction of the change contributed as measured by the two nanopores was opposite between the two techniques. For qEV, a large decrease in average nanoparticle diameter was registered using the NP100, indicating that in the 50-200nm range, larger more than small nanoparticles were dissolved by the treatment. Conversely, the opposite was true for the TEI technique, where the NP100 measured change was positive, indicating that more small nanoparticles than large were dissolved. Both TEI and qEV however displayed the greatest overall change in the direction of smaller nanoparticles after treatment.

3.3.2.2 Vesicle fraction of plasma PC-patient group samples

The vesicle fraction in the PC patient donor EV isolate sample was determined in the same way as described above. The resultant change (Δ) in concentration following treatment with Triton x-100 (0,1% v/v) can be seen below (figure 30), and the corresponding change in mean and mode particle diameters in figure 31. For a full list of all measured concentrations, see appendix section 7.5.1

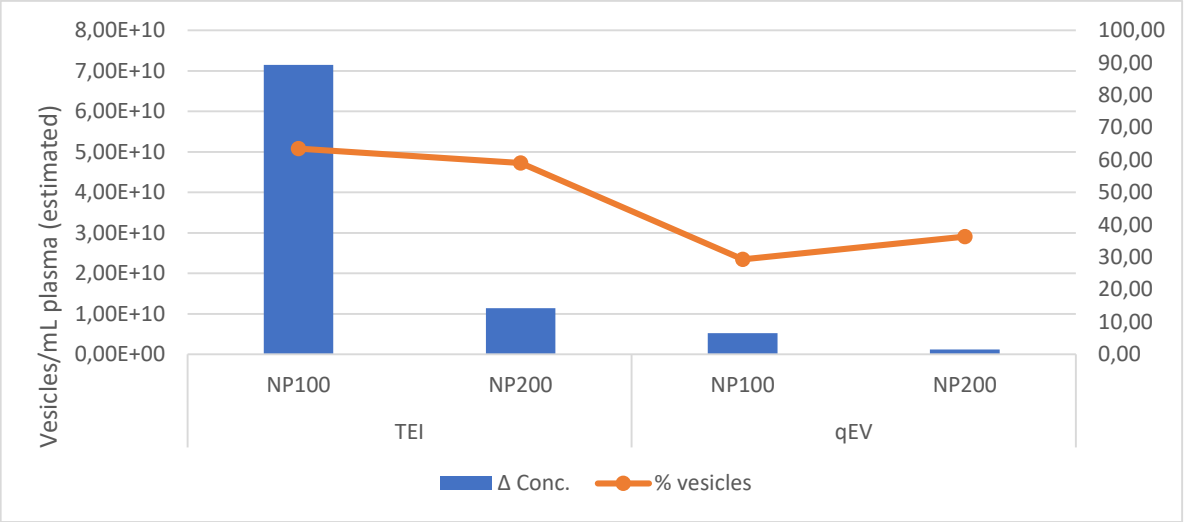

Figure 30: Vesicle concentrations in EV isolates from the plasma PC-patient group. Estimated by TRPS and sample treatment with Triton x-100. The height of each bar (left y-axis) corresponds to the estimated concentration of vesicles or other membrane-bound bodies within the measurement intervals. The orange line corresponds to the relative vesicle fraction (right y-axis) of each sample. ExoEasy concentrations are not included in the diagram in this case, due to low qNano Gold measurement quality of these samples.

With regards to overall vesicle yield, similar trends were observed in the PC patient plasma donor samples as were discovered in those of the control group donor. Much greater concentrations of vesicles were estimated in the NP100 range, than in the NP200 range. Also, in the NP100 range the overall yield of vesicles was much greater in the TEI sample than in the qEV samples. It should be noted however that the TEI estimated purity was much higher here, compared to the control donor, with 63,51% vesicles in the NP100 range, and very nearly that at 59,07% vesicles in the NP200 range. In this manner, the TEI sample vesicle purity came close to that of the purest qEV fraction, qEV 8, with its vesicle% of 61,76 in the NP100 range and 64,36 in the NP200 range. qEV fractions 7 and 9 gave in this case very low vesicle purities in the NP100 range (12,93% and 15,69%) but much higher purities in the NP200 range at 47.01% and 30.27% respectively. The EV isolate from PC-patient plasma vesicle fraction data can be seen illustrated below (figure 30).

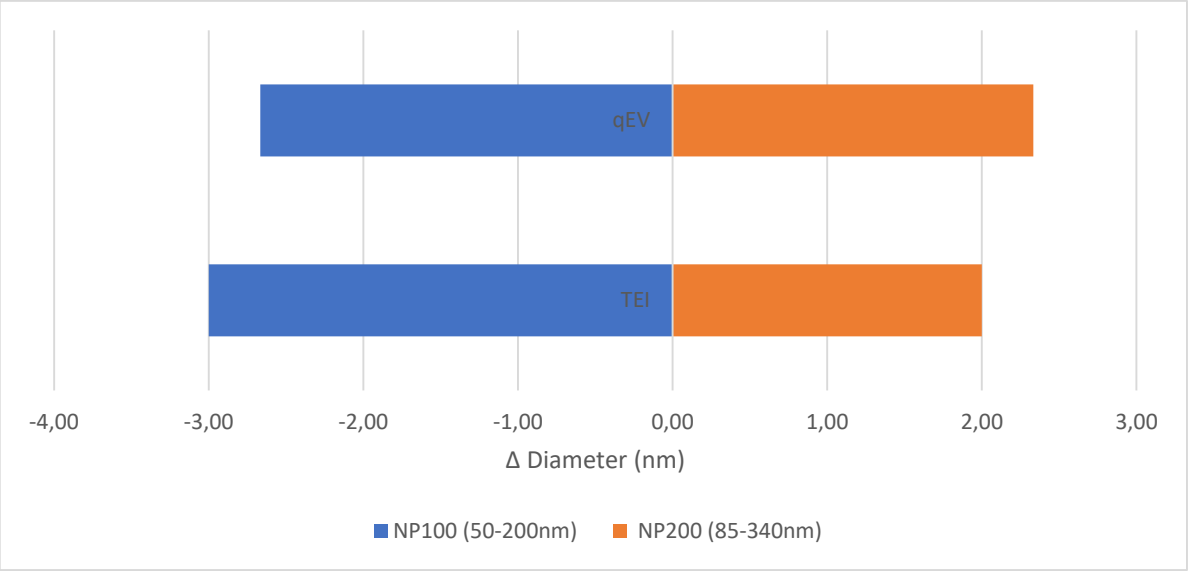

Figure 31: The measured change in mean particle diameter (nm) in the NP100 (50-200nm) and NP200 (85-340) range as a result of treatment with Triton x-100 (0,1%) in EV isolate sample from plasma (PC-patient donor). Change is calculated as diameter after treatment with Triton x-100, subtracted from diameter before treatment. Movement to the left in the figure indicates a measured overall decrease in nanoparticle diameter resulting from the treatment, whereas movement to the right signifies an increase in particle diameter.

Following treatment with triton x-100, a reduction in NP100 mean particle diameter could be observed in both qEV and TEI EV isolates from the PC-patient donor sample (figure 31). Additionally, they both displayed an almost equal increase in NP200 mean. This indicates that the dissolved nanoparticles for both techniques were small relative to the NP200 measured interval (85-340nm), yet large relative to the NP100 measured interval (50-200nm), indicating a size in between the two.

3.3.3 Determination of exosome concentration by enzymatic colorimetric assay

While TRPS allowed for measuring nanoparticle yields of each EV isolation method, it is cannot directly distinguish between for instance exosomes and other nanoparticles within the same size range. We also had challenges measuring the ExoEasy isolates from plasma by the TRPS method. The concentration of exosomes was therefore additionally measured using the ExoCet Exosome Quantitation assay (SBI). Here, samples (70µL) of ExoEasy, TEI, qEV 7, qEV8 and qEV9 from each of the three control group (2 TR) and PC group (1TR) donors were assayed based on their AChE enzyme contents; an enzyme known to be enriched in exosomes (section 1.3.2).

The ExoCet assay was performed on each sample as previously described (section 2.3.4). The average OD405nm for each incubation time was calculated based on the two technical replicates of each ExoCet standard dilution (blank subtracted). The qEV fractions were pooled by adding together the blank-corrected qEV values according to TR (see appendix 7.4) and standard curves constructed. It was determined that the dataset for 20 minutes of incubation provided the optimal relationship between curve linearity and noise. An illustration of the ExoCet standard curve used for the control group samples can be seen below (figure 32).

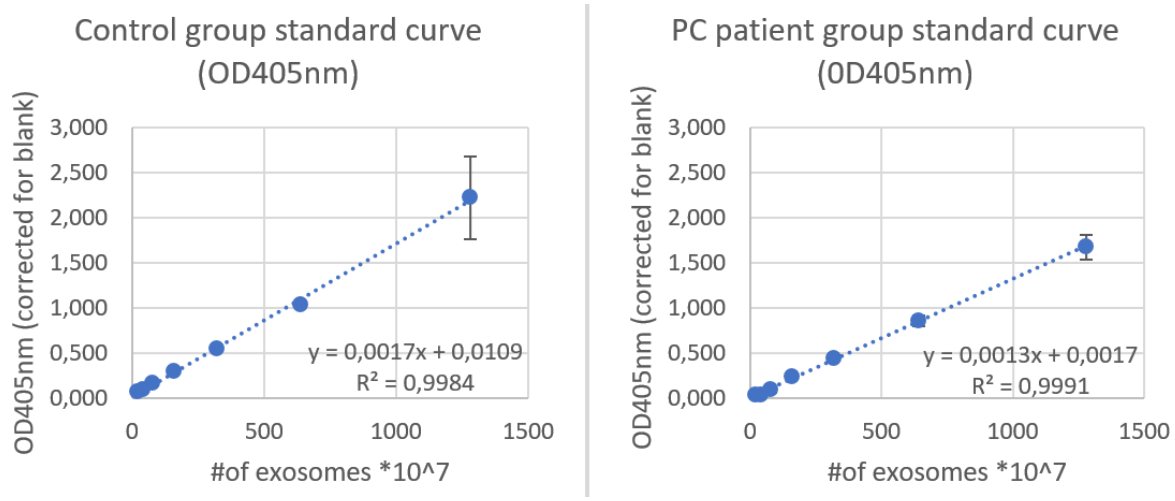

Figure 32: ExoCet standard curve for exosome isolate samples from plasma control group (to the left) and PC patient group (to the right). Each curve represents data collected after 20 minutes of incubation. The formula for each curve, along with its R^2 value is shown below and to the right of each curve. The y-axis in both cases signifies the optical density at 405nm (OD405nm), and the x-axis gives the corresponding number of exosomes divided by 1.0E+07.

Standard curves were subsequently used to calculate the number of exosomes present in each well, as instructed in the protocol provided by the manufacturer (SBI). Blanks were subtracted as described preciously (materials and methods). The average OD405nm and standard deviation for all technical and biological replicates (2BR x 2TR for control group samples, 2xTR only for PC patient group) for each sample was calculated, and the standard curve used to determine the corresponding number of exosomes. This value was in turn divided by the assay sample volume per well (0,025mL) in order to achieve the concentration (exosomes/mL) of the EV isolate sample. This value was multiplied with the total volume of each EV isolate sample (0,5mL) in order to get the ExoCet estimated exosomes/mL plasma (1mL plasma was used for each EV isolate sample).

The TEI sample yielded the overall highest measured concentration of exosomes, with an average Control Group concentration of 1.03E+12 exosomes/mL and a PC-patient average concentration of 8.17E+11. ExoEasy measured out to approximately half the concentrations of TEI for control- and PC patient groups, with 35.4% and 43.8% of the corresponding TEI yields respectively. On average, ExoEasy was estimated to 3.65E+11 exosomes/mL for the control group and 3.58E+11 for the PC patient group. The pooled qEV fraction measured the lowest yield, with only 2.00E+10 control group average, and 6.78E+10 PC-patient group average. The data can be seen visualized in a strip chart below (figure 33)

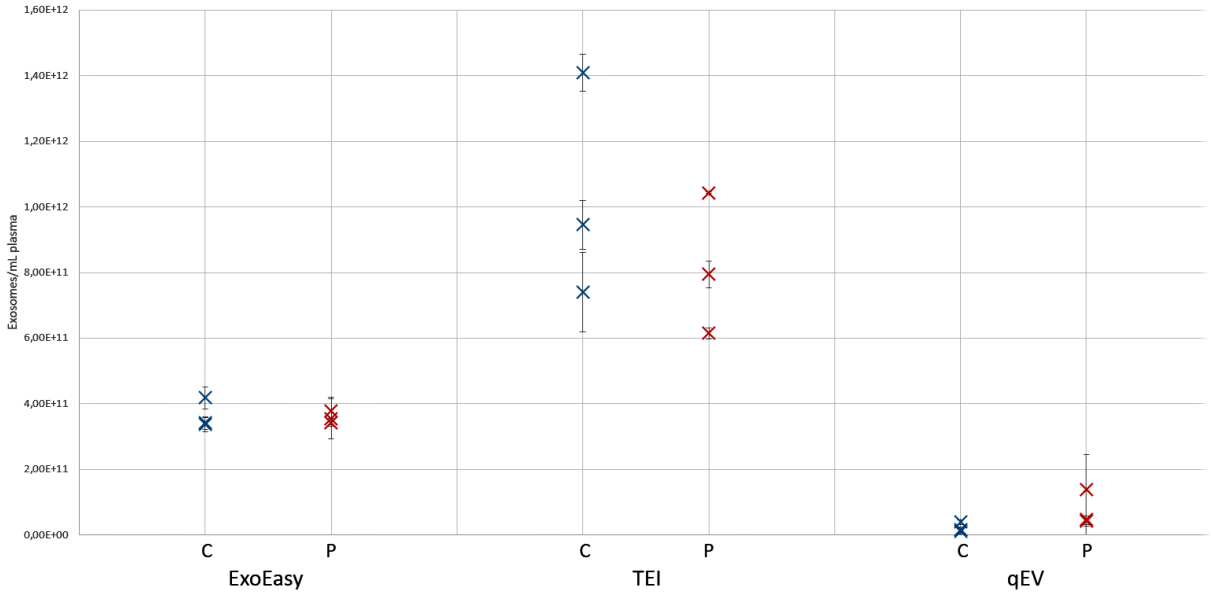

Figure 33: ExoCet measurements of EV samples from plasma. All samples are normalized to reflect exosomes per millilitre of plasma used during EV isolation. Measurements corresponding to the control group (C) are coloured blue, whereas those corresponding to the PC patient group (P) are coloured red. Error bars are constituted by the calculated exosome /mL standard deviation between technical replicates of each individual biological replicate.

Use of the designed specialized blanks resulted in a reduction in estimated exosome concentration of only 15,63% for ExoEasy and 14,88% for ExoEasy. The qEV samples, already close to the assay LOD, was further weakened by more replicates being pushed into the negative section of the standard curve equation. It was determined that the specialized blank results did not offer any benefit over the regular blank (discussion section 4.4.5).

3.3.4 Determination of DNA concentrations in EV isolates

3.3.4.1 concentrations of dsDNA in EV isolate samples from plasma

The overall EV dsDNA cargo was isolated from EVs obtained using ExoEasy, TEI, qEV7, qEV8 and qEV9 on plasma as starting material. A set of EV isolate sample aliquots (100µL) from plasma in two TR from each of the control group blood donors were treated with DNase (see materials and methods) in order to eliminate any extravesicular DNA, and used for isolation of DNA (QiaAmp circulating nucleic acid kit, Qiagen). The same procedure was carried out for a set of EV isolate samples (1 TR) for each of the three PC patient donors. A volume of each resultant DNA isolate sample (100µL) was then used in the Qubit dsDNA assay, and dsDNA/mL CCM was calculated (appendix section 7.1.) The final dsDNA concentration value for each was achieved by taking the average of the three biological replicates of each group (Control group, PC-patient group).

In order to avoid cumulative error from addition of uncertainties, qEV fractions were in this case not pooled. An estimation of the pooled qEV data can however be found in the appendix (section 7.2). A full list of all measured dsDNA by donor can be found in the appendix (section 7.2.2).

As with the CCM derived dsDNA concentration data, TEI proved to be the technique with the overall greatest concentration of dsDNA/mL starting material, with 2.38ng/mL plasma on average in the control group, and 4,21ng/mL in the PC patient group. The qEV fractions for both groups measured as achieving the second third and fourth greatest average dsDNA concentration, with concentrations of 1.67 ng/mL, 1.73 ng/mL and 1.98 ng/mL average in the control group and 1.87 ng/mL, 1.34 ng/mL and 1.40 ng/mL plasma in the PC patient group for qEV 7,8 and 9 respectively. The lowest dsDNA yield was in both groups estimated in the ExoEasy derived samples, with only 1.61ng/mL plasma average in the control group, and 1.16 in the PC patient group (figure 34).

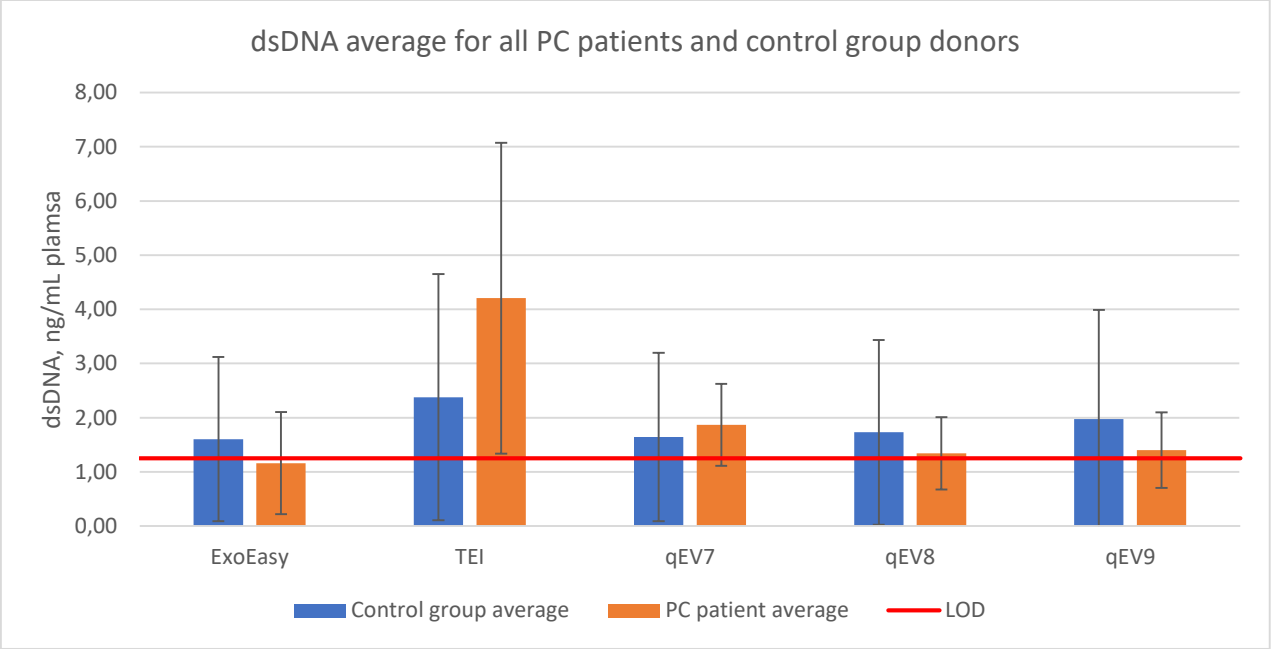

Figure 34: dsDNA /mL plasma from by EV isolation technique, control group average (blue bars) vs. PC patient group average (orange bars). Error bars based on the standard deviation on all actual and estimated dsDNA concentration. Assay corrected limit of detection (LOD) is denoted by the horizontal red line. All EV isolate samples were treated with DNase prior to DNA isolation.

3.3.4.2 correlation between measured dsDNA and corresponding ExoCet measured exosome concentrations in EV isolates from plasma

A scatter plot was created assessing the correlation between ExoCet measured exosome concentrations in EV isolates from plasma and the corresponding dsDNA measurements from the same EV isolate samples (figure 35)

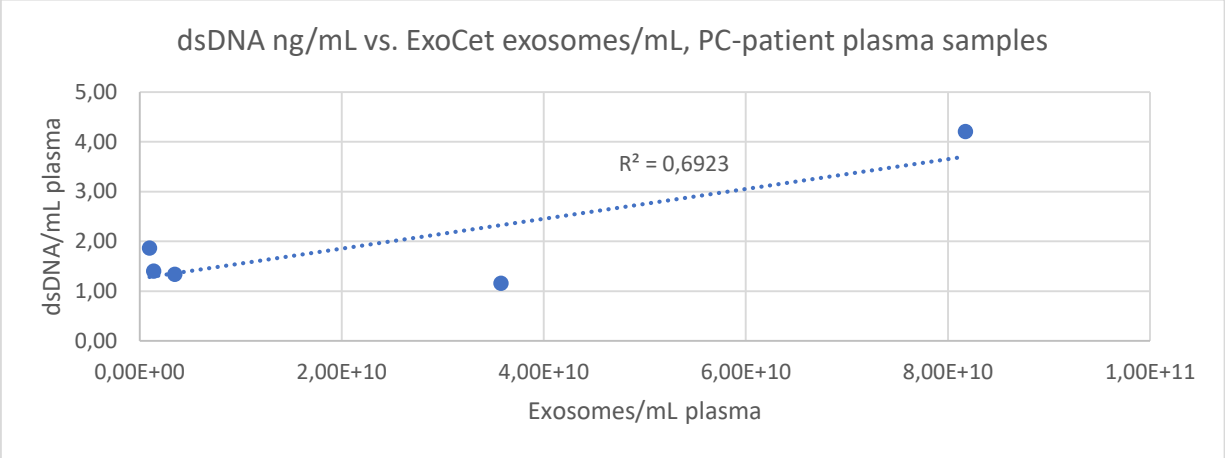

Figure 35: Correlation between the ExoCet Exosome Quantitation Assay estimated exosome concentration (exos/mL plasma), and the corresponding dsDNA ng/mL plasma isolated from the same sample. The R^2 value for the correlation is shown above trend line.

The plot revealed a modest correlation between dsDNA and exosome concentrations, somewhat marred by the clumping of the qEV fraction in the bottom of the chart. The R^2-value for the trend line was 0.69.

3.3.5 Measuring relative tumour DNA concentration in EV isolates from plasma

As discussed in the introduction of this thesis (section 1.2), the reports of EVs containing tumour DNA are becoming steadily more frequent. In order to ascertain the efficacy of each EV isolation technique, it was therefore interesting to measure to what extent DNA isolated from each EV isolation in fact included tumour DNA, as opposed to WT. PNAs are oligonucleotides where the sugar-phosphate backbone has been entirely replaced by protein, and so are not extendable by DNA polymerase [64]. In brief, a PNA oligomer perfectly homologous to wild type (WT) KRAS was added in with the sample DNA a PCR assay. PNA binds well to perfectly homologous sequences, forming a DNA-PNA duplex, but is very sensitive to mismatching bases and is significantly destabilized by even a single base mismatch [65]. This results in the suppression of WT alleles and the selective amplification of mutated alleles in a PNA containing PCR assay. By running parallel real-time PCR (qPCR) sample with and without added PNA, the presence and relative amount of KRAS mutated alleles in the sample can be calculated [64].

EV isolate samples (25µL total volume) from the DNase treated EV isolates of each of the three PC-patient donors were divided into two TRs with PNA (supressing WT alleles) and without PNA (total DNA), and assayed for KRAS mutated allele DNA. The melting temperature Tm of the various PCR products were used to verify that they were a target sequence, and non-target sequence ΔΔCt results were eliminated. In the assay, KRAS mutations were detected in EV isolate samples of all PC-donors,

and at least one positive find in by each EV isolation technique. On average going by Cq values alone, the amount of tumour DNA detected in each EV isolation technique (absolute, not relative to WT) was the same, except for qEV7 in which the average was slightly lower. This reflects the fact that there is a very low total concentration of DNA molecules loaded into the assay, and it is therefore reasonable that the effects of stochastic selection of individual DNA molecules play a major role in determining the absolute Cq values. Because of this statistical weakness, it is likely better to rely on the concentration measurements from Qubit, where relatively more DNA was loaded into each reaction. For a full breakdown of Cq values and results from the PNA-clamp assay, see the appendix (section 7.2.3)

The calculated ΔΔCq values, which are relative to the concentrations of DNA internally within each sample, can however be used to give an idea of the relative purity of KRAS mutated alleles in each sample, when compared to WT (figure 36).

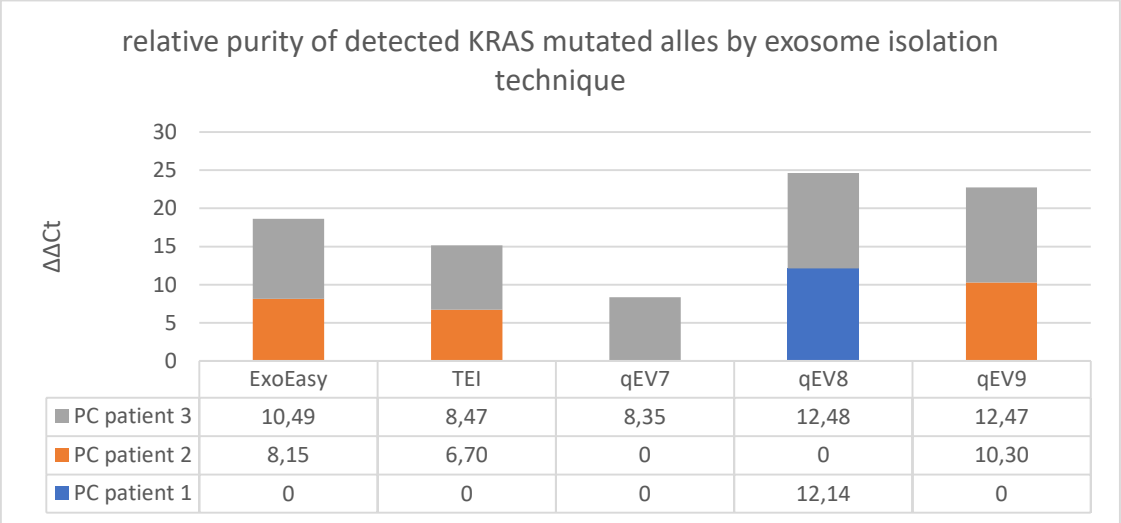

	ExoEasy	TEI	qEV7	qEV8	qEV9
PC patient 3	10,49	8,47	8,35	12,48	12,47
PC patient 2	8,15	6,70	0	0	10,30
PC patient 1	0	0	0	12,14	0

Figure 36: Relative purity of KRAS mutated alleles detected in samples of each EV isolation technique. The ΔΔCq contribution of each KRAS positive sample has been stacked according to the technique in which it was measured. The overall height of each bar is representative of the quantity of KRAS mutated DNA fragments relative to WT detected in EV isolates from the corresponding technique. The individual contributions of samples from a given PC-patient to the total ΔΔCq of each EV isolation technique is given by the key at the bottom left of the figure, and the corresponding ΔΔCq values of each sample in the table to the right of the key. A "0" in the table signifies that no KRAS mutation was detected in the sample.

In the PNA-clamp KRAS assay, again each individual qEV fraction performed as well or better than the TEI and ExoEasy techniques with regards to relative amount of tumour DNA in the sample. This was to some extent with the exception of the qEV7 fraction which apparent performance was somewhat lower than that of the others. In overall quantity of KRAS mutated alleles, the qEV technique as a whole thus proved to extract by far the greatest purity of KRAS mutated alleles. The ExoEasy and TEI techniques performed comparably, although ExoEasy gave a slightly higher overall yield compared to TEI.

4. DISCUSSION

4.1 Brief overview

4.1.0 Criteria for evaluation of techniques

When comparing the EV isolation techniques, there are several aspects of each technique which has to be considered. The goal of an isolation technique is to select for target particles, while discarding non-target particles and contaminants. The amount of particles isolated and their sizes however give only a rough estimate of the efficacy of a given technique, as it cannot discriminate between biologically active EVs and co-isolated biomolecules. Lipoproteins and protein may be found in the target size-range, yet have none of the desired properties of EVs (section 1.2.2) By also treating TRPS samples with a detergent such as Triton x-100, an estimation can be made of the relative amount of vesicles found in each sample, which may give a better idea of the actual amount of EVs present [58]. While exosomes and other EVs are often selected for based primarily by size, their most clinically relevant definition is that of biogenesis, and is tested for by the detection of exosome marker proteins such as the tetraspanins CD9 and CD63 [10]. The next step in assessing sample quality is validation of the actual yield of EVs from each technique therefore relies on the detection of such proteins, as identifying them allows for increased confidence that EVs isolated by a given isolation technique in fact are likely to have the wanted properties as a potential biomarker for cancer. Third is the investigation of DNA cargo found in the EVs isolated in each technique, including measured dsDNA concentrations. In principle, greater DNA recovery by a given EV isolation technique would indicate greater potential prognostic value, as less of any DNA present in a sample would be lost. This however only holds true in the case that said DNA hold a relatively high fraction of tumour DNA, as the selective nature of EV cargo is one of their main features over for instance direct recovery of cell free DNA from plasma. Finally, all these aspects of each EV isolation technique has to be evaluated up against the effort involved in the EV isolation process itself. Due to these many drawbacks of traditional EV isolation through ultracentrifugation coupled with the limitations placed on the possible number of parallel samples by the design of UC-rotors, there is a general consensus that differential centrifugation is not likely to ever been part of a clinical analysis pipeline [66, 67]. The time and effort efficiency of a given EV isolation technique is therefore also an important criterion for evaluation.

4.1.2 Brief summary of findings

The main goal of the project was to evaluate the efficacy of the various EV isolation techniques on human liquid biopsy samples, with the goal of investigating the isolated EVs for potential future use in diagnostics. As high concentrations of EVs were desirable, it was elected to use plasma for this testing, as opposed to other bio fluids (see introduction). By including EV isolate samples from patient of late stage pancreatic cancer, the efficacy of a given technique with regards to isolating EVs with tumour DNA cargo could be estimated. It was however decided that before testing with valuable PC patient samples, the scope of the testing should be narrowed by the elimination of the two least promising EV isolation techniques. This was done using CCM from PANC-1 cells as a stepping stone, and allowed us to get a general idea of the efficacy of each isolation technique.

In general, it was discovered that the ExoEasy, TEI and qEV techniques gave the highest overall nanoparticle and vesicle yields, in measurements using TRPS (figure 6). Additionally, while not a part

of the overall technique comparisons of this thesis, ExoCet Exosome quantitation assay tests were performed on a set of samples from CCM (appendix 7.4 figure 16) showing significant Acetylcholine esterase activity only in samples of TEI and ExoEasy. The same was observed with regards to concentration of dsDNA cargo, UC and ExoQuick again being outperformed by the three above mentioned techniques. In the end it was concluded that ExoQuick and UC did not compete well, and should therefore be eliminated before moving forward with the next phase of the project, in which plasma would be used as starting material for EV isolation.

In samples from plasma qEV resulted in relatively low overall nanoparticle yields compared to the very high TEI concentrations (figure 22). This trend was observed also in the Exosome Quantitation assay, where also ExoEasy appeared to have an overall greater exosome recovery. In overall dsDNA content the TEI technique provided by far the greatest yields (figure 34), yet the PNA clamp assay for KRAS mutations indicated that qEV had a much higher fraction of tumour DNA (figure 36). ExoEasy meanwhile performed reliably yet unexceptionally, never giving the best results of the three, but also rarely performing the worst.

4.1.3 TRPS and the general distribution of isolated nanoparticles

For exosome quantitation, the target window for analysis was the generally accepted window of 50-150nm in which exosomes are known to fall [22]. It was however also interesting to measure the particles of greater diameter than 150nm, as a way to further investigate in the overall distribution of concentrations by particle diameter of the various EV isolation techniques.

The NP100 nanopore can be tuned to measure particles of a minimum diameter range of 50-200nm, thus effectively covering all defined potential exosome diameters. Initial testing however quickly revealed that the vast majority of nanoparticles from all EV isolation techniques was found at the low end of the spectrum, increasing in concentrations as particle diameters approach 50nm. This principle appeared to be valid for all the tested EV isolation techniques for both CCM and plasma. To underscore the significance of this difference, take for instance the measured NP100 and NP200 concentrations of EV isolates from CCM (results, figure 6). As was done in all cases, the NP200 was tuned to a sensitivity range of 85-340nm; the lowest diameter window possible for this nanopore. The NP100 was similarly tuned so as to be sensitive in its lowest possible range, between 50-200nm. The part of the sensitivity window of the NP100 nanopore not also covered by the NP200 thus consists of only the range of particles with diameters between 50-85nm. As illustrated in the figure, the measured NP100 ExoEasy concentration of samples from CCM was 1,13E+09 particles/mL. The corresponding NP200 measurement average of the same samples was of only 1,86E+08 particles/mL, far less than the NP100 measurement, the former constituting more than a six-fold increase in concentration over the latter. This is despite the overlap between pores in the 50-200nm measurement window being an entire 76.67%. As such, more than 83,54% of all measured nanoparticles were in this example found in the small range of 35nm, found in the non-overlapping section between the two nanopores in the range from 50-85nm. This general trend was the observed in all qNano measurements, and can be seen reflected in a more qualitative fashion in the generated CSDHs (results, figures 8,9,25 and 26). Because of this observation, it was decided to include NP200 data also wherever general trends in diameters were to be discussed, as the powerful shift in overall nanoparticles towards the low-end is so significant that particles measured by the two different nanopores often are affected very differently by for instance treatment with a detergent such as Triton x-100 (results, figures 29 and 31).

Additionally, it should be noted that the NP100 is unable to detect particles smaller than 50nm in diameter, and as such a very large amount of particles may be found just below the 50nm threshold. As size decreases below 50nm in diameter however, the likelihood of course increases of any given particle being a protein aggregate or other non-vesicular biomolecule, which, presuming their co-isolation with EV's by the EV isolation techniques, helps in explaining why the overall nanoparticle concentration increases with decreasing particle diameter

All EV isolation techniques were evaluated using the qNano Gold TRPS analysis on EV isolate samples from CCM. It was discovered under measurements however, that due to an apparent incompatibility with the qNano Gold instrument, no measurements of acceptable quality could be obtained of samples of ExoEasy from plasma. Various dilutions of ExoEasy EV isolate were attempted, as well as attempts of measuring using several nanopores of sizes. All attempts failed to provide measurements of acceptable quality. In general, at medium to low dilutions using NP100, the measurement current was observed to skyrocket as pressure was applied in the instrument (essential for calculating concentrations), and measurement stability was immediately lost. At very high dilutions, the current did not trace as expected, and no definitive nanoparticles could be detected. Similarly, using larger nanopores (up to and including NP250), the current trace behaved in an unstable manner, and no definitive nanoparticles could be detected at any dilution. None of the ExoEasy samples from CCM nor any of the other samples from plasma suffered from these issues, indicating that there in fact was some sort of compatibility issue with the plasma derived ExoEasy EV isolates and the qNano Gold instrument. There is reason to believe that the plasma derived samples in general contain several orders of magnitude more very small (<50nm) nanoparticles, than CCM derived samples. One hypothesis for the apparent incompatibility, could be that these nanoparticles just below the measurement interval of the NP100 nanopore is related to the skyrocketing measurement current, and loss of stability. However, this cannot be confirmed definitively.

4.2 EV isolation techniques, practical execution

4.2.1 Differential centrifugation with ultracentrifugation

When performing EV isolations targeting potential future clinical applications, aspects such as hands-on time and overall isolation time are critical for their viability. This is in fact one of the commonly stated grievances regarding ultracentrifugation for exosome and small EV isolation, as the process requires many steps taking several hours, and as such is not likely to ever become clinically viable [20] (figure 3). UC is however one of the most traditional and most widely tested methods of EV isolation, and therefore provides a good standard to evaluate the more modern competing techniques up against, with regards both to time and effort involved, and the quality of the resultant EV isolates [47]. Another hurdle with UC, are the radically variable reported yields, with an EV recovery reports spanning between 2-80% [20]. Furthermore, while no expensive consumable materials are generally required to perform an EV isolation thorough UC, the technique is fundamentally biased in the direction of depositing larger and heavier particles first, as these are the most affected by the high g-forces excreted during centrifugation [33]. Additionally, EV aggregation has been reported as a consequence of the large forces involved in UC [49] and may be a major inconvenience when targeting the very smallest EVs, such as exosomes. With shorter UC centrifugation times and/or lower RCFs, only

the larger EVs will reliably deposit. Conversely, if using very long centrifugation times or high speeds, one risks aggregating or otherwise damaging any larger EVs, while simultaneously co-isolating common contaminating non-vesicular materials such as protein aggregates, lipoproteins, cell organelles and viruses [20].

4.2.2 The precipitation reactions TEI and ExoQuick

In general, the precipitation reactions require very little hands-on time, and are very easily performed. They also scale very well with any volume of starting material, which may be both economical and more environment friendly depending on the circumstances. In brief, the method by which precipitation reagents function, is to reduce the solubility of the target molecule (EVs), typically by binding water molecules and forcing other solutes to precipitate [51]. This however leads to the issue of discriminating against suspended non-EV components. Where TEI simply claims to precipitate any and all vesicles in the solution [68], ExoQuick claims to be able to precipitate exosomes specifically using a proprietary polymer [69]. Polymer precipitation in general has been shown to co-precipitate contaminants such as lipo-proteins [52]. With regards to isolation time, both techniques require overnight incubation before pelleting EV's when using CCM as starting material, and so the complete isolation from CCM cannot be performed in a day. With plasma this incubation time is reduced to a few minutes (or one hour in the case of ExoQuick), and the full EV isolation time from plasma is therefore between 20 and 70 minutes. The TEI technique requires a somewhat higher centrifugation speed for precipitation of the final product in the protocol for CCM than the corresponding protocol for ExoQuick, which when coupled with the large volumes typically associated with EV isolation from CCM may be inconvenient. Large, low concentration starting volumes is inconvenient for these technologies in general, as the resultant pellet after centrifugation (as observed in the case of CCM) is not visible to the naked eye, and must be resuspended directly in the large centrifugation tube into a very small volume of solvent in order to achieve a concentrated EV isolate solution. This makes ensuring complete pellet resuspension versus excessive vortexing or mixing an unfortunate compromise to be made. In the case of TEI for plasma, the opposite is true, where a large yellow pellet is formed which I difficult to fully resuspend. After contact with the manufacturer (Invitrogen), it was determined that the optimal solution is to allow the TEI samples to incubate at RT for up to 3 hours in order to allow the pellet material to dissolve. In the literature, while exosomes and other EV have been found to be very robust, it is still recommended to minimize their stored at room temperature (RT) [20], so this solution is likely not entirely ideal.

4.2.3 ExoEasy affinity spin

With the ExoEasy Maxi kit (Qiagen), large volumes (up to 16mL) of starting material is not an issue, as all is passed through an affinity membrane and the flow through discarded immediately. While there are overall more steps involved, the overall process is comparable to that of the precipitation reactions with regards to time and effort involved in the isolation. The columns and their components are however one-time use, and while less of the liquid components of the kit may be used when isolating from smaller volumes of starting material, there is of course no way to use fewer columns. It can therefore not be said that the kit scales well with various sample volumes with regards to cost and waste generated.

4.2.4 qEV SEC

In the case of the qEV SEC columns (Izon science) there several factors to consider. While the SEC technology promises potentially very high quality isolation of vesicles [20]. It requires much more

preparation prior to EV isolation than the precipitation reactions and ExoEasy. The loading volume of the qEV column is exactly 0.5mL which is important to consider. Depending on the wanted starting volume, a concentrating step may have to be included in any protocol relying on qEV for EV isolation. Additionally, the qEV columns are stored at 4°C, and have to be equilibrated to RT before use. They also have to be rinsed with several millilitres of filtered buffer prior to use, further adding to the overall time required in order to complete the EV isolation process. When isolating EVs, the void volume (buffer in the column below the leading wave of large EV's) must be carefully measured as it passes thorough the column, and the collection tubes rapidly switched out when the EV containing fractions are reached. While the columns are reusable up to 5 times according to the manufacturer, any such column should probably not be used more than once in the case that the EV isolates were to be used in a clinical setting, in order to avoid cross contamination. Using the column rack sold by the manufacturer (Izon) it is however not simple to use several columns at once for parallel EV isolations. Over all, the time required to complete an EV isolation using the qEV columns is approximately 1-2 hours. This time considerably less than the total time required for the precipitation reactions in the case of CCM, and far less than the UC technique. Isolation of EVs through qEV does however consist of many very different steps, and is very much a hands-on process throughout. The overall time required is also much greater than all techniques apart from UC, when isolating EVs from plasma.

4.3 Characterization of EV isolates from CCM

4.3.1 TRPS measured nanoparticle yields from CCM

As described in the results (section 3.2.1), the qNano Gold measurements of nanoparticle concentrations in EV isolates from CCM reveals a large variance between the EV isolation techniques. Focusing on the 50-200nm range, ExoEasy appears to have isolated the most overall nanoparticles, nearly doubling that of the second highest yielding technique (qEV). This relationship between qEV and ExoEasy in particular with regards to raw quantity of particles is as expected, based on the findings of Stranska *et.al.* 2018 [54] The two precipitation reactions, ExoQuick and TEI performed similarly to one another not far behind qEV, while UC resulted in a concentration of only 2.9% that of ExoEasy (figure 6). This particularly low recovery also coincides well with what is generally expected from the technique [20, 51].

4.3.2 Size distributions

With regards to size distributions among EV isolate samples from CCM, some general trends are apparent in the average particle diameter data (figure 7). The largest mean particle diameter in the was found in the UC sample, which is reflected by its very flat particle size distribution seen in the CSDH (figure 9). The ultracentrifugation step would therefore appear to deposit few particles compared to the other techniques, and relatively favour the larger particles present. This is to be expected, considering how the sedimentation rate is dependent primarily on particle mass and density, and could also be indicative of EV clumping [20]. The next largest average particle diameters can be found in the qEV7 fraction, and also here the similar observations with regards to size can be made as already done for UC. This is reasonable, as qEV7 is the first collected vesicle fraction from the SEC column, and should therefore theoretically contain the largest particles. Smaller particles would be hindered by the internal structure of the SEC column, and deposited in a later fraction (qEV8, qEV9) [52].

Simultaneously, qEV7 and UC turned out to be the lowest yielding samples from CCM, with regards to total particle concentration. This apparent correlation would seem to indicate that the majority of the particles not only in the EV isolates (section 4.1.3), but of the raw materials themselves are very small. If this is the case, techniques which to a lesser extent are able to deposit the smallest nanoparticles will exhibit both larger average particle diameters, and lower overall particle concentrations.

Near the opposite end of the size spectrum, TEI and ExoEasy are situated with nearly identical average particle diameters (results, figure 7). This would fit well with both techniques isolating nearly all types of vesicles present in the sample, regardless of size. While the fundamental differences in the two technologies makes this an interesting results, it cannot be said to be entirely surprising based on reports on the ExoEasy column [51] or the general description of TEI by the manufacturer [68]. By to a large extent isolating very small particles (50-70nm) along with the larger ones, the overall particle concentration found in isolates from these techniques increases. Whether these nanoparticles are in fact exosomes, is however yet to be determined. ExoQuick meanwhile yielded an average particle diameter slightly greater than that of TEI, and slightly less than that of qEV8, perhaps indicating that it indeed isolates a different group of EVs than what is isolated by TEI. The very smallest average particle diameter is found in isolates of the qEV9 fraction: the last collected SEC fraction. This fits well with what would theoretically be expected from the SEC column, where the resistance should be the greatest for the smaller particles, which therefore takes longer to pass through. The qEV9 fraction should (also according to the manufacturer) be the one richest in proteins, out of the three collected qEV fractions.

4.3.3 EV isolate vesicle fraction and average vesicle diameter

When treating EV isolate samples with a detergent such as Triton x-100, it is expected that vesicles will have their membranes disrupted and lipids dispersed into the solution [58]. The overall concentration of nanoparticles in the sample will therefore fall. When measuring the same dilutions of samples with and without treatment with Triton x-100, the difference in nanoparticle concentration should theoretically correspond to the number of vesicles in that sample. Based on this reasoning, there are two main aspects of the samples which can be determined in this manner: the total vesicle concentration in the sample, corresponding to the change (Δ) in nanoparticles following treatment, and the relative fraction of vesicles, or “purity” of the sample. Additionally, by measuring the change in average particle diameter following treatment with detergent, something can be said of the size of the vesicles which were dissolved by the treatment. In the case that the average diameter is reduced after treatment, the dissolved particles would have to be on average larger, than the average of those remaining in solution. Conversely, if the average diameter is increased after treatment, the average diameter of the dissolved vesicles has to be smaller than the average of the remaining vesicles. In the EV isolates from CCM, only a somewhat rough idea of the vesicle fraction can be ascertained as only the 85-340nm range was measured (figure 12). This was due to a limited amount of sample material from CCM only allowing for one additional series of measurements with the qNano Gold. Based on these data however, the overall amount of vesicles in each sample followed a pattern similar to the previously discussed overall concentrations, immediately indicating at least some correlation between the isolated particles of each technique and EV’s. ExoEasy showed the overall greatest concentration of vesicles, followed by qEV and TEI. As advertised by the manufacturer, the qEV technique gave a particularly good sample purity (76% vesicles), and in this aspect performed much better than both ExoEasy and TEI, which were both closer to 50%. This increased apparent purity of qEV over ExoEasy is also what was reported by Stranska *et.al.* 2018 [54]. However, TEI was nearly 2% less pure than the

UC sample, which in turn was 12% less pure than ExoEasy. Therefore, in this experiment, the affinity spin technology of Qiagen's ExoEasy appears to be superior to the TEI precipitation and UC. The ExoQuick precipitation technique, while producing the second to least vesicles overall after UC, in fact resulted in a relatively high purity, nearly matching that of qEV.

Perhaps as interesting as the vesicle purity, is the change which occurs following triton x-100 treatment with regards to average particle diameter. In the case of UC, a very large increase in average diameter was observed (figure 13). This indicates that the vesicles disrupted by the detergent on average were smaller than the average diameter of the nanoparticles in the UC sample with no detergent added (149.67nm). Based on the methodology of the UC technique, it is expected that the particles will pellet in order from most to least dense. It is the differential centrifugation steps prior to the ultracentrifugation which are meant to remove large contaminants [20]. As such, any particles not pelleted at 10 000x g 30m at 4°C are expected to be contained in the ultracentrifugation pellet. Additionally, this could be further evidence that these larger bodies are adversely affected by the very large g-forces of the ultracentrifugation to a greater extent than the smaller and less dense vesicles which were apparently dissolved by the triton x-100 treatment. Under this hypothesis, the large undissolved bodies observed after treatment with detergent could be lipoproteins and various other debris which has clumped together, as mixed aggregates [20, 49].

The qEV and ExoEasy technique both experience moderate increases in nanoparticle diameter following the treatment, indicating a dissolved vesicle average diameter of less than 138.11nm and 171.67 respectively. This places the dissolved vesicles of both techniques potentially within the defined size range for exosomes (50-150nm) and within the range of oncosomes (100-400nm) and MVs (50-1000). Interestingly the two polymer precipitation techniques, ExoQuick and TEI techniques both displayed a reduction in average particle diameter. In the case of the ExoQuick sample, with an average diameter already as high as 161.33 before treatment, this indicates that the vesicles predominantly dissolved could not have been exosomes, but rather had to be larger vesicles such as oncosomes or MVs. TEI similarly, with a starting average diameter of 145nm prior to treatment with Triton x-100 experienced the largest decrease of all the techniques in average particle diameter, also indicating that a sizable fraction of the dissolved nanoparticles is likely membrane bound bodies of a diameter larger than that of exosomes.

4.3.4 Characterisation of isolated nanoparticles by bead-assisted flow cytometry analysis

By virtue of the technology behind the BAFC, exact quantitation of proteins per vesicle is impossible. This is due to the fact that the amount of protein adsorbed to each individual bead is unknown (see materials and methods). However, samples in the same assay can still be compared relative to one another in terms of the total vesicle-associated amount of the studied protein in a semi quantitative manner.

Our results showed that both CD9 (figure 14) and CD63 (figure 15) can be found in all tested EV isolate samples from CCM. However, the qEV technique in both cases contained by far the most of both proteins again hinting at a very good EV purity. In the case of CD9 in particular, the individual qEV fractions gave the by far the strongest signal, and in increasing order from qEV 7 to 9. As previously discussed under trends in nanoparticle size distributions, the qEV fractions displayed decreasing particle diameter as the fraction number increased. It therefore follows, based on the BAFC assay, that the smallest qEV isolated EVs (qEV9) in fact contain the most CD9 protein. Notably, the ExoEasy and

TEI techniques by comparison gave the second and third smallest average particle diameter in the same measurement series, and additionally had 6.07 and 2.72 times greater particle concentration than the qEV9 fraction in the 50-200nm range (appendix section 7.5). Further emphasizing this trend, the qEV 8 fraction which was measured using TRPS to have a larger average particle diameter than both ExoQuick and ExoEasy, was in the BAFC measured to produce the third greatest signal, just 3% less than that of ExoEasy. This underscores that average nanoparticle size not necessarily is a reliable indicator of the type of particle present in a sample. While TEI and ExoEasy isolate many nanoparticles, the number of vesicles and exosomes, in particular, seems substantially lower. When considering overall concentration of vesicles (figure 12), the concentration of TEI and ExoEasy actually were very similar to that of qEV, with 113% as many in the case of ExoEasy and 95% as many in the case of TEI. The overall concentration of CD9 protein in the qEV sample per particle therefore appears to be very high compared to these two techniques. It is therefore tempting to assume that the qEV technique overall isolates a large fraction of EVs which at the very least have a different biogenesis to those isolated by the other techniques. The exact same pattern, apart from a relatively greater signal from the ExoEasy sample, can be observed in the BAFC for CD63 protein.

When considering these and the above results, it should be kept in mind that the three qEV fractions all stem from the same initial volume of starting material, and as such each qEV fraction is 3 times as dilute as any other EV isolate sample. It would therefore appear the qEV SEC technique is extremely effective at isolating nanoparticles with the CD9 and CD63 proteins, and the results further indicate that there is a definitive difference in the sort of particles isolated by each technique. While on the surface ExoEasy may appear to have differentiated itself from TEI in the CD9 BAFC by producing 2.13 greater MFI fold change (figure 14), it should be noted that the ExoEasy sample in this case was measured to be 2.23 times the TEI concentration. It is therefore plausible that there is not additional purity of CD9 containing nanoparticles in the ExoEasy sample, which cannot be explained by the greater concentration. In the CD63 BAFC on the other hand, this difference has increased to 10.22 times greater signal in favour of ExoEasy, indicating that perhaps there is indeed some difference in the particles isolated between the two, at least with regards to CD63 specifically. The ExoQuick and UC samples in both cases performed only as well as could be expected, considering their overall low nanoparticle yields, indicating correspondingly low MFI fold changes.

4.3.5 dsDNA in EV isolates from CCM

In general, DNase treatment proved to have little effect on the final concentration of isolated dsDNA in the case of ExoEasy and TEI, reducing their overall dsDNA concentrations by only 13.89% and 2.26% respectively. This may indicate that the majority of the dsDNA contained in these samples is protected from the action of the DNase enzyme by being enveloped by a vesicle. ExoQuick and qEV conversely, lost 65.82 and 55,94% of their measured dsDNA during DNase treatment, indicating that more than half of their dsDNA contents are without the protection provided by vesicles, and as such are accessible to the DNase enzyme. The UC sample, while already having a very low dsDNA yield, was observed to suffer a further reduction by as much as 36.36% in dsDNA following DNase treatment.

When considering only dsDNA remaining in each sample after DNase treatment, the technique yielding the decidedly greatest dsDNA ng/ml CCM, was TEI, with more than twice the dsDNA/mL of the second best yielding technique, ExoEasy. ExoEasy in turn produced a yield of 3.65 times the dsDNA/mL of the third highest yielding technique, qEV. Returning to the previously made points during discussion of the nanoparticle size distributions (section 4.3.2) and BAFC results (section 4.3.4), this would appear to

coincide well with the hypothesis that ExoEasy and TEI to a large extent isolate the same range of particles, but as discussed in the BAFC chapter; that ExoEasy also overlaps more with qEV than does TEI. The latter technique appears to isolate some distinct EV very rich in DNA and AChE-enzyme, yet relatively very poor in CD9 and CD63 indicating that it is perhaps not an exosome. A non-exosome DNA rich EV isolated primarily by TEI and to a lesser extent by ExoEasy, would also fit in well with the observation that ExoEasy and TEI DNA isolates both have high overall dsDNA yields which are unaffected by treatment of samples with DNase (figure 16). This EV may very well be an oncosome, as reported by Meehan *et.al.* [18]. It should be noted however, that the overall high concentrations of dsDNA in the two samples at least to some extent could be explained by their very high particle concentration, when compared to the other techniques.

4.3.6 Purity of dsDNA-containing nanoparticles: dsDNA/particle

On the topic of isolating the vesicles with the greatest dsDNA yield, a direct method of viewing the problem would perhaps be to take the dsDNA (after DNase treatment) concentration data and divide by the corresponding nanoparticle data, in order to get a "dsDNA/nanoparticle" value. (figure 17)

When interpreting this figure, it is first important to note that the nanoparticles in the EV isolates were not filtered so as to include only those of diameters 50-200nm prior to DNA isolation. As such, any isolated DNA may stem from particles both smaller than 50nm, or much larger. This comparison can however still be useful in estimating what particle size is likely to contain dsDNA. Additionally, it may be used to give an indication of the relative amount of contaminating particles in a sample i.e. the abundance of particles in the 50-200nm range which do not contribute any dsDNA. Based on the trends observed in the CSDHs (figures 10,11), it would seem very unlikely that large amounts of particles (relative to the total) of size greater than 200nm is present in any of the samples.

When viewing the comparison (figure 17), what is immediately apparent is how it underscores the fact that while the ExoEasy technique isolated by far the most particles, the relative amount of DNA contained in these is very low compared to that of TEI. As previously discussed under size distributions (section 4.3.2), ExoEasy and TEI have very similar mean (and even mode) isolated nanoparticle diameters. It is therefore perhaps counter-intuitive that such a large disparity should be observed when comparing their relative yield of dsDNA from the same substrate. Returning to the CSDH of the two techniques however (figure 8), it may appear that the ExoEasy technique isolates nanoparticles in a slightly more concentrated fashion specifically in the 50-200nm diameter range. TEI conversely gives a much smoother and more rounded size-distribution profile, isolating relatively more particles in the above 200nm. As the exclusion of many smaller particles seems to lead to an increase in relative dsDNA concentration, this again leads back to the previously hypothesized non-exosome EV (section 4.3.5) which the TEI technique is superior to ExoEasy with regards to isolating, whereas the latter co-isolates very many smaller nanoparticles not necessarily associated with dsDNA.

4.3.7 Correlations between isolated dsDNA and measured nanoparticles from CCM

The speculation on purity of dsDNA containing isolates makes the direct comparison between measured nanoparticle concentration and dsDNA an interesting one. By plotting the TRPS measured 50-200nm particle concentration in the various EV isolation technique against the dsDNA isolated from DNase treated aliquots of the same sample, an estimate of how strongly the trends correlate can be established (figure 18). As with the dsDNA yield per nanoparticle (figure 17), it was not possible to

separate out nanoparticles not within the range of the NP100 nanopores. As such, the dsDNA data for this comparison is based on any isolated EV present in the EV isolate, whereas the concentration values are based on nanoparticles in the 50-200nm range only.

As is clearly demonstrated by comparison (figure 18), the correlation between dsDNA and measured nanoparticles/mL scores an R-value of only 0,28 in the 50-200nm range when all samples are included. There is however a very clear outlier around y=45. By removing this outlier, the R^2 increases drastically to 0,95. This outlier corresponds to the measurements made of TEI. This emphasizes the previously discussed observations that based on the trend collectively set by all the other samples, the measured dsDNA concentration from TEI is disproportionally higher than what would be expected based solely on its measured particle concentration in the 50-200nm range alone.

One potential explanation for this discrepancy would be that the TEI vesicle concentration somehow has been underestimated, and that the relative DNA-yield subsequently should be far lower. Based on the curves in figure 18, for the TEI sample to fall in on the curve, its concentration would have to be more than twice that of ExoEasy, the otherwise most highly concentrated sample. Previous data from the testing phase using ExoCet (not included in the main part of this thesis) however lends some additional credence to the ExoEasy exosome concentration in CCM is in fact being greater than the TEI concentration (appendix section 7.4 figure 16)

By making the same plot as before but looking at the correlation between the NP200 measured nanoparticles and the isolated dsDNA, a much higher R^2 score of 0.93 is achieved, even with all samples included (see figure 19). Notably, due to the previously discussed large overlap between the NP100 and NP200 measurement intervals (section 4.1.3), plotting against the NP200 concentration data effectively equates to removing the “diluting” effects off nanoparticles between 50 and 85nm in diameter from the comparison. As also previously discussed, the CSDH for TEI (figure 8) would seem to indicate that the raw nanoparticle numbers contribution from particles of size greater than 200nm is relatively very small, yet cannot be ruled out as the source of the very high concentrations of measured dsDNA. The most notable outlier in this dataset (the data point closest to the graph origin) here (figure 19) corresponds to the UC sample, which displays a disproportionately high dsDNA concentration compared to the trend set by the other techniques.

Based on these plots, there would appear to be a general correlation between the concentration of isolated nanoparticles, and concentration of dsDNA. Furthermore, based on how the TEI value fits much better into the correlation when comparing NP200 values than NP100, there is further reason to believe that the dsDNA yield from the TEI sample predominantly originates from particles larger than what is predominantly isolated by any of the other EV isolation techniques.

Similar plots were attempted for triton x-100 determined vesicle concentrations vs. measured dsDNA, but no correlation with an R-value of greater than 0.42 could be found. This could have several explanations. One possibility would be that some of the samples have dsDNA content not contained within membrane bound bodies which can be disrupted using the described Triton x-100 treatment (section 2.3.2). This would however require said dsDNA to avoid digestion during the RQ-1 DNase treatment the EV isolates were subjected to prior to DNA isolation. It is therefore a much more likely scenario that the triton x-100 treatment was insufficient for entirely dissolving all vesicles in at least some of the samples, thus yielding inconsistent results. This somewhat weakens the credibility of the triton x-100 treated samples as a reliable estimate of the vesicle fraction, as it would likely result in

falsely low relative vesicle fraction estimates for samples containing overall very many vesicles, relative to samples containing very few. This, however, would go counter to the findings of Osteikoetxea *et.*al 2015 [58], who concluded that a concentration of 0.1% (v/v) of Triton x-100 should be more than sufficient. A likely alternative is that the limited number of data points and random noise may have caused the relatively low R^2-value. No matter the reason, it would still likely not invalidate conclusions drawn regarding vesicle sizes, as these do not depend on the complete dissolution of all vesicle to be accurate.

4.3.8 Comparing dsDNA yield with BAFC measured CD9 and CD63 concentration

Another interesting relationship to consider is that between an EV sample's content of exosome marker proteins and the measured dsDNA yield. By comparing the two (figure20) it becomes clear that the dsDNA yield follows the same pattern for the qEV fractions as described previously, increasing in accordance with the fraction number and decreasing average particle diameter. Again it bears mentioning that for these comparisons the qEV fractions have not been pooled, and as such are three times as dilute as the other samples relative to the amount starting material (16mL CCM) which is the volume all three qEV fractions originate from.

The ExoEasy sample, at 6.07 times the NP100 particle concentration of qEV9, gave 8.50 times the isolated dsDNA concentration. The ExoEasy sample did however also produce the largest CD63 signal, and the second largest CD9 signal, making conclusions on the relationship between BAFC signal intensity and dsDNA difficult to draw. It would however seem plausible that the ExoEasy technique may have co-isolated many of the same dsDNA rich nanoparticles typical of TEI, and simultaneously several EVs rich in CD9 and CD63. ExoEasy would in this manner fall in between the qEV and TEI techniques, with regards to the sort of overall nanoparticles isolated. The TEI sample, at only 2.72 times the qEV9 overall NP100 concentration, displayed 18.95 times the concentration of isolated dsDNA. Simultaneously, the qEV9 sample produced a 3.23 SD9 signal and 9.61 times the CD63 signal compared to TEI, perhaps indicating that there the particles containing the largest amount of dsDNA are not necessarily rich in CD9 or CD63 protein.

4.3.9 Summarizing overall performance of EV isolation techniques from CCM

Taking all the above points into consideration, it is now possible to give a rough estimate of the performance of each individual technique. While no simple scoring system could take into account all the relevant factors discussed above, a simplified system may be used to give a rough estimate. One way of doing this is listing the most important criteria each technique is to be evaluated up against, and arranging the performance of each isolation technique from best to worst. By making the best performer by a certain criteria get the highest score of 5 and the worst performer the lowest score of

1, a higher total score across all criteria would mean a better performing technique. As per the defined criteria for comparison of EV isolation methods (section 4.1.0) these would be the total EV yield ([EV]), the EV purity (EV%), the amount of exosome marker protein (CD9/CD63), the dsDNA yield ([dsDNA]) and the effort required to complete the isolation. Considering that the final aim of the EV isolation is potential use as a biomarker for cancer, extra weight was given to the overall EV content and dsDNA yield. The summary is shown in table 6.

Table 6: Each EV isolation technique from CCM scored against the defined criteria for ideal EV isolation. The overall yielded concentration of EVs ([EV]) has been weighted slightly, with a modifier of 1.5 on its original score to emphasize the importance of a high vesicle yield. The relative sample vesicle purity (EV%), relative amount of exosome marker proteins (CD9/CD63) and overall effort of the isolation process (Effort) has been weighted normally. The total dsDNA yield has been weighted with a 2x modifier, as the DNA content is perhaps the most interesting target EV-cargo molecule with regards to future clinical applications of EVs. Numbers in parenthesis are the original scores of the EV isolation technique, prior to applying the weighting modifier.

	[EV] (x1.5)	EV %	CD9/CD63	[dsDNA] (x2)	Effort	**Sum**
ExoEasy	7.5 (5)	3	4	8 (4)	5	**27.5**
qEV	6 (4)	4	5	6 (3)	2	**23**
TEI	4.5 (3)	1	1	10 (5)	3	**19.5**
ExoQuick	3 (2)	5	2	4 (2)	4	**18**
UC	1.5 (1)	2	3	2 (1)	1	**9.5**

4.4 Findings in EV isolates from Plasma

4.4.1 TRPS measured nanoparticle yields from plasma

Due to the previously described complications with the qNano Gold and samples from plasma (section 4.1.3), only TEI and qEV were left for direct comparisons with samples from CCM. For these samples however, TEI resulted in very high concentrations of nanoparticles with a yield 6.6 times higher than qEV (figure 22). It is notable how far out of proportion this is, when compared to the corresponding CCM results, where qEV in fact had a greater overall nanoparticle concentration than did TEI. Additionally, the measurements of TEI and qEV fractions revealed overall much higher nanoparticle concentrations in plasma samples, than was measured in the CCM-derived EV isolates. This can be illustrated by placing the qNano Gold data of the corresponding data samples from CCM and plasma in the same diagram (figure 23). It should be noted that a logarithmic scale has to be used, as the overall difference spans several orders of magnitude. This is despite the CCM-samples being based on

16 times as much starting material by volume as the plasma derived samples, with 16mL CCM being used compared to only 1mL plasma per technique.

In addition to the generally higher concentrations of nanoparticles in the plasma samples, the plasma control group donor displayed a much higher nanoparticle yield per mL plasma, than did the selected PC patient. This is noteworthy at this point, as it constitutes the first of several indications of a potentially very large inherent variance in plasma nanoparticle content between individuals.

4.4.2 Size distributions of samples from plasma

With regards to the average nanoparticle diameter compared with concentration, similar trends to what was previously described for samples from CCM (section 4.3.2) can be observed also in the plasma samples (figure24). For both the control group donor and the PC patient derived EV isolates, the qEV fractions yield increasing numbers of total nanoparticles as the SEC fraction number increases. Additionally, the qEV7 fraction in both cases yield both the smallest overall number of nanoparticles, and simultaneously has the largest mean particle diameter. For the PC patient sample EV isolates, the particle diameters further follow the same pattern as described for CCM, with qEV8 having larger average particle diameter than TEI, which in turn has larger average particle diameter than qEV9.

When comparing qNano particle measurements of CCM and Plasma there is further a striking difference in the overall spread of the data. As can be seen from the generated CSDH (figures 25, 26 vs. 8, 9) the plasma data appear relatively much more tightly focused around 60nm than the CCM data. By again taking a look at figures showing the mean particle diameter spread for samples from CCM and Plasma (figures 7, 24) it becomes clear that this is reflected here. In general, the CCM derived EV isolates have the larger mean diameter. In numbers, the average diameter of all plasma values (TEI, qEV7, qEV8, qEV9) is 85.81nm (appendix section 7.5). The average of the same samples from CCM is 91.44nm. This again coincides with the previously discussed observation that smaller particle diameters appear to correlate to higher particle concentrations (section 4.3.2). As has already been established, CCM samples have much lower overall particle concentrations than Plasma samples (figure 23). It is at this stage important to note however, that this does not equate to actually fewer large particles being present in the plasma samples than in the CCM samples, only that relatively more small particles are present thus affecting the average. In fact, in absolute numbers, the amount of nanoparticles with a diameter greater than 200nm appear to be much greater in the plasma derived samples (figure 27).

4.4.3 EV isolate vesicle fraction and average vesicle diameter

For the samples from plasma, both NP100 and NP200 data is available, allowing for comparisons of particles also in the interval of 50-85nm. By looking at the plasma derived EVs in the 85-340nm range and comparing to the samples from CCM, it becomes clear that also the overall amount of vesicles is much greater in the plasma samples than in the CCM samples, reflecting the overall increase in nanoparticles. In the case of the control group sample from plasma, qEV gave a higher overall vesicle yield than TEI, but this relationship appeared reversed in the PC-patient sample. More interesting was the changes observed in sample purity. In the NP200 interval, a very large drop in relative vesicle fraction for both techniques, with some exceptions (see table 7)

Table 7: Comparison of the measured vesicle purities of TEI and qEV EV isolates from PC-patient and control plasma, as illustrated in results figures 28 and 30.

	Control donor sample		**PC patient donor sample**	
	NP100	NP200	NP100	NP200
TEI	19,51	2,50	63,51%	59,07%
qEV	29,57	41,63	29,36%	36,37%

As can be seen from table 15, a large reduction can be seen in both TEI measurements from the control donor sample, and all measurements from qEV, relative to samples from CCM. Strangely, and overall increase the vesicle fraction was observed specifically in TEI samples from the PC patient donor, holding true in both NP100 and NP200 intervals. In general, it can only be concluded that the what is isolated from various donors apparently may varies greatly between individual donors, especially when using the TEI technique. However, while the qEV technique proved the most consistent with regards to vesicle fraction quality, the TEI sample still provided the overall greatest number of vesicles in all but one instance.

4.4.4 Average EV size distribution

As previously done with the CCM samples, some general facts concerning the sizes of the plasma vesicles may be inferred by looking at the changes in nanoparticle diameters following treatment with detergent (figures 29, 31). In the control donor sample's NP200 range qEV showed an increase in particle diameter following treatment, while TEI showed a decrease. This indicated qEV vesicles smaller than 145.17nm (the average measured NP100 diameter with no Triton x-100) and TEI vesicles larger than 129.5nm. This places them both potentially within the range of exosomes [8]. Additionally, as NP100 data are available for these samples, even more can be said of these vesicle's sizes. In the case of the qEV samples, a large decrease was observed in average nanoparticle diameter in the NP100 range, implying that the dissolved vesicles were much larger than the average NP100 diameter measured without treatment of detergent of 84.33nm. It can therefore be said that the average vesicle size of the qEV sample in this case was between 84.33nm and 145.17nm, placing it very nicely within the set size range for exosomes. In the case of the TEI sample however, a moderate increase in nanoparticle diameter was observed in the NP100 range. This implies that the dissolved vesicles in the 50-200nm range were on average smaller than the measured TEI average NP100 nanoparticle diameter with no Triton x-100, of 78.50nm. Considering that these vesicles would be below the detection limit of the NP200, this could indicate that in the case of the TEI sample, there is a large population of vesicles in the 50-78nm range, as well as a separate population of vesicles with an average diameter greater than 145nm. The reason this population of very small vesicles would have to be so large, is that the NP100 range extends to 200nm, and thus encompasses the mentioned large 145nm average vesicles. The impact on average size by the removal of these larger particles needs to be negated by many small vesicles getting dissolved, in order to explain the observed results.

Looking at the PC patient plasma sample a reduction in diameter following treatment with detergent was observed in the NP100 measurements from both qEV and TEI. In the NP200 range, the opposite was true, with an observed increase in average nanoparticle diameter following treatment. Following the same reasoning as previously, this would correspond to an estimated average qEV vesicle diameter of between 89.5nm and 149.33, positioning it perfectly for exosomes with respect to EV diameter. The corresponding TEI average diameter would be in between 86.50nm and 124.00nm, which is also within

the defined range. It should be noted that no conclusions can be drawn comparing the control and PC patient donors in these cases, other than that there appears to be some interpersonal variance affecting results, when working with EV isolates from plasma.

4.4.5 Exosome quantitation using the ExoCet assay

EV isolation technique performance in exosome isolation

As has been discussed, comparing nanoparticles or even vesicles with size as the only metric is insufficient when trying to determine the technique best suited for isolating complex and biologically active biomolecules such as exosomes (section 4.1.0). As such, the ExoCet Exosome Quantitation Assay was used in order to further examine the relationship between the products of the various exosome isolation techniques. In this case, concentration measurements were based on the activity of the exosome-associated Acetylcholinesterase enzyme.

In the ExoCet Exosome Quantitation Assay (SBI) on samples from plasma, TEI was estimated to be the decidedly highest yielding technique (figure 33), followed by ExoEasy with the second highest concentration barely registering above the LOD. While unfortunately no corresponding qNano Gold measurement could be made to verify this relation between the TEI and ExoEasy samples, the relative relationship between TEI and qEV can be confirmed for both control group and PC patient donor samples (figure 22). Notably, this is a very different relationship compared to what was observed in samples from CCM, where the relative concentration between ExoEasy and TEI samples was reversed. These results would appear to indicate that the ExoEasy technique performs poorly either with plasma as a substrate, or with the very small volumes used.

A potential weakness with the enzyme-linked assay technology

With regards to the estimated concentrations of exosomes in each sample by the ExoCet assay, TEI in the plasma control and PC patient group was estimated at 4,19 and 7,23 times the corresponding TRPS measurements of nanoparticles in the 50-200nm range. Similarly, qEV was estimated at 0,53 and 3,80 times the corresponding NP100 values. When also taking into account the fact that the NP100 interval encompasses 50-200nm, and hence the entire possible range of diameters for exosomes, it would appear that the ExoCet assay may be overestimating the actual exosome concentration in the samples derived from qEV and TEI.

Such an overestimation of the TEI sample concentration may be caused by inherent OD405nm in the TEI sample, unrelated to the enzymatic activity measured by the ExoCet assay. This was in part due to the appearance of the TEI EV isolates from plasma appearing somewhat opaque to the naked eye. In order to control for this, a series of specialized blanks were designed in order to account for sample opacity caused by potential colloid particles. When conducting ExoCet measurements, a significant increase in OD405 is associated with the addition of the strongly yellow coloured ExoCet buffer B. However, sample cannot be added to complete reaction mix without causing an enzymatic reaction. Simultaneously, the 1:1 dilution of the EV isolate sample in reaction mix is likely to affect any inherent non-enzymatic optical density contribution of the EV isolate sample. The OD405nm from the buffer a given sample is dissolved in when combined with the ExoCet lysis buffer (buffer A+B) therefore has to be measured separately in completed reaction mix and the, contribution of the sample diluted 1:1 in

ExoCet buffer A in a different microtiter plate well. With this in mind, the specialized blanks were designed to consist of two ExoCet TRs of the various EV isolates treated as normal samples during the assay preparation phase (see materials and methods), but loaded into wells on the microtiter plate with inert reaction buffer (no ExoCet buffer B added). By adding the measured OD405nm of this sample to that of the appropriate normal blank at a given time of incubation, a specialized blanking value which accounts for static opacity due to colloidal occlusion of the sample for that incubation time is obtained. This was done in an effort to improve accuracy by taking into account any opacity in the solution caused by colloid or other suspended particles in the various samples when subtracting blank OD405.

Use of the specialized blanking values gave only minor reductions in the ExoCet assay estimated exosome concentrations (see results). The ExoEasy and TEI samples had very different apparent opacity (judging by eye) yet both experienced an approximate 15% reduction in estimated exosome concentration when using the specialized blanks. This does little to explain the sevenfold increase in estimated ExoCet exosome concentration relative to the qNano Gold estimated total 50-200nm nanoparticle concentration. There is therefore little reason to believe that the specialized blanks had their intended effect, when also considering that the relative relation between samples did not change in any meaningful way. It would appear that the other measures taken to negate the effects of inherent sample opacity, such as increasing the centrifugation time of samples post-lysis (see materials and methods), in order to collect more debris, as well as the long RT incubation of the TEI samples prior to the assay, were sufficient for counteracting any ill-effects from internal opacity ad 405nm. Additionally, the long incubation time (20 minutes) selected so as to minimize the effects of noise further abates the issue. With this in mind, it was concluded that there was not sufficient evidence of gained benefits by use of specialized blanks, to justify deviating from the protocol provided by the manufacturer (SBI) by their inclusion in the sample blanking process.

An alternative hypothesis would be that the already discussed large differences between even vesicles of similar size isolated by the different EV isolation techniques may play an important role in explaining this issue. The manufacturer of ExoCet, System Bio, also produces the ExoQuick EV isolation kits. The Exosome quantitation in the ExoCet assay is based on measured AChE-activity in samples of isolated exosomes, which have been quantified using NanoSight (NTA) analysis. NTA analysis, like the TRPS-based qNano Gold, cannot easily discriminate between nanoparticles of the same diameter. According to the documentation provided by the manufacturer (SBI), the standard solutions used to produce the standard curve upon which the exosome quantitation is based, does not contain actual exosomes, but rather a predetermined concentration of AChE-enzyme. As such, the quantitation is highly dependent on the relative amount of AChE-enzyme per unit of nanoparticles isolated in the correct size range for exosomes (50-150nm) being consistent between isolations. Based on the differences in results between EV isolation techniques already discussed in this thesis, there may be reason to believe that the relative fractions of different types of nanoparticles isolated differs between exosome isolation techniques. In the case that the EV isolation technique used by SBI isolates a smaller relative fraction of AChE-containing nanoparticles in the correct size range, other techniques which isolate nanoparticles with more AChE-content will have their numbers overestimated. There is however not enough data to conclude strongly on the validity of this hypothesis.

4.4.6 dsDNA in samples from plasma

With regards to the Qubit measured concentrations some issues were met with regards to low sample concentrations of dsDNA. Initially, the same Allprep (Qiagen) kit was attempted used for isolating DNA from plasma samples as were used for CCM samples. When in the testing phase no dsDNA could be measured using the Qubit dsDNA HS assay, it was decided that the issue may be related to the high DNA size cut-off of the AllPrep DNA Mini Spin columns of 15-30kb. It was therefore decided to switch to the QiaAmp Circulating nucleic acid kit (Qiagen) instead, for isolation of DNA from plasma, which performed better under testing.

In general, only very low concentrations of dsDNA could be found in EV isolates from plasma. This turned out to pose some obstacles to overcome with regards to as representatively as possible portraying the estimated concentrations of dsDNA yielded by each technique. This came about as several of the samples measured in the Qubit dsDNA HS assay proved to have concentrations of dsDNA lower than the limit of detection (LOD) for the Qubit dsDNA HS assay for one or more of the biological replicates of each group. All values in the raw data (appendix section 7.2) were however hovering close to the LOD, providing reason to believe that the actual concentration in the non-measureable samples were >0ng/mL. Excluding these samples when calculating the average dsDNA concentration would therefore likely lead to an overestimation of the actual concentration, whereas setting them to 0ng/mL would equally likely result in an underestimation of the actual dsDNA concentration. It was therefore decided that when calculating the average of biological replicates, samples below the LOD should be set to LOD/2, thus minimizing the chance of radical misrepresentation of dsDNA concentrations. For a breakdown of the dsDNA concentration calculations, please refer to the appendix (Appendix 7.1, calculations).

With this in mind, the results of the measurements of dsDNA from plasma derived EV isolates can be compared. Perhaps unsurprisingly considering the CCM results, TEI resulted in the greatest overall yield of dsDNA, when compared to ExoEasy and each individual qEV fraction. Interestingly, the ExoEasy technique in general gave very low concentrations from plasma, averaging just barely above the LOD in the control group, and in fact slightly below in the PC patient group. This is particularly interesting as it is less than each individual qEV fraction. The qEV isolation technique overall therefore in these experiments greatly exceed the efficacy of the ExoEasy technique with regards to isolating measurable quantities of dsDNA (figure 34). This relation between ExoEasy and TEI is also what was observed in the previously discussed ExoCet estimated exosome concentrations. This may be related to the fact that the ExoEasy spin column, in its effort to be simple and universally compatible, is dimensioned to support volumes of up to 16mL of starting material. The volume of starting material processed by the same type of column is therefore reduced 16-fold when moving from CCM samples to plasma samples. The qEV column conversely, is intended for use with small volumes (0,5mL loading volume), and subsequently requires a concentrating step prior to loading if large volumes of starting materials are to be processed. It may be the case that the efficacy of DNA isolation from very small volumes is even more adversely affected when using small volumes with the ExoEasy spin column technology, with its unchanging solid phase dimensions despite greatly changing volumes of starting material, than with the qEV SEC-columns. The TEI technique, relying on precipitation in solution without elusion through a solid phase, appears to scale well with different volumes.

.

4.4.7 Correlations between isolated exosomes from plasma and measured nanoparticles

In the case of ExoCet estimated exosomes from the plasma control group, the contribution in OD405nm of each individual qEV fraction was below the LOD determined by the standard curve equation for both qEV 7 and 8. As such there are too few data points in this series for any meaningful scatterplots looking for correlation to be made. An estimation could however be made based on the dataset from the PC-patient samples, showing at some apparent correlation (figure 35).

Based on this estimation, it would appear that there is some correlation, albeit not a very strong one, with an R^2 value of only 0,69 (figure 35). It would appear that relative to the trend set by the qEV fractions (clustered in the bottom left) and that of TEI (top right), ExoEasy is relatively underperforming with regards to dsDNA content. The way the qEV fractions cluster indicate that qEV9 (topmost of the three) has a relatively higher dsDNA concentration than the norm, whereas qEV7 and 8 are in the middle. Interestingly, this perfectly reflects what was previously discussed in the dsDNA per nanoparticle plot for CCM (figure 18).

4.4.8 PNA clamp assay for KRAS mutated alleles

As progress has been made in EV research in the last decade, several observations of tumour DNA being carried by EVs has been reported (section 1.2) In order to measure the levels of such DNA in the EV isolates produced by the various techniques using plasma as starting material, a PNA clamp assay for KRAS mutation was performed.

As previously mentioned, the KRAS gene has been shown to be present in 80-90% of pancreatic cancers [62]. One particularly interesting metric for evaluating the success of the EV isolation techniques, is therefore the PNA clamp assay for KRAS mutation. This is an important aspect, as it confirms the presence and relative purity of tumour mutated alleles in the DNA contained within each sample, and thus gives a very strong indication as to whether or not the EVs of each EV isolation technique contain nucleic acids usable for diagnostic purposes in the future.

As with the BAFC analysis (figures 14, 15) the PNA clamp assay revealed very strong results for the qEV fractions, where qEV8 and 9 individually gave the greatest and second greatest total ΔΔCq across all PC-patient donors (figure 36). Also the qEV7 fraction, although contributing less, resulted in a KRAS detection, and with a respectable purity. As such, the overall qEV technique may be considered to isolate the EV's with the greatest purity of relevant DNA.

Both ExoEasy and TEI techniques however each collected DNA determined to be positive for KRAS mutation from two out of three PC-patient donors. This shows that both these techniques, although yielding less pure fractions of tumour DNA vs. WT, still isolate the correct EV's to an extent measureable using PNA clamp assay. It must be noted however, that one of the main goals of using EV's such as exosomes for DNA isolation, is their suggested ability to selectively enrich themselves with tumour DNA, as such purity is a very important factor to consider.

One interesting observation at this point would be that qEV distinguishes itself particularly in exosome marker protein (section 4.3.4) and KRAS mutated alleles. This falls well in line with the numerous reports linking exosomes and tumour DNA [6, 17, 39], indicating a link also here in this study.

4.4.9 Summarizing overall performance of EV isolation techniques from plasma

As the overall EV concentration and purity could not be reliable measured in the ExoEasy samples, these cannot be included in the final summary evaluation of the techniques. Instead, the relationship between the techniques as measured by the ExoCet Exosome Quantitation assay will be used. Furthermore, the results for CD9 and CD63 protein could not be successfully measured in samples from plasma, and requires more experimentation. The primary focus of the weighting will therefore in the plasma phase be on the ability of each technique to extract DNA from samples, and particularly tumour DNA. In addition, the effort scores from the last phase will be included also this time. Like before, the general scoring will be that of rating the techniques from best (3 points) to worst performance (1 point), and summing together the points of the EV isolation technique across all the evaluation criteria. Additionally, a modifier of x1.5 will be placed on the quantity of isolated dsDNA ([dsDNA]) and a modifier of x2.0 on the relative amount of detected KRAS mutated alleles (KRAS). The summary is shown below (table 8)

Table 8: Each EV isolation technique from plasma scored against the defined criteria for ideal EV isolation. The overall yielded concentration of dsDNA ([dsDNA]) has been weighted slightly, with a modifier of x1.5 on its original score to emphasize the importance of a high dsDNA yield. The relative sample estimated exosome concentration ([Exos]) and the overall effort of the isolation process (Effort) has been weighted normally. The total relative fraction of mutated KRAS alleles in the sample (KRAS) has been weighted with a 2x modifier. Numbers in parenthesis are the original scores of the EV isolation technique, prior to applying the weighting modifier.

	[Exos]	[dsDNA] (x1.5)	KRAS (x2.0)	Effort	**Sum**
TEI	3	4.5 (3)	2 (1)	2	**11.5**
qEV	1	3 (2)	6 (3)	1	**11**
ExoEasy	2	1.5 (1)	4 (2)	3	**10.5**

5. CONCLUSIONS AND FUTURE PERSPECTIVE

This study has shown that UC, the most traditional and widely used technique for EV isolation [70] is greatly outperformed by newly available cheaper, quicker and more effective methods of EV isolation. A distinct increase in EV yield, purity and quality was demonstrated for EV isolation by polymer precipitation, affinity chromatography and SEC over UC. Recovered dsDNA concentrations were also low, and findings indicate many large co-isolates which are not EVs. ExoQuick was found to isolate a relatively pure EV fraction, but to be unable to compete with the overall performance of TEI and ExoEasy with regards to factors such as overall vesicle yield, abundance of exosome marker proteins and dsDNA yield.

qEV was shown to isolate the purest EVs of any technique, yielding nanoparticles in the ideal range for exosomes while also showing a significantly higher content of exosome marker proteins than any other tested technique. qEV additionally isolated by far the greatest fraction of KRAS mutated dsDNA alleles, falling in line with reports of a link between the two [8, 11]. qEV was shown to perform marginally better than ExoEasy with regard to overall dsDNA isolation. The total yield of dsDNA, however, in EV isolates from qEV were shown to be much lower than that of TEI in samples from both CCM and plasma. The TEI technique was shown to isolate a disproportionally large amount of dsDNA from both CCM and plasma when compared to any of the other techniques tested. TEI was also observed to co-isolate a very large amount of non-vesicle macromolecules. Findings indicated that TEI may isolate large EVs such as oncosomes or MVs to a much greater extent than the other EV isolation techniques, and that the disproportionate dsDNA yield may originate from these larger EVs. While KRAS mutated alleles were identified in TEI samples, the relative fraction of these was less than that which was found in both qEV and ExoEasy. The TEI isolated EVs were found to be poor in exosome marker proteins. EVs isolated by the ExoEasy techniques were characterized by a very small average size and very high concentrations. The relative fraction of CD63 in EVs from ExoEasy was found to be greater than that of those from TEI, while CD9 was equal between the two. Findings indicated a heterogeneous nanoparticle population with a slightly better overall yield than qEV of dsDNA from CCM, but marginally less from plasma. The relative fraction of exosome marker proteins in EVs from ExoEasy was found to be greater than that of TEI, and the relative fraction of KRAS mutated alleles to be marginally better. It was found that overall, the performance of TEI and qEV was somewhat superior to that of ExoEasy, and overall the best when weighted against criteria deemed the most relevant for EV isolation with prospects of use as a biomarker for PC.

In the short term, the findings in this study calls for future investigation of the specific properties of the EVs isolated by the qEV and TEI techniques in particular. Further testing needs to be done on EV isolates in order to more directly determine the types of vesicles present by further testing for different biomarkers, and preferably techniques such as electron microscopy. Further study is necessary in order to determine to what extent the lower measured concentration of EVs and dsDNA in qEV isolate is due to the exclusion of irrelevant material, and the dsDNA contents of the two techniques should be investigated in order to uncover any differences in fragment length and origin. While on one hand qEV appears to isolate very pure fractions of EVs and tumour DNA, overall low concentrations and EV yields make TEI a tempting option. Barring their low concentration, while the qEV isolates may appear to hold a much higher purity of relevant EVs and dsDNA, the process of SEC EV isolation is still significantly more laborious and time consuming than the process required for EV isolation by TEI. As such, it should

be studied if the TEI isolate quality is sufficiently high, as it would be preferable with a quicker process for any potential future clinical routine EV isolation. Finally, the extent to which SEC and polymer precipitation isolated dsDNA with the current methodology holds prognostic qualities which are different or superior to that of general cell-free DNA isolated directly from plasma, and if not; what changes can be made to increase their viability.

The tumour DNA content taken into account, there can be little doubt that EVs and EV isolation will play a central role in future cancer diagnosis. As technologies within EV purification and next generation sequencing continue to progress, EVs are likely to provide a non-invasive window into the internal environment of organs and tissues which would otherwise require a large medical intervention. With further research, their circulating nature and general abundance may make exosomes and other EVs an invaluable tool for early detection of pancreatic cancer, as well as other malignancies.

6. REFERENCES

1. Lewis, A.R., J.W. Valle, and M.G. McNamara, *Pancreatic cancer: Are "liquid biopsies" ready for prime-time?* World Journal of Gastroenterology, 2016. **22**(32): p. 7175-7185.
2. Kaur, S., et al., *Early diagnosis of pancreatic cancer: challenges and new developments.* Biomarkers in medicine, 2012. **6**(5): p. 597-612.
3. Haque, I.S. and O. Elemento, *Challenges in Using ctDNA to Achieve Early Detection of Cancer.* bioRxiv, 2017.
4. Costa-Silva, B., et al., *Pancreatic cancer exosomes initiate pre-metastatic niche formation in the liver.* Nature cell biology, 2015. **17**(6): p. 816-826.
5. Armstrong, D. and D.E. Wildman, *Extracellular Vesicles and the Promise of Continuous Liquid Biopsies.* Journal of Pathology and Translational Medicine, 2018. **52**(1): p. 1-8.
6. Kahlert, C., et al., *Identification of Double-stranded Genomic DNA Spanning All Chromosomes with Mutated KRAS and p53 DNA in the Serum Exosomes of Patients with Pancreatic Cancer.* The Journal of Biological Chemistry, 2014. **289**(7): p. 3869-3875.
7. *Journal of Extracellular Vesicles*. 2018 [cited 2018 07. june]; Available from: https://www.tandfonline.com/toc/zjev20/current.
8. *ExoCarta Exosome Protein, RNA and Lipid Database*. 2018 [cited 2018 08. june]; Available from: http://www.exocarta.org/.
9. Yáñez-Mó, M., et al., *Biological properties of extracellular vesicles and their physiological functions.* Journal of Extracellular Vesicles, 2015. **4**: p. 10.3402/jev.v4.27066.
10. Willms, E., et al., *Extracellular Vesicle Heterogeneity: Subpopulations, Isolation Techniques, and Diverse Functions in Cancer Progression.* Frontiers in Immunology, 2018. **9**: p. 738.
11. Huang, X., et al., *Characterization of human plasma-derived exosomal RNAs by deep sequencing.* BMC Genomics, 2013. **14**: p. 319-319.
12. Cheng, L., et al., *Characterization and deep sequencing analysis of exosomal and non-exosomal miRNA in human urine.* Kidney Int, 2014. **86**(2): p. 433-44.
13. Ogawa, Y., et al., *Exosome-Like Vesicles with Dipeptidyl Peptidase IV in Human Saliva.* Biological and Pharmaceutical Bulletin, 2008. **31**(6): p. 1059-1062.
14. Melo, S.A., et al., *Glypican-1 identifies cancer exosomes and detects early pancreatic cancer.* Nature, 2015. **523**: p. 177.

15. Das, K., et al., *The Protease Activated Receptor2 Promotes Rab5a Mediated Generation of Pro-metastatic Microvesicles.* Scientific Reports, 2018. **8**: p. 7357.
16. Muhsin-Sharafaldine, M.-R. and A.D. McLellan, *Tumor-Derived Apoptotic Vesicles: With Death They Do Part.* Frontiers in Immunology, 2018. **9**: p. 957.
17. Abak, A., A. Abhari, and S. Rahimzadeh, *Exosomes in cancer: small vesicular transporters for cancer progression and metastasis, biomarkers in cancer therapeutics.* PeerJ, 2018. **6**: p. e4763.
18. Meehan, B., J. Rak, and D. Di Vizio, *Oncosomes – large and small: what are they, where they came from?* Journal of Extracellular Vesicles, 2016. **5**: p. 10.3402/jev.v5.33109.
19. Gould, S.J. and G. Raposo, *As we wait: coping with an imperfect nomenclature for extracellular vesicles.* Journal of Extracellular Vesicles, 2013. **2**: p. 10.3402/jev.v2i0.20389.
20. Coumans, F.A.W., et al., *Methodological Guidelines to Study Extracellular Vesicles.* Circ Res, 2017. **120**(10): p. 1632-1648.
21. Kastelowitz, N. and H. Yin, *Exosomes and Microvesicles: Identification and Targeting By Particle Size and Lipid Chemical Probes.* Chembiochem : a European journal of chemical biology, 2014. **15**(7): p. 923-928.
22. Kalluri, R., *The biology and function of exosomes in cancer.* J Clin Invest, 2016. **126**(4): p. 1208-15.
23. Batagov, A.O. and I.V. Kurochkin, *Exosomes secreted by human cells transport largely mRNA fragments that are enriched in the 3'-untranslated regions.* Biology Direct, 2013. **8**: p. 12-12.
24. Taylor, D.D., H.D. Homesley, and G.J. Doellgast, *Binding of Specific Peroxidase-labeled Antibody to Placental-type Phosphatase on Tumor-derived Membrane Fragments.* Cancer Research, 1980. **40**(11): p. 4064.
25. Takahashi, A.e.a., *Exosomes maintain cellular homeostasis by excreting harmful DNA from cells.* Nature Communications, 2017. **8**.
26. Salem, K.Z., et al., *Exosomes in Tumor Angiogenesis.* Methods Mol Biol, 2016. **1464**: p. 25-34.
27. Elmore, S., *Apoptosis: A Review of Programmed Cell Death.* Toxicologic pathology, 2007. **35**(4): p. 495-516.
28. Jiang, L., et al., *Determining the contents and cell origins of apoptotic bodies by flow cytometry.* Scientific Reports, 2017. **7**(1): p. 14444.
29. Atkin-Smith, G.K., et al., *A novel mechanism of generating extracellular vesicles during apoptosis via a beads-on-a-string membrane structure.* Nature Communications, 2015. **6**: p. 7439.

30. Bergsmedh, A., et al., *Horizontal transfer of oncogenes by uptake of apoptotic bodies.* Proceedings of the National Academy of Sciences of the United States of America, 2001. **98**(11): p. 6407-6411.
31. Gregory, C.D. and I. Dransfield, *Apoptotic Tumor Cell-Derived Extracellular Vesicles as Important Regulators of the Onco-Regenerative Niche.* Frontiers in Immunology, 2018. **9**: p. 1111.
32. Johnstone, R.M., et al., *Vesicle formation during reticulocyte maturation. Association of plasma membrane activities with released vesicles (exosomes).* J Biol Chem, 1987. **262**(19): p. 9412-20.
33. Li, P., et al., *Progress in Exosome Isolation Techniques.* Theranostics, 2017. **7**(3): p. 789-804.
34. Sun, Y.-Z., et al., *Extracellular Vesicles: A New Perspective in Tumor Therapy.* BioMed Research International, 2018. **2018**: p. 2687954.
35. Fernando, M.R., et al., *New evidence that a large proportion of human blood plasma cell-free DNA is localized in exosomes.* PLoS One, 2017. **12**(8): p. e0183915.
36. Skog, J., et al., *Glioblastoma microvesicles transport RNA and protein that promote tumor growth and provide diagnostic biomarkers.* Nature cell biology, 2008. **10**(12): p. 1470-1476.
37. Chahar, H.S., X. Bao, and A. Casola, *Exosomes and Their Role in the Life Cycle and Pathogenesis of RNA Viruses.* Viruses, 2015. **7**(6): p. 3204-25.
38. Di Vizio, D., et al., *Oncosome formation in prostate cancer: Association with a region of frequent chromosomal deletion in metastatic disease.* Cancer research, 2009. **69**(13): p. 5601-5609.
39. Minciacchi, V.R., M.R. Freeman, and D. Di Vizio, *Extracellular Vesicles in Cancer: Exosomes, Microvesicles and the Emerging Role of Large Oncosomes.* Seminars in cell & developmental biology, 2015. **40**: p. 41-51.
40. Wolf, P., *The nature and significance of platelet products in human plasma.* Br J Haematol, 1967. **13**(3): p. 269-88.
41. Hulsmans, M. and P. Holvoet, *MicroRNA-containing microvesicles regulating inflammation in association with atherosclerotic disease.* Cardiovasc Res, 2013. **100**(1): p. 7-18.
42. Gatti, S., et al., *Microvesicles derived from human adult mesenchymal stem cells protect against ischaemia-reperfusion-induced acute and chronic kidney injury.* Nephrol Dial Transplant, 2011. **26**(5): p. 1474-83.
43. Martinez, M.C., et al., *Transfer of differentiation signal by membrane microvesicles harboring hedgehog morphogens.* Blood, 2006. **108**(9): p. 3012-20.

44. Diehl, P., et al., *Microparticles: major transport vehicles for distinct microRNAs in circulation.* Cardiovasc Res, 2012. **93**(4): p. 633-44.
45. Szatanek, R., et al., *Isolation of extracellular vesicles: Determining the correct approach (Review).* International Journal of Molecular Medicine, 2015. **36**(1): p. 11-17.
46. Lötvall, J., et al., *Minimal experimental requirements for definition of extracellular vesicles and their functions: a position statement from the International Society for Extracellular Vesicles.* Journal of Extracellular Vesicles, 2014. **3**: p. 10.3402/jev.v3.26913.
47. Benedikter, B.J., et al., *Ultrafiltration combined with size exclusion chromatography efficiently isolates extracellular vesicles from cell culture media for compositional and functional studies.* Scientific Reports, 2017. **7**: p. 15297.
48. Pedersen, K., et al., *Direct Isolation of Exosomes from Cell Culture: Simplifying Methods for Exosome Enrlchment and Analysis*. Vol. 6. 2015. 1-9.
49. Linares, R., et al., *High-speed centrifugation induces aggregation of extracellular vesicles.* Journal of Extracellular Vesicles, 2015. **4**: p. 10.3402/jev.v4.29509.
50. Webber, J. and A. Clayton, *How pure are your vesicles?* Journal of Extracellular Vesicles, 2013. **2**: p. 10.3402/jev.v2i0.19861.
51. Zeringer, E., et al., *Strategies for Isolation of Exosomes*. Vol. 2015. 2015. pdb.top074476.
52. Batrakova, E.V. and M.S. Kim, *Using exosomes, naturally-equipped nanocarriers, for drug delivery.* Journal of controlled release : official journal of the Controlled Release Society, 2015. **219**: p. 396-405.
53. Welton, J.L., et al., *Ready-made chromatography columns for extracellular vesicle isolation from plasma.* Journal of Extracellular Vesicles, 2015. **4**: p. 10.3402/jev.v4.27269.
54. Stranska, R., et al., *Comparison of membrane affinity-based method with size-exclusion chromatography for isolation of exosome-like vesicles from human plasma.* Journal of Translational Medicine, 2018. **16**: p. 1.
55. Scientific, T.F. *Overview of Affinity Purification*. 2018 [cited 2018 09. june]; Available from: https://www.thermofisher.com/no/en/home/life-science/protein-biology/protein-biology-learning-center/protein-biology-resource-library/pierce-protein-methods/overview-affinity-purification.html.
56. Coumans, F.A.W., et al., *Reproducible extracellular vesicle size and concentration determination with tunable resistive pulse sensing.* Journal of Extracellular Vesicles, 2014. **3**: p. 10.3402/jev.v3.25922.

57. Izon_Science. *The qNano Gold*. 2018 [cited 2018 09. June]; Available from: http://izon.com/qnano-gold/.
58. Osteikoetxea, X., et al., *Differential detergent sensitivity of extracellular vesicle subpopulations.* Org Biomol Chem, 2015. **13**(38): p. 9775-82.
59. *Exosome Quantitation*. 2018 2018 [cited 2018 09. june]; Available from: https://www.systembio.com/products/exosome-research/exosome-quantitation/.
60. H, S., et al., *Development of a bead-assisted flow cytometry method for the semi-quantitative analysis of EVs*. 2015.
61. *Multiplex Cytometric Bead Array: The ABCs of CBAs*. 2018 [cited 2018 09. june]; Available from: https://bitesizebio.com/31909/multiplex-cytometric-bead-array/.
62. Gilje, B., et al., *High-Fidelity DNA Polymerase Enhances the Sensitivity of a Peptide Nucleic Acid Clamp PCR Assay for K-ras Mutations.* The Journal of Molecular Diagnostics : JMD, 2008. **10**(4): p. 325-331.
63. *The R project for Statistical Computing*. 2018 [cited 2018 27.05.2018]; Available from: https://www.r-project.org/.
64. Tjensvoll, K., et al., *Clinical relevance of circulating KRAS mutated DNA in plasma from patients with advanced pancreatic cancer.* Mol Oncol, 2016. **10**(4): p. 635-43.
65. Däbritz, J., et al., *Detection of Ki-ras mutations in tissue and plasma samples of patients with pancreatic cancer using PNA-mediated PCR clamping and hybridisation probes.* British Journal of Cancer, 2005. **92**(2): p. 405-412.
66. Sáenz-Cuesta, M., et al., *Methods for Extracellular Vesicles Isolation in a Hospital Setting.* Frontiers in Immunology, 2015. **6**: p. 50.
67. Andreu, Z., et al., *Comparative analysis of EV isolation procedures for miRNAs detection in serum samples.* Journal of Extracellular Vesicles, 2016. **5**: p. 10.3402/jev.v5.31655.
68. *Invitrogen Total Exosome Isolation Reagent (From cell culture media)*. 2018 [cited 2018 06. june]; Available from: https://www.thermofisher.com/order/catalog/product/4478359.
69. *ExoQuick-TC*. 2018 [cited 2018 06. june]; Available from: https://www.systembio.com/products/exosome-research/exosome-isolation/exoquick-tc/.
70. Gardiner, C., et al., *Techniques used for the isolation and characterization of extracellular vesicles: results of a worldwide survey.* Journal of Extracellular Vesicles, 2016. **5**: p. 10.3402/jev.v5.32945.

7. APPENDIX

7.1 Calculations

Calculation of dsDNA/mL starting material (Qubit dsDNA HS assay)

For determination of dsDNA/ml CCM/plasma used during EV isolation, the calculation performed was structured as follows:

1) $Qubit\ output\left(\frac{ng}{mL}\right) * volume\ of\ total\ DNA\ eluate\ (mL) = total\ DNA\ isolated\ (ng) = "a"$

Note: this volume = 100µL for all Allprep samples (= all CCM samples) and 50µL for all QiaAmp samples (= all plasma samples).

2) "a" has to be scaled by a factor in order to reflect the DNA present in the volume of EV isolate which was not used for DNA isolation. This factor is obtained by dividing the full EV isolate volume by the volume used for DNA isolation:

   a. Allprep/QiaAmp on 100µL EV isolate sample; full EV isolate sample = 500µL. $\frac{500}{100} = 5 = scaling\ factor$
   b. Allprep on 70µL EV isolate sample; full EV isolate volume = 500µL.
   $$\frac{500}{70} \approx 7{,}143 = scaling\ factor$$

$a * scaling\ factor$
$= theoretical\ total\ DNA(ng) isolated\ form\ the\ full\ exosome\ isolate\ stock\ volume = "b"$

3) Total volume of raw material (CCM or plasma) used during EV isolation for a given technique = "c"
   Note: c= 16mL for all techniques other than UC, and 16,5 for UC.

4) $\frac{b}{c} = theoretical\ total\ dsDNA(ng) obtained\ per\ mL\ raw\ materal$

   Note: in the case of plasma, the volume C =1mL, and as such steps 3 and 4 may be disregarded when calculating dsDNA/mL plasma.

The qEV (Izon science) column protocol (Izon) dictates that the optimal EV concentration and purity is achieved by collecting the eluate in 3 separate fractions, each of 500µL. After discarding the column void volume of 3mL, this equates to qEV fractions 7, 8 and 9. While these qEV fractions were treated as separate samples during subsequent testing and measurements, they all originate from the same

volume of raw material. As such, these fractions were pooled together mathematically in order to better be able to compare the total dsDNA yields of the various EV isolation techniques:

1. $Qubit\ output\ \left(\frac{ng}{mL}\right) * volume\ of\ DNA\ eluate(mL) = total\ DNA\ isolated\ (ng) = "a"$
2. $\left(a_{qEV7} + a_{qEV8} + a_{qEV9}\right) = total\ dsDNA\ (ng)\ isolated\ from\ all\ qEV\ fractions = "\sum a"$

   ∑a has to be scaled by a factor in order to reflect the DNA present in the EV isolate not used in the DNA isolation technique. This factor is obtained by dividing the full EV isolate volume by the volume used for DNA isolation:
   Ex:

   Allprep on 100µL EV isolate sample * 3 qEV fractions = 300µL
   Full EV isolate volume of 3 qEV fractions = 500µL *3

$$\frac{1500}{300} = 5 = scaling\ factor$$

3. $\sum a * scaling\ factor =$
   $total\ dsDNA(ng)\ theoretically\ isolated\ from\ all\ 3\ full\ qEV\ exosome\ isolate\ fractions = "b"$
4. Total volume of CCM used for all three qEV fractions = 16mL.
5. $\frac{b}{16mL} = Total\ dsDNA(ng)\ isolated\ per\ mL\ of\ CCM\ used\ during\ exosome\ isolation$

   Note: in the case of EV isolates from plasma, the starting volume was 1mL. As such, steps 4 and 5 may be disregarded when calculating total qEV dsDNA/mL plasma.

<u>Calculation of dsDNA from plasma, taking the Qubit LOD into consideration</u>

The Qubit LOD corresponding to dsDNA/mL plasma was calculated as follows:

1. The LOD in the assay reaction mix = [dsDNA] ≥ 0,5ng/mL. For each assay, 20µL od DNA-isolate sample + 180µL of Qubit working solution was used, resulting in a 1:10 dilution of the stock DNA isolate.
2. $0{,}5\ \frac{ng}{mL} * 10 = 5\frac{ng}{mL} =$
   The minimum concentration of dsDNA required in the stock DNA isolate, in order to exceed the Qubit LOD

   The total elution volume of the DNA isolate (QiaAmp) = 50µL = 0,05mL

3. $5\frac{ng}{mL} * 0{,}05mL = 0{,}25ng =$
   The mass of dsDNA required to be present in the full stock DNA isolate in order to exceed the Qubit LOD

(100µL/500µl) =1/5 of the full EV isolate sample volume was used for DNA isolation

4. $0{,}25ng * 5 = 1{,}25ng =$
   The mass of dsDNA required to be present in the full EV isolate stock, in order to exceed the Qubit LOD
   The full EV isolate volume stems in each case from only 1mL of plasma.
5. $1{,}25\ ng/1mL =$
   The concentration of dsDNA required per mL of plasma in order to exceed the Qubit LOD

This method of minimizing estimation error however makes it all the more important to provide an accurate estimation of the uncertainty introduced by the method. In order to achieve the most accurate standard deviation when calculating across several parallel measurements, calculations were carried out as follows:

1) Each Qubit measurement was split into two values, "Val1" and "Val2"
   a. For measurements falling below the LOD, Val1= 0 and Val2= 1,25. In this way, the average contribution of each below-LOD measurement would be 0,625ng/mL (= LOD/2). Additionally, as the number of included values increases, calculated STDAV will approach 0,625. This will allow error bars to reflect the uncertainty of ± ½*LOD.
   b. For measurements above the LOD, VAL1 = VAL2 = the measured concentration. Thus, the average contribution of each such value will be the actually measured concentration, and the local STDAV contribution = 0.
2) The overall averages were then calculated using all data points (estimated and actual). This resulted in a large amount of data points for each dataset, bolstering the accuracy of the calculated STDAV.

<u>On calculating the number of exosomes from the ExoCet Exosome Quantitation Assay</u>

1. The OD405nm data from each well in the 96-well microtiter plate was correlated to its sample name according to the loading order
2. Each value was corrected by its appropriate blanking value
3. qEV fractions 7,8 and 9 were pooled by taking adding together the blanked OD405 of qEV 7, 8 and 9 of the same biological replicate and with the same technical replicate # (ex: qEV7 control group donor #1 TR1 + qEV8 control group donor #1 TR 1 + qEV9 control group donor #1 TR1)
4. Any negative values (those with an OD405nm lower than that of their respective blank) were removed.
5. The blanked values for the various standard solutions were averaged, and a standard curve constructed.
6. The formula of the standard curve was used in order to calculate the number of exosomes estimated to be present in each well.
7. The calculated number of exosomes was divided by 0,025mL, in order to get the value for Exosomes/mL sample. For the pooled qEV values, this number was 0,075mL.

   This is because 50µL of sample (diluted 1:1 with ExoCet lysis buffer) was divided across two wells on the microtiter plate during loading. Each well was therefore loaded with the

equivalent of 0,025mL sample. As the qEV-pooled values are the OD405 values of 3 such wells (corrected for blank), the total loaded sample volume also has to be multiplied by 3.

8. The value from (7) was multiplied by 0,5mL in order to get the value for total number of exosomes in the full EV isolate sample (the total elution volume of each EV isolation technique). For the pooled qEV values, this number was 1,5.

   This is because the total volume of EV isolate for each technique is 0,5mL. For the qEV sample, each fraction is 0,5mL. As such, when pooling the three, the total EV isolate volume is 1,5mL.
9. The value from 8 was divided by the volume of starting material used, in order to get a value for exosomes isolated/mL starting material. Because 1mL of plasma was used for all isolations (All three qEV fractions stem from the same 1mL plasma), this value is 1.

7.2 DNA

7.2.1 dsDNA from EV isolates from CCM

Summary: Qubit dsDNA from CCM isolated from EV isolates treated/untreated with DNase

Table 11: Qubit dsDNA HS assay corrected concentrations of dsDNA from CCM derived EVs. The left of the table shows measured dsDNA (ng) from EV isolates with no DNase treatment prior to DNA isolation, whereas the right of the table shows those DNase treated prior to DNA isolation. To the right of each column of concentrations, is a column showing the associated standard deviation (STDAV) for each value, based on the two technical replicate samples.

	No DNase treatment		**With DNase treatment**	
Sample ID	dsDNA ng/mL CCM	STDAV	dsDNA ng/mL CCM	STDAV
ExoEasy	23,18	3,41	19,96	3,36
TEI	45,36	3,17	44,34	8,64
ExoQuick	14,29	6,26	4,88	0,90
UC	2,65	1,09	1,69	0,70
qEV7	2,00	2,48	0,96	0,85
qEV8	4,20	2,08	2,17	0,39
qEV9	6,23	0,27	2,35	1,73

Qubit dsDNA unprocessed data from CCM derived exoDNA isolate samples, no DNase treatment

Table xx : Qubit dsDNA measurement data from 100µL non-DNase treated EV isolate samples from CCM. Each isolation techniques was measured in two technical replicated on the EV isolation from plasma level (ID 1 and 2), and each technical replicate was measured three times using the Qubit ("Meas.No." 1,2 and 3). The concentration of dsDNA measured directly in the Qubit assay is displayed in the column "[dsDNA]assay, and the value corrected to reflect the actual concentration in the stock DNA isolate is show under "[dsDNA]"

Sample #	ID	Meas. No.	[dsDNA]assay	[dsDNA] ng/mL
1	ExoEasy 1	1	84,30	843,00
		2	81,40	814,00
		3	80,00	800,00
2	ExoEasy2	1	67,20	672,00
		2	66,30	663,00
		3	65,90	659,00
3	qEV7 1	1	0,75	7,50
		2	0,79	7,90
		3	0,79	7,90
4	qEV7 2	1	11,60	116,00
		2	12,00	120,00
		3	12,40	124,00
5	qEV8 1	1	18,50	185,00
		2	18,00	180,00
		3	17,90	179,00
6	qEV8 2	1	8,71	87,10
		2	8,62	86,20

		3	8,84	88,40
7	qEV9 1	1	19,40	194,00
		2	19,20	192,00
		3	19,40	194,00
8	qEV9 2	1	21,50	215,00
		2	21,10	211,00
		3	19,10	191,00
9	TEI 1	1	153,00	1530,00
		2	152,00	1520,00
		3	152,00	1520,00
10	TEI 2	1	139,00	1390,00
		2	138,00	1380,00
		3	137,00	1370,00
11	ExoQuick 1	1	60,00	600,00
		2	59,70	597,00
		3	60,00	600,00
12	ExoQuick 2	1	31,50	315,00
		2	31,50	315,00
		3	31,70	317,00
13	UC 1	1	6,42	64,20
		2	6,20	62,00
		3	6,03	60,30
14	UC 2	1	11,70	117,00
		2	11,20	112,00
		3	11,00	110,00

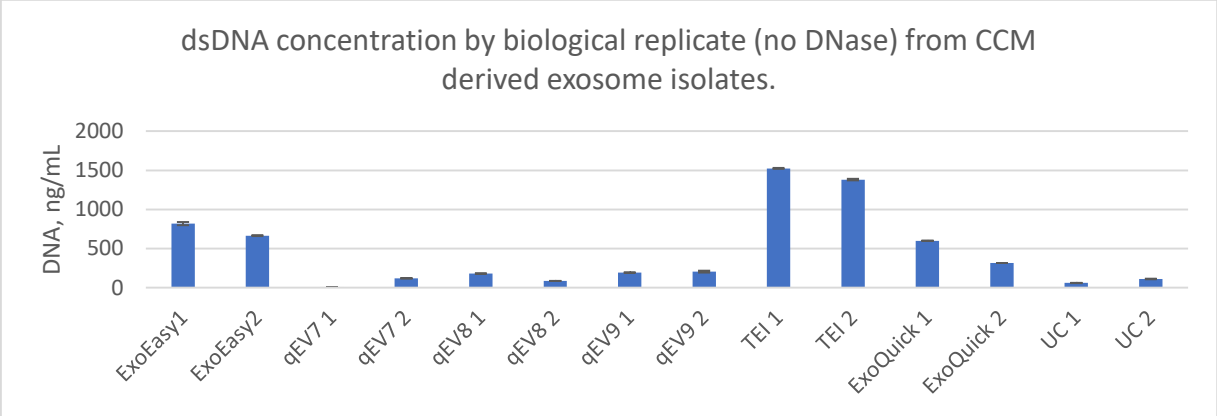

Figure xx: Qubit dsDNA HS assay measured dsDNA concentration per mL of CCM used, all TRs. DNA isolated from EV isolate material untreated with DNase. Error bare reflect the standard deviation between three sequential measurements of each prepared sample on the Qubit 2.0 fluorometer.

Qubit dsDNA from CCM **with** EV DNase treatment, raw data

Table xx: dsDNA measurement data (Qubit dsDNA HS assay) from 70µL of DNase treated EV isolate samples from CCM. Each isolation technique was measured in two technical replicates (ID 1 and 2), and each physical replicate measured three times on the Qubit 2.0 fluorometer (Meas. No. 1,2 and 3). The concentration of dsDNA measured directly in the Qubit assay is listed in the column labelled "[dsDNA]assay", whereas the dsDNA concentration corrected to reflect that of the stock DNA isolate is shown in the column labelled "[dsDNA]".

Sample #	ID	Meas. #	[dsDNA]assay	[dsDNA] ng/mL
1	ExoEasy BR1	1	39,40	394,00
		2	38,70	387,00

		3	38,20	382,00
2	ExoEasyBR2	1	50,10	501,00
		2	50,10	501,00
		3	49,90	499,00
3	TEI BR1	1	86,70	867,00
		2	85,30	853,00
		3	84,90	849,00
4	TEI BR2	1	114,00	1140,00
		2	113,00	1130,00
		3	112,00	1120,00
5	ExoQuick BR1	1	10,10	101,00
		2	9,25	92,50
		3	9,20	92,00
6	ExoQuick BR2	1	12,50	125,00
		2	12,40	124,00
		3	12,20	122,00
7	UC BR1	1	2,75	27,50
		2	2,77	27,70
		3	2,76	27,60
8	UC BR2	1	5,16	51,60
		2	5,05	50,50
		3	4,92	49,20
9	qEV7 BR1	1	0,79	7,90
		2	0,79	7,90
		3	0,79	7,90
10	qEV7 BR2	1	3,54	35,40
		2	3,44	34,40
		3	3,50	35,00
11	qEV8 BR1	1	5,52	55,20
		2	5,47	54,70
		3	5,48	54,80
12	qEV8 BR2	1	4,33	43,30
		2	4,22	42,20
		3	4,17	41,70
13	qEV9 BR1	1	8,20	82,00
		2	8,11	81,10
		3	7,68	76,80
14	qEV9 BR2	1	2,61	26,10
		2	2,50	25,00
		3	2,44	24,40

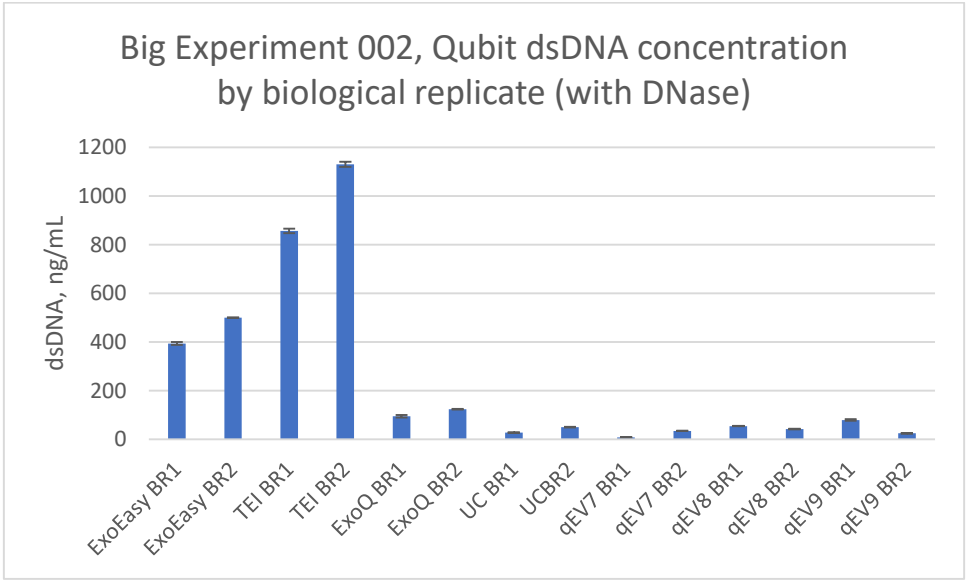

Figure xx: Error bars reflect the standard deviation between the three measurements on the Qubit instrument.

Table xx: Qubit measured concentrations of dsDNA from CCM derived EVs without DNase treatment (average of TR's)

Sample ID	dsDNA/mL CCM	STDAV
ExoEasy	23,18	3,41
TEI	45,36	3,17
ExoQuick	14,29	6,26
UC	2,65	1,09
qEV	12,43	2,39

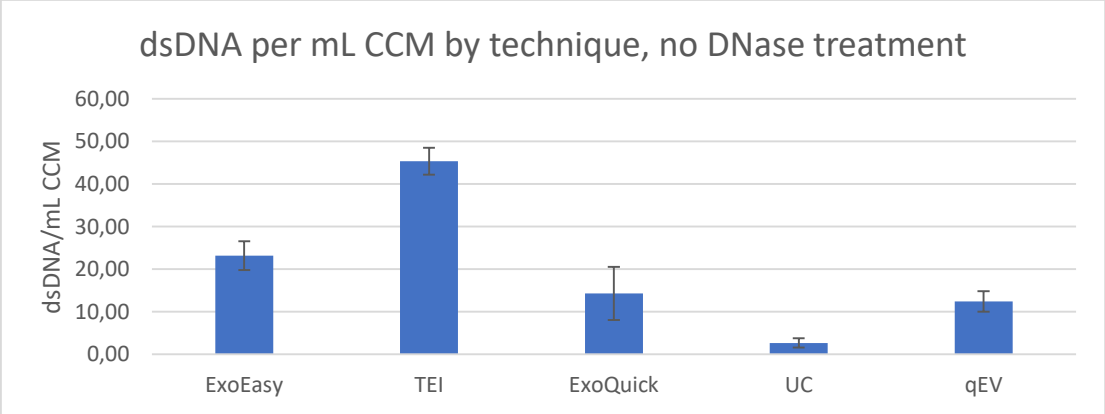

Figure xx: dsDNA /mL CCM by EV isolation technique, without DNase treatment

CCM with DNase

Table xx: Qubit measured concentrations of dsDNA from CCM derived EVs with DNase treatment (average of TR's)

Sample ID	dsDNA/mL CCM	STDAV
ExoEasy	19,96	3,36
TEI	44,34	8,64
ExoQuick	4,88	0,90
UC	1,69	0,70
qEV	5,47	1,11

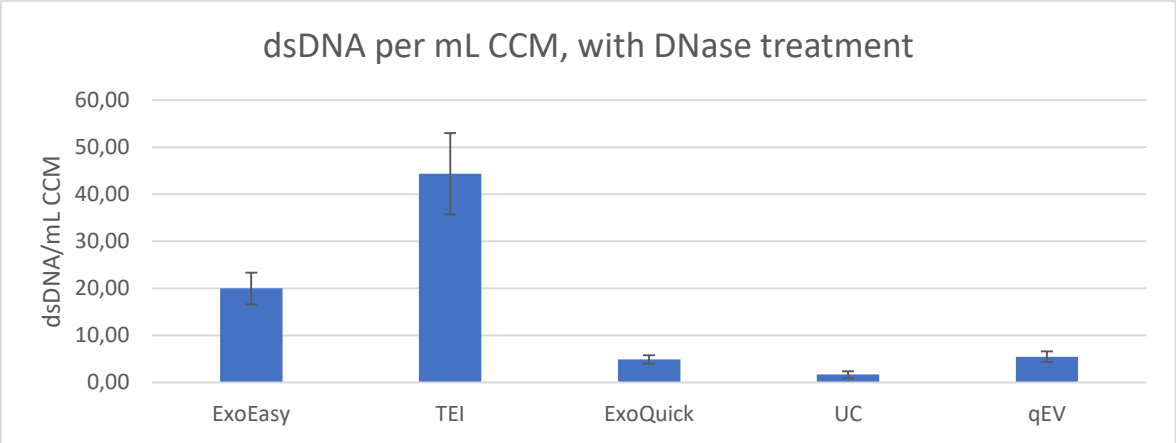

Figure xx: dsDNA /mL CCM by EV isolation technique with DNase treatment

Table xx: Qubit measured concentrations of dsDNA from CCM derived EVs with and without DNase treatment, compared (average of TR's).

Sample ID	dsDNA (ng) /mL CCM No DNase	STDAV	dsDNA (ng) /mL CCM With DNase	STDAV2
ExoEasy	23,18	3,41	19,96	3,36
TEI	45,36	3,17	44,34	8,64
ExoQuick	14,29	6,26	4,88	0,90
UC	2,65	1,09	1,69	0,70
qEV	12,43	2,39	5,47	1,11

7.2.2 dsDNA (Qubit) from plasma derived EV isolates

Summary of corrected values for EV dsDNA/mL plasma can be seen below (table 13).

Table 13: Qubit dsDNA HS assay corrected concentrations of dsDNA from plasma derived EV isolates. The left of the table shows measured dsDNA from control group samples, whereas the right of the table shows measured dsDNA from PC-patient samples. To the right of each column of concentrations is a column showing the associated standard deviation (STDAV) for each concentration value, based on the three biological replicates for each EV isolation technique. Note that the limit of detection (LOD) of the assay is 1.25ng dsDNA/mL plasma (normalized).

	Control group		**PC patient group**	
Sample ID	dsDNA /mL CCM	STDAV	dsDNA /mL CCM	STDAV
ExoEasy	1,61	1,51458518	1,16	0,94
TEI	2,38	2,27157513	4,21	2,87
qEV7	1,64	1,55188378	1,87	0,76
qEV8	1,73	1,70423434	1,34	0,67
qEV9	1,98	2,01041731	1,40	0,70

(all data from DNase treated EV isolate)

SE003 (control group donor #1)

sample #	Sample Set	Sample ID	Meas. #	Assay ng/mL	dsDNA ng/mL
1	SE003	ExoEasy BR1	1	<0,50	N/A
			2	<0,50	N/A
			3	<0,50	N/A
2	SE003	ExoEasy BR2	1	<0,50	N/A
			2	<0,50	N/A
			3	<0,50	N/A
3	SE003	TEI BR1	1	<0,50	N/A
			2	<0,50	N/A
			3	<0,50	N/A
4	SE003	TEI BR2	1	0,63	6,3
			2	0,64	6,4
			3	0,66	6,6
5	SE003	qEV7 BR1	1	<0,50	N/A
			2	<0,50	N/A
			3	<0,50	N/A
6	SE003	qEV7 BR2	1	<0,50	N/A
			2	<0,50	N/A
			3	<0,50	N/A
7	SE003	qEV8 BR1	1	<0,50	N/A
			2	<0,50	N/A
			3	<0,50	N/A
8	SE003	qEV8 BR2	1	<0,50	N/A
			2	<0,50	N/A
			3	<0,50	N/A

9	SE003	qEV9 BR1	1	<0,50	N/A
			2	<0,50	N/A
			3	<0,50	N/A
10	SE003	qEV9 BR2	1	<0,50	N/A
			2	<0,50	N/A
			3	<0,50	N/A

SE004 (control group donor #2)

sample #	Sample Set	Sample ID	Meas. #	Assay ng/mL	dsDNA ng/mL
1	SE004	ExoEasy BR1	1	<0,50	N/A
			2	<0,50	N/A
			3	<0,50	N/A
2	SE004	ExoEasy BR2	1	<0,50	N/A
			2	<0,50	N/A
			3	<0,50	N/A
3	SE004	TEI BR1	1	<0,50	N/A
			2	<0,50	N/A
			3	<0,50	N/A
4	SE004	TEI BR2	1	<0,50	N/A
			2	<0,50	N/A
			3	<0,50	N/A
5	SE004	qEV7 BR1	1	<0,50	N/A
			2	<0,50	N/A
			3	<0,50	N/A
6	SE004	qEV7 BR2	1	<0,50	N/A
			2	<0,50	N/A
			3	<0,50	N/A
7	SE004	qEV8 BR1	1	<0,50	N/A
			2	<0,50	N/A
			3	<0,50	N/A
8	SE004	qEV8 BR2	1	<0,50	N/A
			2	<0,50	N/A
			3	<0,50	N/A
9	SE004	qEV9 BR1	1	<0,50	N/A
			2	<0,50	N/A
			3	<0,50	N/A
10	SE004	qEV9 BR2	1	<0,50	N/A
			2	<0,50	N/A
			3	<0,50	N/A

SE005 (control group donor #3)

sample #	Sample Set	Sample ID	Meas. #	Assay ng/mL	dsDNA ng/mL
1	SE005	ExoEasy	1	1,37	13,70
			2	1,37	13,70

			3	1,33	13,30
2	SE005	ExoEasy	1	1,76	17,60
			2	1,38	13,80
			3	1,35	13,50
3	SE005	TEI	1	2,30	23,00
			2	1,95	19,50
			3	1,83	18,30
4	SE005	TEI	1	2,66	26,60
			2	2,15	21,50
			3	2,60	20,60
5	SE005	qEV7	1	1,45	14,50
			2	1,41	14,10
			3	1,39	13,90
6	SE005	qEV7	1	1,56	15,60
			2	1,54	15,40
			3	1,48	14,80
7	SE005	qEV8	1	1,26	13,60
			2	1,32	13,20
			3	1,36	13,60
8	SE005	qEV8	1	1,79	17,90
			2	1,84	18,40
			3	1,80	18,00
9	SE005	qEV9	1	1,91	19,10
			2	1,93	19,30
			3	1,82	18,20
10	SE005	qEV9	1	1,96	19,60
			2	1,85	18,50
			3	1,77	17,70

SE006 (PC patient donor #1)

sample #	Sample Set	Sample ID	Meas. #	Assay ng/mL	dsDNA ng/mL
1	PC39B11	ExoEasy	1	<0,50	N/A
			2	<0,50	N/A
			3	<0,50	N/A
2	PC39B11	TEI	1	0,95	9,5
			2	0,95	9,5
			3	0,94	9,4
3	PC39B11	qEV7	1	1,18	11,8
			2	1,16	11,6
			3	1,14	11,4
4	PC39B11	qEV8	1	<0,50	N/A
			2	<0,50	N/A
			3	<0,50	N/A
5	PC39B11	qEV9	1	<0,50	N/A
			2	<0,50	N/A
			3	<0,50	N/A

SE007 (PC patient donor #2)

Sample #	SE	ID	Meas #	Assay ng/mL	dsDNA ng/mL
1	PC47B7B	ExoEasy	1	0,93	9,30
			2	0,88	8,80
			3	0,87	8,70

2	PC47B7B	TEI	1	3,30	33,00
			2	3,24	32,40
			3	3,23	32,30
3	PC47B7B	qEV7	1	0,59	5,90
			2	0,58	5,80
			3	0,56	5,60
4	PC47B7B	qEV8	1	0,79	7,90
			2	0,76	7,60
			3	0,76	7,60
5	PC47B7B	qEV9	1	0,81	8,10
			2	0,80	8,00
			3	0,78	7,80

SE008 (PC patient donor #3)

Sample #	SE	ID	Meas #	Assay ng/mL	dsDNA ng/mL
1	PC48B7	ExoEasy	1	<0,50	N/A
			2	<0,50	N/A
			3	<0,50	N/A
2	PC48B7	TEI	1	0,83	8,30
			2	0,85	8,50
			3	0,85	8,50
3	PC48B7	qEV7	1	0,51	5,10
			2	0,50	5,00
			3	0,50	5,00
4	PC48B7	qEV8	1	0,60	6,00
			2	0,60	6,00
			3	0,57	5,70
5	PC48B7	qEV9	1	0,65	6,50
			2	0,64	6,40
			3	0,62	6,20

Control group

Table xx: Qubit measured concentrations of dsDNA from control group plasma derived EVs with EV DNase treatment

ID	dsDNA ng/mL	STDAV	LOD
ExoEasy	1,61	1,51458518	1,25
TEI	2,38	2,27157513	1,25
qEV7	1,64	1,55188378	1,25
qEV8	1,73	1,70423434	1,25
qEV9	1,98	2,01041731	1,25

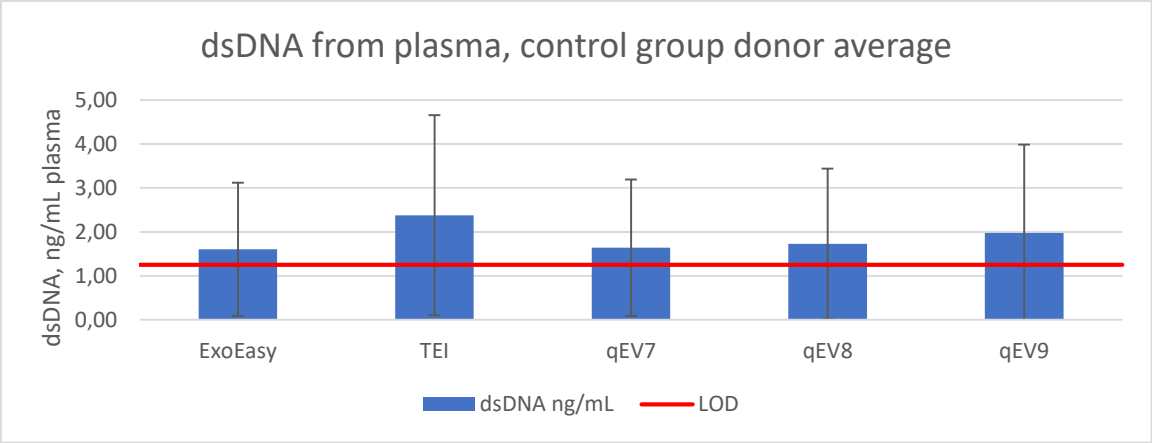

Figure xx: dsDNA /mL plasma from control group by EV isolation technique, with EV DNase treatment

Table xx: Qubit measured concentrations of dsDNA from control group plasma derived EVs with EV DNase treatment, qEV fractions pooled

ID	dsDNA ng	STDAV	LOD
ExoEasy	1,61	1,51	1,25
TEI	2,38	2,27	1,25
qEV	5,35	1,76	1,25

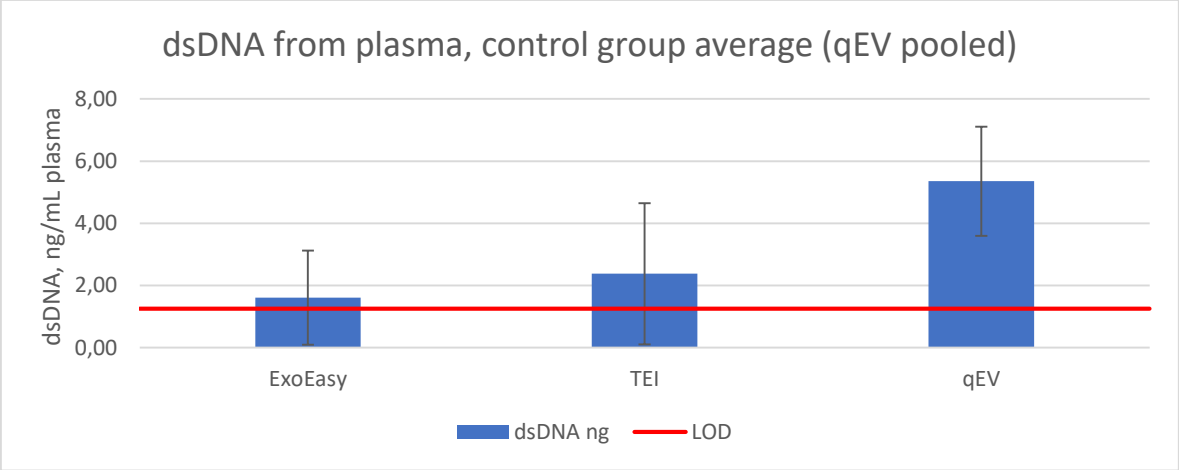

PC patient group:

Table xx: Qubit measured concentrations of dsDNA from patient group plasma derived EVs with EV DNase treatment

ID	dsDNA ng/mL	STDAV	LOD
ExoEasy	1,16	0,94	1,25
TEI	4,21	2,87	1,25
qEV7	1,87	0,76	1,25
qEV8	1,34	0,67	1,25
qEV9	1,40	0,70	1,25

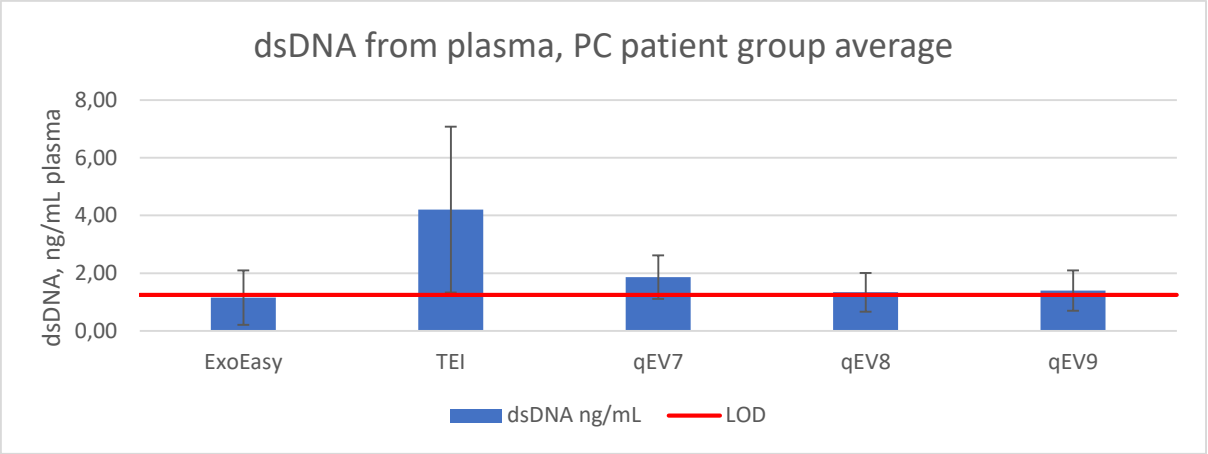

Figure xx: dsDNA /mL plasma from PC patient group by EV isolation technique, with EV DNase treatment

Table xx: Qubit measured concentrations of dsDNA from partient group plasma derived EVs with EV DNase treatment

ID	dsDNA ng	STDAV	LOD
ExoEasy	1,16	0,94	1,25
TEI	4,21	2,87	1,25
qEV	4,61	0,73	1,25

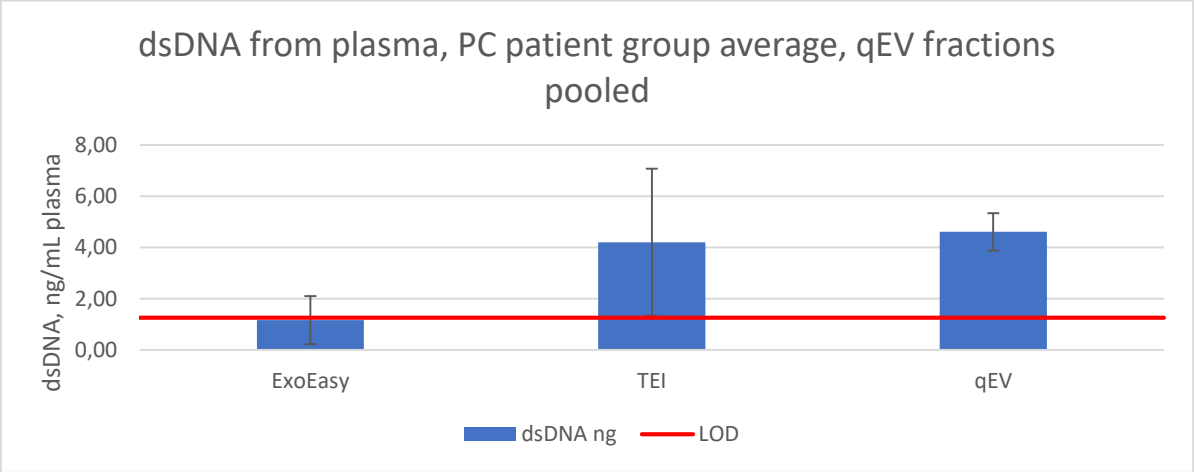

Figure xx: dsDNA /mL plasma from patient group by EV isolation technique, with EV DNase treatment

Comparisons

Table xx: Qubit measured concentrations of dsDNA from plasma derived EVs with EV DNase treatment, patient vs. control group

ID	Control group average	STDAV	PC patient average	STDAV2	LOD
ExoEasy	1,61	1,51	1,16	0,94	1,25

TEI	2,38	2,27	4,21	2,87	1,25
qEV7	1,64	1,55	1,87	0,76	1,25
qEV8	1,73	1,70	1,34	0,67	1,25
qEV9	1,98	2,01	1,40	0,70	1,25

Table xx: Qubit measured concentrations of dsDNA from plasma derived EVs with EV DNase treatment, patient vs. control group. qEV fractions pooled

ID	Control group average	STDAV	PC patient group average	STDAV2	LOD
ExoEasy	1,61	1,51	1,16	0,94	1,25
TEI	2,38	2,27	4,21	2,87	1,25
qEV	5,35	1,76	4,61	0,73	1,25

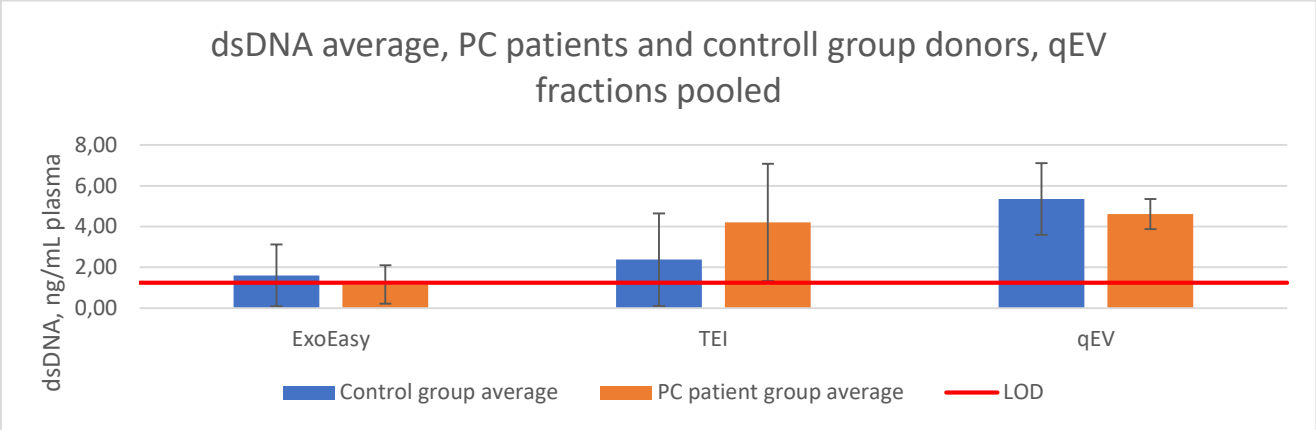

Figure xx: dsDNA /mL plasma from by EV isolation technique, control group vs. patient group. With EV DNase treatment, qEV fractions pooled

7.2.3 PNA clamping Assay for KRAS mutation data

PC patient #1

Table xx: PC patient #1 PNA assay for KRAS mutated alleles real-time PCR data. The sample ID column reflects the given ID anonymized tag of the PC-patient donor. The threshold (dR) denotes the florescence threshold for the real-time PCR assay.

The Cq value reflects the number of cycles required for each sample to reach the fluorescence threshold. Value(s) deemed to be of the wrong melting temperature (Tm), and therefore off-target sequences are marked in red.

Well	Sample ID	Well Type	Replicate	Threshold (dR)	Cq (dR)
A1	PC39B11_ExoEasy+PNA	Unknown	1	500	No Ct
A2	PC39B11_ExoEasy+PNA	Unknown	1	500	No Ct
A3	PC39B11_ExoEasy-PNA	Unknown	2	500	32,40
A4	PC39B11_ExoEasy-PNA	Unknown	2	500	32,25
B1	PC39B11_TEI+PNA	Unknown	3	500	No Ct
B2	PC39B11_TEI+PNA	Unknown	3	500	No Ct
B3	PC39B11_TEI-PNA	Unknown	4	500	32,51
B4	PC39B11_TEI-PNA	Unknown	4	500	32,32
C1	PC39B11_qEV7+PNA	Unknown	5	500	34,40
C2	PC39B11_qEV7+PNA	Unknown	5	500	No Ct
C3	PC39B11_qEV7-PNA	Unknown	6	500	35,67
C4	PC39B11_qEV7-PNA	Unknown	6	500	No Ct
D1	PC39B11_qEV8+PNA	Unknown	7	500	34,29
D2	PC39B11_qEV8+PNA	Unknown	7	500	No Ct
D3	PC39B11_qEV8-PNA	Unknown	8	500	No Ct
D4	PC39B11_qEV8-PNA	Unknown	8	500	35,16
E1	PC39B11_qEV9+PNA	Unknown	9	500	No Ct
E2	PC39B11_qEV9+PNA	Unknown	9	500	No Ct
E3	PC39B11_qEV9-PNA	Unknown	10	500	41,80
E4	PC39B11_qEV9-PNA	Unknown	10	500	No Ct

Table xx: PC patient #1 calculated ΔCq and ΔΔCq values, based on the average of the two replicates for each of the PNA positive and negative samples detailed in table xx. Value(s) deemed to be of the wrong melting temperature (Tm), and therefore off-target sequences are marked in red.

ID	ΔCq	ΔΔCq
ExoEasy	#DIV/0!	#DIV/0!
TEI	#DIV/0!	#DIV/0!
qEV7	-1,27	12,54
qEV8	-0,87	12,14
qEV9	#DIV/0!	#DIV/0!

PC patient #2

Table xx: : PC patient #2 PNA assay for KRAS mutated alleles real-time PCR data. The sample ID column reflects the given ID anonymized tag of the PC-patient donor. The threshold (dR) denotes the florescence threshold for the real-time PCR assay. The Cq value reflects the number of cycles required for each sample to reach the fluorescence threshold. Value(s) deemed to be of the wrong melting temperature (Tm), and therefore off-target sequences are marked in red.

Well	Sample ID	Well Type	Replicate	Threshold (dR)	Cq (dR)
F1	PC47B7_ExoEasy+PNA	Unknown	11	500	35,18
F2	PC47B7_ExoEasy+PNA	Unknown	11	500	36,67
F3	PC47B7_ExoEasy-PNA	Unknown	12	500	32,18
F4	PC47B7_ExoEasy-PNA	Unknown	12	500	33,42
G1	PC47B7_TEI+PNA	Unknown	13	500	35,64

G2	PC47B7_TEI+PNA	Unknown	13	500	33,33
G3	PC47B7_TEI-PNA	Unknown	14	500	29,96
G4	PC47B7_TEI-PNA	Unknown	14	500	29,86
H1	PC47B7_qEV7+PNA	Unknown	15	500	No Ct
H2	PC47B7_qEV7+PNA	Unknown	15	500	No Ct
H3	PC47B7_qEV7-PNA	Unknown	16	500	No Ct
H4	PC47B7_qEV7-PNA	Unknown	16	500	No Ct
A5	PC47B7_qEV8+PNA	Unknown	17	500	No Ct
A6	PC47B7_qEV8+PNA	Unknown	17	500	38,30
A7	PC47B7_qEV8-PNA	Unknown	18	500	35,09
A8	PC47B7_qEV8-PNA	Unknown	18	500	33,95
B5	PC47B7_qEV9+PNA	Unknown	19	500	No Ct
B6	PC47B7_qEV9+PNA	Unknown	19	500	35,94
B7	PC47B7_qEV9-PNA	Unknown	20	500	36,31
B8	PC47B7_qEV9-PNA	Unknown	20	500	33,62

Table xx: PC patient #2 calculated ΔCq and ΔΔCq values, based on the average of the two replicates for each of the PNA positive and negative samples detailed in table xx. Value(s) deemed to be of the wrong melting temperature (Tm), and therefore off-target sequences are marked in red.

ID	ΔCq	ΔΔCq
ExoEasy	3,13	8,15
TEI	4,58	6,70
qEV7	#DIV/0!	#DIV/0!
qEV8	3,78	7,49
qEV9	0,97	10,30

PC patient #3

Table xx: PC patient #3 PNA assay for KRAS mutated alleles real-time PCR data. The sample ID column reflects the given ID anonymized tag of the PC-patient donor. The threshold (dR) denotes the florescence threshold for the real-time PCR assay. The Cq value reflects the number of cycles required for each sample to reach the fluorescence threshold. Value(s) deemed to be of the wrong melting temperature (Tm), and therefore off-target sequences are marked in red.

Well	Sample ID	Well Type	Replicate	Threshold (dR)	Cq (dR)
C5	PC48B7_ExoEasy+PNA	Unknown	21	500	35,77
C6	PC48B7_ExoEasy+PNA	Unknown	21	500	No Ct
C7	PC48B7_ExoEasy-PNA	Unknown	22	500	36,08
C8	PC48B7_ExoEasy-PNA	Unknown	22	500	33,89
D5	PC48B7_TEI+PNA	Unknown	23	500	35,38
D6	PC48B7_TEI+PNA	Unknown	23	500	No Ct
D7	PC48B7_TEI-PNA	Unknown	24	500	32,58
D8	PC48B7_TEI-PNA	Unknown	24	500	No Ct
E5	PC48B7_qEV7+PNA	Unknown	25	500	No Ct
E6	PC48B7_qEV7+PNA	Unknown	25	500	36,34
E7	PC48B7_qEV7-PNA	Unknown	26	500	34,01
E8	PC48B7_qEV7-PNA	Unknown	26	500	32,83
F5	PC48B7_qEV8+PNA	Unknown	27	500	35,47
F6	PC48B7_qEV8+PNA	Unknown	27	500	No Ct
F7	PC48B7_qEV8-PNA	Unknown	28	500	36,17
F8	PC48B7_qEV8-PNA	Unknown	28	500	37,18

G5	PC48B7_qEV9+PNA	Unknown	29	500	34,07
G6	PC48B7_qEV9+PNA	Unknown	29	500	33,46
G7	PC48B7_qEV9-PNA	Unknown	30	500	34,94
G8	PC48B7_qEV9-PNA	Unknown	30	500	34,98

Table xx: PC patient #3 calculated ΔCq and ΔΔCq values, based on the average of the two replicates for each of the PNA positive and negative samples detailed in table xx. Value(s) deemed to be of the wrong melting temperature (Tm), and therefore off-target sequences are marked in red.

ID	ΔCq	ΔΔCq
ExoEasy	0,79	10,49
TEI	2,80	8,47
qEV7	2,92	8,35
qEV8	-1,21	12,48
qEV9	-1,19	12,47

7.4 ExoCet

7.4.1. Exosome isolation from plasma, control group samples

EV samples from blood plasma collected from 3 presumed healthy donors, constituting the EVs from plasma control group.

Below is shown a summary of corrected ExoCet exosome quantitation result data for exosome isolates from plasma can be seen below (table 12)

Table 12: ExoCet Exosome Quantitation Assay data for EV isolate samples from plasma. The rightmost column displays each sample ID in the format "control group ID/ PC patient group ID". Control group data is found to the left in the table, and PC patient group data to the right. All concentration data is normalized to reflect exosomes isolated/mL of plasma used. Standard deviations are based on 4 technical replicates of each sample for the control group, and 2 technical replicates for each sample for the PC patient group.

	Control Group		**PC Patient Group**	
	Exosomes/mL Plasma	STDAV	Exosomes/mL plasma	STDAV
ExoEasy	3,65E+11	4,52E+10	3,58E+11	3,73E+10

TEI	1,03E+12	3,03E+11	8,17E+11	1,93E+11
qEV	2,00E+10	1,38E+10	6,78E+10	4,78E+10

Loading order (96 well microtiterplate):

Table 1: Loading order for the ExoCet assay 96-well microtiter plate. See next page for Legend.

	1	2	3	4	5	6	7	8	9	10	11	12
A	3EE 1-1	3q7 1-1	3q9 1-1	4TEI 1-1	4q8 1-1	5EE 1-1	5q7 1-1	5q9 1-1	AChE 1	S.NC q8 1	STD 1-1	STD 5-1
B	3EE 1-2	3q7 1-2	3q9 1-2	4TEI 1-2	4q8 1-2	5EE 1-2	5q7 1-2	5q9 1-2	AChE 2	S.NC q8 2	STD 1-2	STD 5-2
C	3EE 2-1	3q7 2-1	3q9 2-1	4TEI 2-1	4q8 2-1	5EE 2-1	5q7 2-1	5q9 2-1	S.NC EE 1	S.NC q9 1	STD 2-1	STD 6-1
D	3EE 2-2	3q7 2-2	3q9 2-2	4TEI 2-2	4q8 2-2	5EE 2-2	5q7 2-2	5q9 2-2	S.NC EE 2	S.NC q9 2	STD 2-2	STD 6-2
E	3TEI 1-1	3q8 1-1	4EE 1-1	4q7 1-1	4q9 1-1	5TEI 1-1	5q8 1-1	XE 1	S.NC TEI 1	-	STD 3-1	STD 7-1
F	3TEI 1-2	3q8 1-2	4EE 1-2	4q7 1-2	4q9 1-2	5TEI 1-2	5q8 1-2	XE 2	S.NC TEI 2	-	STD 3-2	STD 7-2
G	3TEI 2-1	3q8 2-1	4EE 2-1	4q7 2-1	4q9 2-1	5TEI 2-1	5q8 2-1	PBS 1	S.NC q7 1	-	STD 4-1	STD 8-1
H	3TEI 2-2	3q8 2-2	4EE 2-2	4q7 2-2	4q9 2-2	5TEI 2-2	5q8 2-2	PBS 2	S.NC q7 2	-	STD 4-2	STD 8-2

Control group sample loading order, Legend:

TR= Technical replicate,

BR= Biological replicate,

SE= Big experiment #

3EE 1-1: **3** = SE003, **EE**= ExoEasy sample, **1-1**= TR (EV isolate level) 1 – TR (ExoCet level) 1

3EE 1-2: **3** = SE003, **EE** = ExoEasy sample, **1-2**= TR TR (EV isolate level) 1 – TR (ExoCet level) 2

3EE 2-1: **3** = SE003, **EE**= ExoEasy sample, **2-1**= TR (EV isolate level) 2 – TR (ExoCet level) 1

3EE 2-2: **3** = SE003, **EE** = ExoEasy sample, **2-2**= TR TR (EV isolate level) 2 – TR (ExoCet level) 2

3TEI 1-1: **3 =**SE003, **TEI**= Total Exosome Isolation sample, **1-1**= TR (EV isolate level) 1 – TR (ExoCet level) 1

…

3q7 1-1: **3=** SE003, **q7**= qEV7 sample, **1-1**= TR (EV isolate level) 1 – TR (ExoCet level) 1

…

3q8 1-1: 3= SE003, **q8**= qEV8 sample, **1-1**= TR (EV isolate level) 1 – TR (ExoCet level) 1

…

3q9 1-1: 3= SE003, **q9**= qEV9 sample, **1-1**= TR (EV isolate level) 1 – TR (ExoCet level) 1

4EE 1-1: 4 = SE004, **EE**= ExoEasy sample, **1-1**= TR (EV isolate level) 1 – TR (ExoCet level) 1

…

S.NC: Specialized negative control for a given sample, constituted of 50µL of the sample loaded in a microtiter plate well containing (inert) reaction buffer A (no substrate-containing buffer B added)

XE: ExoEasy (Qiagen) elution buffer XE (negative control, blank for ExoEasy samples)

PBS: 1x PBS (negative control, blank for qEV and TEI samples)

AChE: Acetylcholine esterase (from eel [details from bottle] 1mg/mL stock) diluted to a concentration of 1µg/mL (positive control)

STD 1-1: ExoCet standard solution dilution 1 (no dilution), parallel 1

STD 1-2: ExoCet standard solution dilution 1 (no dilution), parallel 2

STD 2-1: ExoCet standard solution dilution 2 (1:2 dilution), parallel 1

…

Table xx: OD 405nm, EV isolation samples from plasma control group, 10 minutes of incubation (RT)

	1	2	3	4	5	6	7	8	9	10	11	12
A	0,713	0,448	0,467	0,979	0,453	0,641	0,405	0,421	1,666	0,052	1,594	0,54
B	0,68	0,431	0,431	0,949	0,44	0,624	0,434	0,435	1,609	0,049	2,041	0,521
C	0,668	0,445	0,452	1,017	0,451	0,647	0,439	0,45	0,052	0,051	1,039	0,491
D	0,665	0,421	0,441	0,993	0,443	0,623	0,442	0,451	0,048	0,058	1,066	0,497
E	1,259	0,442	0,626	0,438	0,446	0,907	0,443	0,449	0,128	N/A	0,756	0,475
F	1,27	0,432	0,632	0,445	0,444	0,899	0,452	0,46	0,133	N/A	0,75	0,468
G	1,267	0,45	0,641	0,434	0,455	0,801	0,451	0,448	0,043	N/A	0,605	0,451
H	1,217	0,432	0,645	0,436	0,446	0,794	0,432	0,433	0,043	N/A	0,611	0,404

Table xx: OD 405nm, EV isolation samples from plasma control group, 15 minutes of incubation (RT):

	1	2	3	4	5	6	7	8	9	10	11	12
A	0,783	0,447	0,457	1,101	0,453	0,698	0,403	0,421	2,053	0,052	1,97	0,565
B	0,749	0,429	0,431	1,059	0,44	0,697	0,432	0,434	1,97	0,049	2,513	0,542
C	0,732	0,444	0,452	1,169	0,45	0,707	0,435	0,448	0,05	0,052	1,245	0,504
D	0,729	0,42	0,441	1,13	0,441	0,68	0,442	0,45	0,048	0,051	1,273	0,511
E	1,465	0,44	0,674	0,436	0,447	1,038	0,438	0,446	0,129	N/A	0,863	0,482
F	1,477	0,43	0,682	0,443	0,445	1,027	0,448	0,453	0,133	N/A	0,855	0,475
G	1,475	0,448	0,694	0,433	0,455	0,894	0,448	0,444	0,044	N/A	0,655	0,45
H	1,398	0,431	0,702	0,435	0,447	0,889	0,431	0,431	0,043	N/A	0,665	0,403

Table xx: OD 405nm, EV isolation samples from plasma control group, 20 minutes of incubation (RT):

	1	2	3	4	5	6	7	8	9	10	11	12
A	0,853	0,446	0,467	1,227	0,453	0,759	0,403	0,421	2,403	0,056	2,326	0,598
B	0,818	0,429	0,432	1,176	0,438	0,734	0,431	0,433	2,303	0,049	2,973	0,564
C	0,793	0,443	0,455	1,324	0,449	0,767	0,433	0,45	0,049	0,052	1,447	0,513
D	0,793	0,419	0,443	1,271	0,441	0,738	0,44	0,45	0,048	0,053	1,477	0,523
E	1,662	0,44	0,727	0,435	0,447	1,171	0,437	0,445	0,128	N/A	0,969	0,489
F	1,678	0,429	0,735	0,442	0,444	1,156	0,445	0,452	0,133	N/A	0,963	0,481
G	1,664	0,447	0,749	0,432	0,455	0,988	0,446	0,442	0,043	N/A	0,707	0,449
H	1,573	0,43	0,77	0,433	0,447	0,985	0,43	0,428	0,043	N/A	0,72	0,4

7.4.2. EV isolation from plasma, PC patient group samples

EV samples from blood plasma collected from 3 pancreatic cancer (PC) patient blood plasma samples, constituting the PC patient group.

Loading order (96 well microtiterplate):

Table 1: Loading order for the ExoCet assay 96-well microtiter plate. See next page for Legend.

	1	2	3	4	5	6	7	8	9	10	11	12
A	6EE 1	6q9 1	7q8 1	8q7 1	PBS 1	SpecNC q7 1	STD 1-1	STD 5-1	-	-	-	-
B	6EE 2	6q9 2	7q8 2	8q7 2	PBS2	SpecNC q7 2	STD 1-2	STD 5-2	-	-	-	-
C	6TEI 1	7EE 1	7q9 1	8q8 1	AChE 1	SpecNC q8 1	STD 2-1	STD 6-1	-	-	-	-
D	6TEI 2	7 EE 2	7q9 2	8q8 2	AChE 2	SpecNC q8 2	STD 2-2	STD 6-2	-	-	-	-
E	6q7 1	7 TEI 1	8EE 1	8q9 1	SpecNC EE 1	SpecNC q9 1	STD 3-1	STD 7-1	-	-	-	-
F	6q7 2	7 TEI 2	8EE 2	8q9 2	SpecNC EE 2	SpecNC q9 2	STD 3-2	STD 7-2	-	-	-	-
G	6q8 1	7q7 1	8TEI 1	XE 1	SpecNC TEI 1	-	STD 4-1	STD 8-1	-	-	-	-
H	6q8 2	7q7 2	8TEI 2	XE 2	SpecNC TEI 2	-	STD 4-2	STD 8-2	-	-	-	-

PC patient group sample loading order, Legend:

TR= Technical replicate,

BR= Biological replicate,

SE= Big experiment #

6EE 1: **6** = SE006, **EE**= ExoEasy sample, **1**= TR (ExoCet level) 1

6EE 2: **6** = SE006, **EE** = ExoEasy sample, **2**= TR (ExoCet level) 2

6TEI 1: **6 =**SE006, **TEI**= Total EV Isolation sample, **1**= TR (ExoCet level) 1

…

6q7 1: **6=** SE006, **q7**= qEV7 sample, **1**= TR (EV isolate level) 1 – TR (ExoCet level) 1

…

6q8 1: 6= SE006, **q8**= qEV8 sample, **1**= TR (ExoCet level) 1

…

6q9 1: 6= SE006, **q9**= qEV9 sample, **1**= TR (ExoCet level) 1

7EE 1: 7 = SE007, **EE**= ExoEasy sample, **1**= TR (ExoCet level) 1

…

S.NC: Specialized negative control for a given sample, constituted of 50µL of the sample loaded in a microtiter plate well containing (inert) reaction buffer A (no substrate-containing buffer B added)

XE: ExoEasy (Qiagen) elution buffer XE (negative control, blank for ExoEasy samples)

PBS: 1x PBS (negative control, blank for qEV and TEI samples)

AChE: Acetylcholine esterase (from eel [details from bottle] 1mg/mL stock) diluted to a concentration of 1µg/mL (positive control)

STD 1-1: ExoCet standard solution dilution 1 (no dilution), parallel 1

STD 1-2: ExoCet standard solution dilution 1 (no dilution), parallel 2

STD 2-1: ExoCet standard solution dilution 2 (1:2 dilution), parallel 1

…

Table xx: OD 405nm, EV isolation samples from plasma PC patient group, 10 minutes of incubation (RT):

	1	2	3	4	5	6	7	8
A	0,597	0,439	0,457	0,43	0,42	0,049	1,456	0,502
B	0,561	0,409	0,43	0,428	0,422	0,044	1,343	0,476
C	0,676	0,548	0,452	0,431	1,148	0,054	0,945	0,428
D	0,65	0,557	0,412	0,427	1,091	0,046	0,894	0,48
E	0,424	0,792	0,572	0,434	0,048	0,045	0,683	0,472
F	0,42	0,757	0,579	0,428	0,047	0,044	0,686	0,456
G	0,427	0,415	0,83	0,418	0,087	N/A	0,584	0,437
H	0,387	0,41	0,825	0,442	0,09	N/A	0,569	0,46

Table xx: OD 405nm, EVisolation samples from plasma PC patient group, 15 minutes of incubation (RT):

	1	2	3	4	5	6	7	8
A	0,643	0,441	0,458	0,429	0,421	0,05	1,847	0,527
B	0,605	0,408	0,431	0,427	0,421	0,044	1,679	0,489
C	0,751	0,596	0,453	0,431	1,427	0,056	1,143	0,434
D	0,737	0,605	0,416	0,427	1,337	0,046	1,076	0,482
E	0,423	0,874	0,623	0,433	0,048	0,045	0,787	0,474
F	0,42	0,84	0,632	0,428	0,048	0,044	0,779	0,457
G	0,427	0,413	0,965	0,415	0,088	N/A	0,634	0,433
H	0,386	0,407	0,964	0,438	0,091	N/A	0,616	0,454

Table: OD 405nm, EV isolation samples from plasma PC patient group, 20 minutes of incubation (RT):

	1	2	3	4	5	6	7	8
A	0,69	0,442	0,485	0,429	0,42	0,051	2,214	0,552
B	0,651	0,408	0,431	0,426	0,419	0,045	2,017	0,508
C	0,828	0,642	0,454	0,432	1,693	0,056	1,337	0,446
D	0,813	0,653	0,415	0,427	1,579	0,046	1,256	0,493
E	0,423	0,956	0,627	0,434	0,048	0,046	0,889	0,479
F	0,418	0,919	0,683	0,428	0,047	0,44	0,87	0,462
G	0,426	0,411	1,098	0,412	0,088	N/A	0,686	0,43
H	0,384	0,406	1,1	0,435	0,091	N/A	0,662	0,45

<u>ExoCet on samples from CCM</u>

While results using the ExoCet exosome quantitation assay (SBI) was considered generally too weak to be worth including in the main section of this thesis, some general observations could be made concerning the samples giving the strongest signal. In EV isolates from CCM, while most samples proved too weak to give a reliable signal over noise, ExoEasy and TEI were reliably giving an sufficiently strong signal to register. Additionally, the ExoEasy sample was observed to be stronger than that of the TEI sample.

Note that the ExoCet data from CCM (figure 16) stems from a different (although identically prepared) batch of CCM ("SE001"), and can therefore not be considered directly comparable to the one discussed in the main portion of this thesis ("SE002").

ExoCet SE001 (EV Isolates from CCM) Loading order:

	1	2	3	4	5	6	7
A	PBS	qEV7 1	qEV9 1	TEI 1	AChE 10-3	Std 4	Std 8
B	PBS	qEV7 1	qEV9 1	TEI 1	AChE 10-3	Std 4	Std 8
C	XE	qEV7 2	qEV9 2	TEI 2	Std 1	Std 5	
D	XE	qEV7 2	qEV9 2	TEI 2	Std 1	Std 5	
E	ExoEasy 1	qEV8 1	ExoQuick 1	UC 1	N/A	Std 2	
F	ExoEasy 1	qEV8 1	ExoQuick 1	UC 1	Std 2	Std 6	
G	ExoEasy 2	qEV8 2	ExoQuick 2	UC 2	Std 3	Std 7	
H	ExoEasy 2	qEV8 2	ExoQuick 2	UC 2	Std 3	Std 7	

Table xx: ExoCet on EV isolates from CCM, raw data (samples) after 15 minutes of incubation. Note that the batch of CCM used for this experiment, while similarly prepared, is not the same as the one discussed in the main section of this paper and so is not directly comparable.

Kolonne1	1	2	3	4	5
A	0,406	0,396	0,399	0,488	1,992
B	0,379	0,375	0,367	0,463	1,147
C	0,413	0,392	0,374	0,451	
D	0,393	0,375	0,362	0,419	
E	0,616	0,38	0,387	0,36	
F	0,606	0,375	0,37	0,36	
G	0,596	0,376	0,381	0,486	
H	0,595	0,358	0,361	0,351	

Table xx: ExoCet on EV isolates from CCM, raw data for standard curve after 15 minutes of incubation. Note that the batch of CCM used for this experiment, while similarly prepared, is not the same as the one discussed in the main section of this paper and so is not directly comparable.

Kolonne1	Kolonne2	Kolonne3	Kolonne4	Kolonne5	Kolonne6	Kolonne7	Kolonne8
Standard:	OD 405nm	Subtract blank		Standard:	#Exos x10^7	Average	STDAV
Std 1	2,45	2,0865		Std 1	1280	2,051	0,05020458
Std 1	2,379	2,0155		Std 2	640	1,145	0,05444722
Std 2	1,547	1,1835		Std 3	320	0,5735	0,00989949
Std 2	1,47	1,1065		Std 4	160	0,289	0,02757716
Std 3	0,944	0,5805		Std 5	80	0,1405	0,01272792
Std 3	0,93	0,5665		Std 6	40	0,0755	0,0311127
Std 4	0,672	0,3085		Std 7	20	0,0265	N/A
Std 4	0,633	0,2695		Std 8	0	0	0,00070711
Std 5	0,513	0,1495					
Std 5	0,495	0,1315					
Std 6	0,461	0,0975		Well of STD	7 Double	Laoded.	
Std 6	0,417	0,0535		Ignore value	Use only	Parallell 1	
Std 7	0,39	0,0265					
Std 7	0,479	0,1155					
Std 8	0,364	0,0005					
Std 8	0,363	-0,0005					

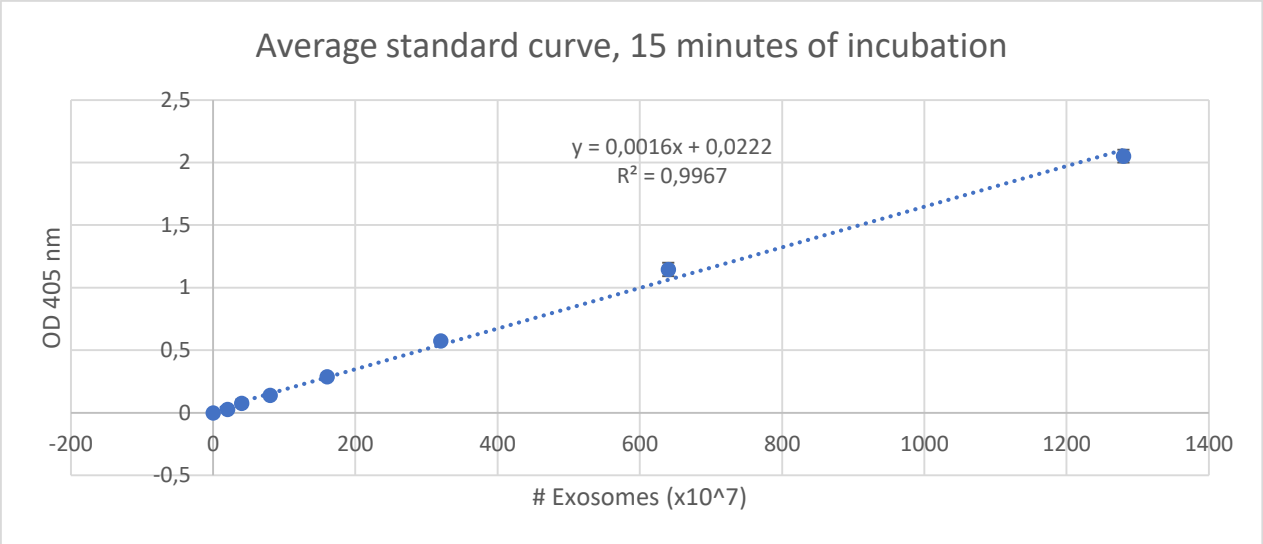

Figure xx: ExoCet on EV isolates from CCM standard curve

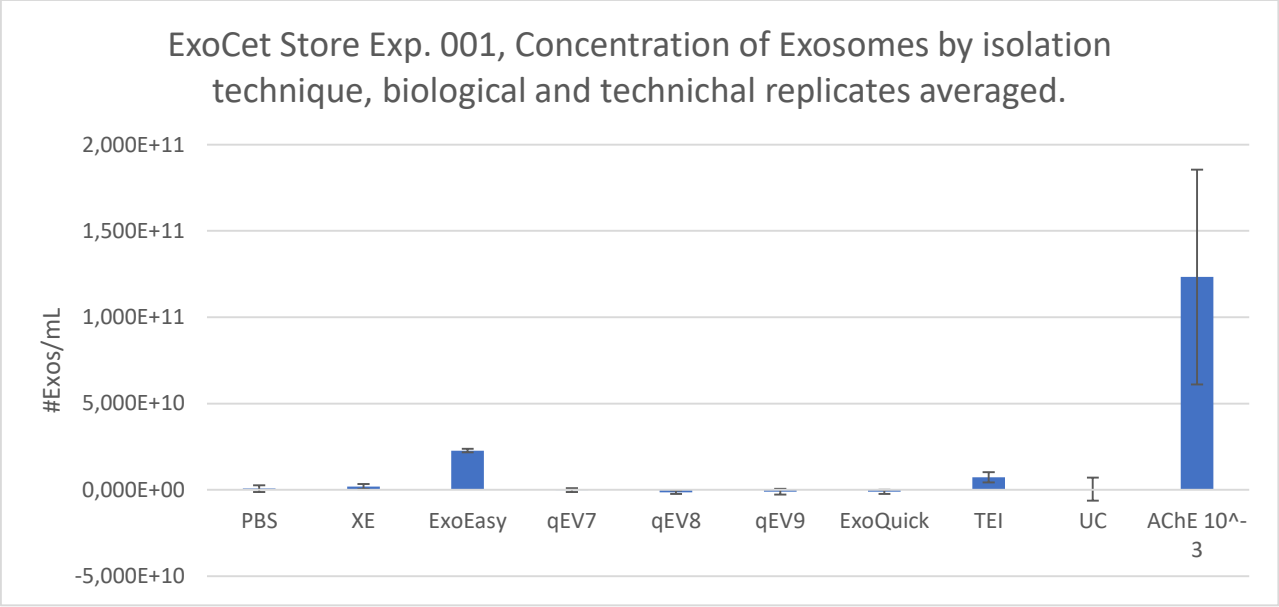

Figure 1: ExoCet Exosome Quantitation Assay (SBI) results from samples of EV isolates from CCM. The y-axis reflects the calculated number of exosomes/mL based on the optimal standard curve (15 minutes of incubation). Error-bars are based on the calculated standard deviation between 2 technical replicates (EV isolate level) in 2 technical replicates (ExoCet assay) for a total of 4 TR per sample. PBS and XE are negative controls. AChE 10^-3 is a Acetylcholine esterase positive control. Only the ExoEasy and TEI samples showed significant enzyme activity after subtraction of blank.

7.5 qNano Gold (Izon Science)

EV isolates from CCM, processed qNano gold concentration and average particle diameter data.

Table 4: qNano gold NP100 (top of table) and NP200 (bottom of table) measured concentrations of EVs isolate samples from CCM. P/mL CCM equates to the measured nanoparticles within the nanopore sensitivity range (50-200nm for NP100, 85-340nm for NP200). All values have been normalized so as to represent the concentration of nanoparticles within the given size-range isolated from 1mL of the starting material (CCM)

EV isolate from CCM, NP100 (50-200nm)							
ID	P/mL CCM	STDAV	STDAV%	P.Mean	STDAV	P.Mode	STDAV
ExoEasy	1,13E+09	2,56E+08	22,75	90,75	6,54	68,25	4,40
ExoQuick	4,19E+08	2,38E+08	56,92	91,33	5,82	71,00	6,66
qEV7	1,15E+08	8,78E+07	76,47	95,78	5,95	74,89	14,87
qEV8	2,99E+08	6,72E+07	22,44	93,00	5,73	70,50	7,97
qEV9	1,86E+08	3,80E+07	20,48	86,67	5,96	68,67	6,50
TEI	5,05E+08	3,31E+07	6,57	90,33	5,32	68,83	5,78
UC	3,28E+07	3,45E+07	105,15	98,17	17,09	97,67	4,04
EV Isolate from CCM, NP200 (85-340nm)							
ExoEasy	1,86E+08	7,16E+07	38,56	162,83	19,51	128,33	22,07
ExoQuick	1,14E+08	5,46E+07	47,69	151,56	10,25	111,67	7,14
qEV7	6,38E+07	4,80E+07	75,15	140,78	7,17	108,22	7,31
qEV8	4,32E+07	5,43E+06	12,57	143,78	9,99	111,44	7,88
qEV9	7,44E+07	6,63E+06	8,91	134,83	12,29	107,67	7,03
TEI	3,11E+08	1,03E+08	33,17	144,93	7,46	109,00	10,32
UC	6,67E+06	1,74E06	26,10	139,80	9,82	124,00	18,30

EV isolates from Plasma, processed qNano gold concentration and average particle diameter data.

*Table 5: qNano gold measured concentrations (NP100, NP200) of EV isolate samples from blood plasma. P/mL CCM equates to the measured nanoparticles within the nanopore sensitivity range, calculated back so as to represent the concentration of such nanoparticles in 1mL of the CCM starting material. The top section of the table is constituted of Control group data, and the bottom section of PC patient data. "P.Mean" refers to the nanoparticle mean diameter within the given sensitivity interval. "P.mode" refers to the mode particle diameter. *The qNano Gold measurement of the ExoEasy sample concentrations was in this case considered to be of insufficient quality, and is therefore disregarded in all comparisons.*

	NP100 (50-200nm)				**NP200 (85-340nm)**			
	Control group samples							
Sample ID	P/mL plasma	P. Mean	STDAV	P .Mode	P/mL plasma	P. Mean	STDAV	P .Mode
ExoEasy	1,99E+10 *	72,00	19,00	61,00	N/A	N/A	N/A	N/A
TEI	2,46E+11	78,50	19,70	68,50	6,00E+10	129,50	39,75	105,00
qEV7	3,84E+08	89,50	31,45	67,00	1,66E+08	147,00	57,80	129,00
qEV8	8,75E+09	78,50	24,10	64,50	3,61E+09	149,00	47,60	119,50
qEV9	2,81E+10	85,00	24,10	68,00	8,15E+09	139,50	41,85	114,00
	PC patient group samples							
Sample ID	P/mL plasma	P.Mean	STDAV	P.Mode	P/mL plasma	P. Mean	STDAV	P .Mode
ExoEasy	N/A	N/A	N/A	N/A	N/A	N/A	N/A	N/A
TEI	1,13E+11	86,50	21,60	72,50	1,93E+10	124,00	31,20	108,50
qEV7	2,17E+09	97,50	30,25	71,00	1,67E+08	157,50	60,00	118,50
qEV8	5,40E+09	91,50	32,60	71,50	5,05E+08	142,50	50,65	110,50
qEV9	1,02E+10	79,50	23,75	66,50	2,61E+09	148,00	47,90	115,50

7.5.1 Triton x-100 (0,1% v/v) measured concentrations

The CCM derived EV isolate samples, a separate set of measurements using the NP200 nanopore was performed in order to estimate the vesicle fraction. Twin dilutions were prepared, one featuring 0,1% v/v triton x-100, and the two were measured immediately following one another. The processed result data is show in tables 6 and 7 below. All values normalized to correspond to mL CCM used during EV isolation.

Table 6: CCM sample measured changes following treatment with 0,1% Triton x-100. ΔConc. Signifies the change in concentration, equating to the estimated vesicles/mL plasma. The corresponding change in particle mean and mode diameter (nanometres) can be seen in the two subsequent columns, "ΔP.Mean." And "ΔP.Mode" respectively. The final column tagged "%Vesicles", shows the calculated percentage of nanoparticles in the sample estimaterd to be vesicles, based on the calculated ΔConc.

Sample ID	ΔConc.	ΔP.Mean (nm)	ΔP.Mode (nm)	%Vesicles
ExoEasy	1,04E+08	3,67	8,00	57,12
ExoQuick	6,44E+07	-2,33	13,00	76,30
TEI	8,75E+07	-7,67	-7,33	43,34
qEV7	6,72E+07	7,33	28,33	86,73
qEV8	2,21E+07	4,33	1,33	56,56
qEV9	2,49E+06	2,00	-22,00	59,48
UC	2,28E+06	27,33	29,33	45,09

The unprocessed concentration data are shown below (tables xx, xx, xx, xx.). All values normalized to correspond to mL CCM used during EV isolation.

Table 1: No triton x-100 treatment, CCM derived EV isolate samples measured using the NP200 nanopore.

ID	P/mL CCM	P Mean	P Mode	STDAV mean	STDAV mode
ExoEasy	1,82E+08	171,67	109,33	1,53	6,81
ExoQuick	8,44E+07	161,33	107,00	7,23	0,00
TEI	2,02E+08	145,33	110,00	10,21	9,85
qEV7	7,75E+07	144,00	107,00	12,29	6,08
qEV8	3,91E+07	142,00	113,33	11,36	6,03
qEV9	4,19E+06	128,33	115,67	3,21	6,03
UC	5,06E+06	149,67	138,67	24,95	22,72

Table 2: No triton x-100 treatment, CCM derived EV isolate samples measured using the NP200 nanopore, qEV fractions pooled.

ID	P/mL CCM	P Mean	P Mode	STDAV mean	STDAV mode
ExoEasy	1,82E+08	171,67	109,33	1,53	6,81
ExoQuick	8,44E+07	161,33	107,00	7,23	0,00
TEI	2,02E+08	145,33	110,00	10,21	9,85
UC	5,06E+06	149,67	138,67	24,95	22,72
qEV	1,21E+08	138,11	112,00	8,95	6,05

Table 3: With triton x-100 treatment, CCM derived EV isolate samples measured using the NP200 nanopore.

ID	P/mL CCM	P Mean	P Mode	STDAV mean	STDAV mode
ExoEasy	7,81E+07	175,33	117,33	10,69	9,87
ExoQuick	2,00E+07	159,00	120,00	15,62	19,29
TEI	1,14E+08	137,67	102,67	7,09	6,66
qEV7	1,03E+07	151,33	135,33	9,07	22,14
qEV8	1,70E+07	146,33	114,67	14,64	0,58
qEV9	1,70E+06	130,33	93,67	13,20	2,89
UC	2,78E+06	177,00	168,00	N/A	N/A

Table 4: With triton x-100 treatment, CCM derived EVe isolate samples measured using the NP200 nanopore. qEV fractions pooled

ID	P/mL CCM	P Mean	P Mode	STDAV mean	STDAV mode
ExoEasy	7,81E+07	175,33	117,33	10,69	9,87
ExoQuick	2,00E+07	159,00	120,00	15,62	19,29
TEI	1,14E+08	137,67	102,67	7,09	6,66
UC	2,78E+06	177,00	168,00	N/A	N/A
qEV	2,89E+07	142,67	114,56	12,31	8,54

For the plasma derived EV isolate samples, a separate set of measurements using the NP100 and NP200 nanopores were performed in order to estimate the vesicle fraction. Twin dilutions were prepared, one featuring 0,1% v/v triton x-100, and the two were measured immediately following one another. The processed result data is show in tables 16 and 17 below. All values normalized to correspond to mL CCM used during EV isolation.

*Table 16: Control donor plasma sample measured changes following treatment with 0,1% Triton x-100. ΔConc. Signifies the change in concentration, equating to the estimated vesicles/mL plasma. The corresponding change in particle mean and mode diameter (nanometres) can be seen in the two following columns, tagged "ΔP.Mean" and "ΔP.Mode" respectively. The final column named "%vesicles" gives the calculated percentage of nanoparticles estimated to be vesicles, based on the previously calculated ΔConc. *The qNano Gold measurement of the ExoEasy sample concentrations was in this case considered to be of insufficient quality, and is therefore disregarded in all comparisons.*

	NP100				**NP200**			
Sample ID	ΔConc.	ΔP.Mean (nm)	ΔP.Mode (nm)	%Vesicles	ΔConc.	ΔP.Mean (nm)	ΔP.Mode (nm)	%Vesicles
ExoEasy	1,75E+10*	10,5	9,50	88,04*	N/A	N/A	N/A	N/A
TEI	4,80E+10	1,00	0,50	19,51	1,50E+09	-2,00	0,00	2,50
qEV7	9,65E+07	-14,00	-2,00	25,16	7,50E+07	-18,00	-27,50	45,32
qEV8	4,00E+08	0,00	4,00	4,57	1,79E+09	14,00	4,50	49,58
qEV9	1,05E+10	-0,50	-0,50	37,43	3,10E+09	5,00	0,00	38,04

Table 17: PC patient plasma sample measured changes following treatment with 0,1% Triton x-100. ΔConc. Signifies the change in concentration, equating to the estimated vesicles/mL plasma. The corresponding change in particle mean and mode diameter can be seen in the two following columns, tagged "ΔP.Mean" and "ΔP.Mode" respectively. The final column named "%vesicles" gives the calculated percentage of nanoparticles estimated to be vesicles, based on the previously calculated ΔConc.

	NP100				**NP200**			
Sample ID	ΔConc.	ΔP.Mean	ΔP.Mode	%Vesicles	ΔConc.	ΔP.Mean	ΔP.Mode	%Vesicles
ExoEasy	N/A	N/A	N/A	N/A	N/A	N/A	N/A	N/A
TEI	7,15E+10	-3,00	2,50	63,51	1,14E+10	2,00	-8,00	59,07
qEV7	2,80E+08	-6,50	5,50	12,93	7,85E+07	-7,50	-1,50	47,01
qEV8	3,34E+09	-5,00	-3,00	61,76	3,25E+08	15,00	17,00	64,36
qEV9	1,60E+09	3,50	6,00	15,69	7,90E+08	-0,50	5,00	30,27

The unprocessed concentration data for triton x-100 experiments on samples from plasma are shown below (tables xx, xx, xx, xx.). All values normalized to correspond to mL CCM used during EV isolation.

Table 16: qNano Gold measured nanoparticle concentrations from plasma derived EV isolate samples as with and without treatment with triton x-100. NP100 and NP200 nanopores.

Control donor	No triton x-100						
SE003 NP100	50-200nm						
All:				qEV fractions pooled:			
ID	P/mL plasma	P Mean	P Mode				
ExoEasy	1,99E+10	72,00	61,00				
TEI	2,46E+11	78,50	68,50	ID	P/mL plasma	P Mean	P Mode
qEV7	3,84E+08	89,50	67,00	ExoEasy	1,99E+10	72,00	61,00
qEV8	8,75E+09	78,50	64,50	TEI	2,46E+11	78,50	68,50
qEV9	2,81E+10	85,00	68,00	qEV	3,72E+10	84,33	66,50
Control donor	with triton x-100						
SE003 NP100	50-200nm						
All:				qEV fractions pooled:			
ID	P/mL plasma	P Mean	P Mode				
ExoEasy	2,38E+09	82,50	70,50				
TEI	1,98E+11	79,50	69,00	ID	P/mL plasma	P Mean	P Mode
qEV7	2,87E+08	75,50	65,00	ExoEasy	2,38E+09	82,50	70,50
qEV8	8,35E+09	78,50	68,50	TEI	1,98E+11	79,50	69,00
qEV9	1,76E+10	84,50	67,50	qEV	2,62E+10	79,50	67,00

Control donor	No triton x-100						
SE003 NP200	80-340nm						
All:				qEV fractions pooled:			
ID	P/mL plasma	P Mean	P Mode				
ExoEasy	N/A	N/A	N/A				
TEI	6,00E+10	129,50	105,00	ID	P/mL plasma	P Mean	P Mode
qEV7	1,66E+08	147,00	129,00	ExoEasy	N/A	N/A	N/A
qEV8	3,61E+09	149,00	119,50	TEI	6,00E+10	129,50	105,00
qEV9	8,15E+09	139,50	114,00	qEV	1,19E+10	145,17	120,83

Control donor	with triton x-100						
SE003 NP200	80-340nm						
All:				qEV fractions pooled:			
ID	P/mL plasma	P Mean	P Mode				
ExoEasy	N/A	N/A	N/A				
TEI	5,85E+10	127,50	105,00	ID	P/mL plasma	P Mean	P Mode
qEV7	9,05E+07	129,00	101,50	ExoEasy	N/A	N/A	N/A
qEV8	1,82E+09	163,00	124,00	TEI	5,85E+10	127,50	105,00
qEV9	5,05E+09	144,50	114,00	qEV	6,96E+09	145,50	113,17
PC patient SE006 NP100 (50-200nm), NO triton x-100							
All:				qEV fractions pooled:			
ID	P/mL plasma	P Mean	P Mode				
ExoEasy	N/A	N/A	N/A				
TEI	1,13E+11	86,50	72,50	ID	P/mL plasma	P Mean	P Mode
qEV7	2,17E+09	97,50	71,00	ExoEasy	N/A	N/A	N/A
qEV8	5,40E+09	91,50	71,50	TEI	1,13E+11	86,50	72,50
qEV9	1,02E+10	79,50	66,50	qEV	1,78E+10	89,50	69,67
PC patient SE006 NP100 (50-200nm), WITH triton x-100							

All:				qEV fractions pooled:			
ID	P/mL plasma	P Mean	P Mode				
ExoEasy	N/A	N/A	N/A				
TEI	4,11E+10	83,50	75,00	ID	P/mL plasma	P Mean	P Mode
qEV7	1,89E+09	91,00	76,50	ExoEasy	N/A	N/A	N/A
qEV8	2,07E+09	86,50	68,50	TEI	4,11E+10	83,50	75,00
qEV9	8,60E+09	83,00	72,50	qEV	1,26E+10	86,83	72,50
PC patient SE006 NP200 (85-340nm), NO triton x-100							
All:				qEV fractions pooled:			
ID	P/mL plasma	P Mean	P Mode				
ExoEasy	N/A	N/A	N/A				
TEI	1,93E+10	124,00	108,50	ID	P/mL plasma	P Mean	P Mode
qEV7	1,67E+08	157,50	118,50	ExoEasy	N/A	N/A	N/A
qEV8	5,05E+08	142,50	110,50	TEI	1,93E+10	124,00	108,50
qEV9	2,61E+09	148,00	115,50	qEV	3,28E+09	149,33	114,83
PC patient SE006 NP200 (85-340nm), WITH triton x-100							
All:				qEV fractions pooled:			
ID	P/mL plasma	P Mean	P Mode				
ExoEasy	N/A	N/A	N/A				
TEI	7,90E+09	126,00	100,50	ID	P/mL plasma	P Mean	P Mode
qEV7	8,85E+07	150,00	117,00	ExoEasy	N/A	N/A	N/A
qEV8	1,80E+08	157,50	127,50	TEI	7,90E+09	126,00	100,50
qEV9	1,82E+09	147,50	120,50	qEV	2,09E+09	151,67	121,67

7.5.2. Combined Size Distribution Histograms (CSDH) from CCM

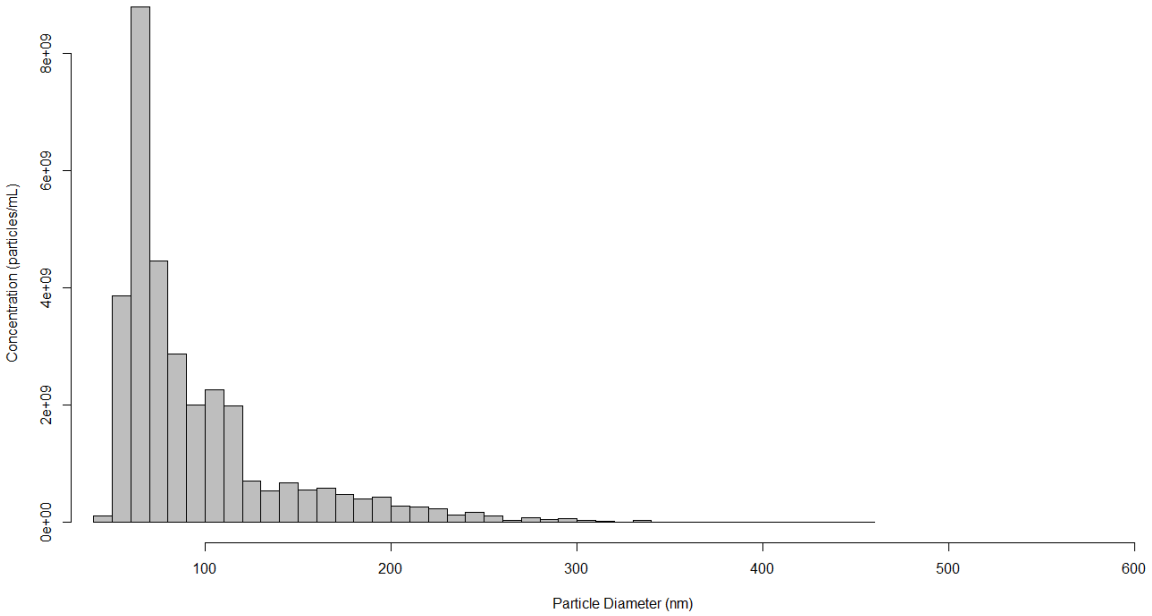

Figure xx, ExoEasy from CCM CSDH

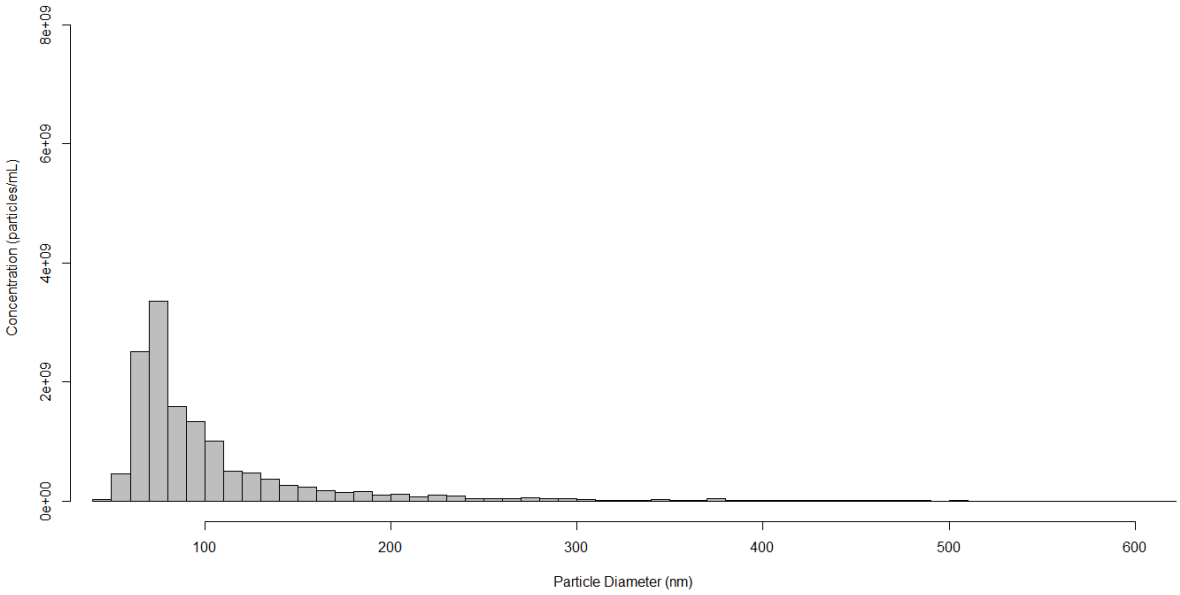

Figure xx, ExoQuick from CCM CSDH

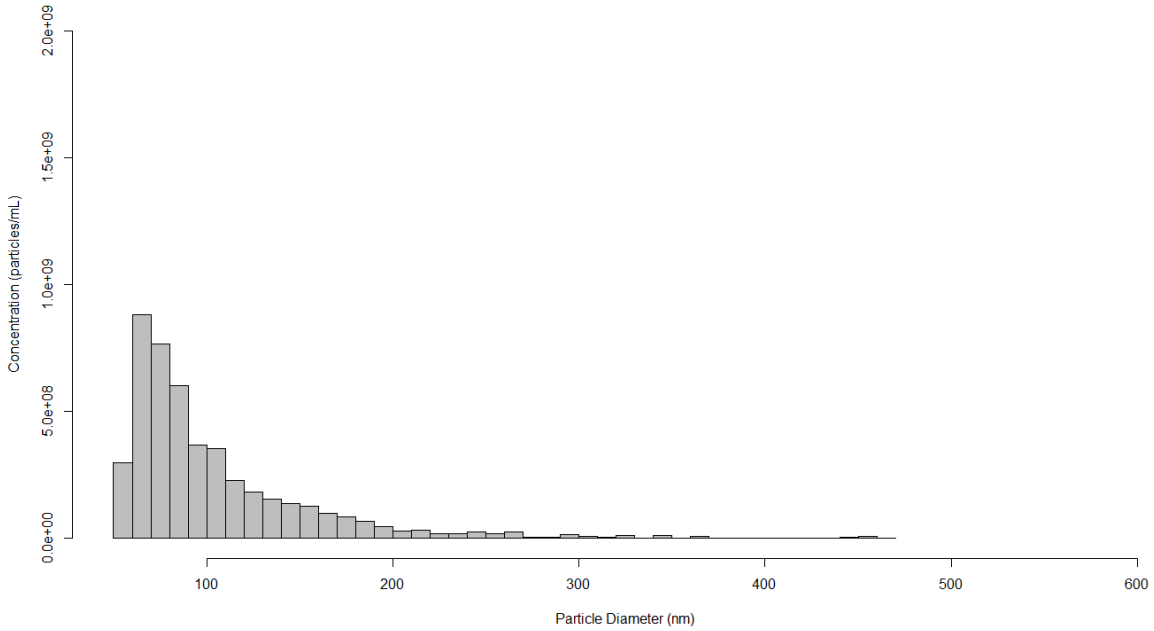

Figure xx, qEV 7 from CCM CSDH

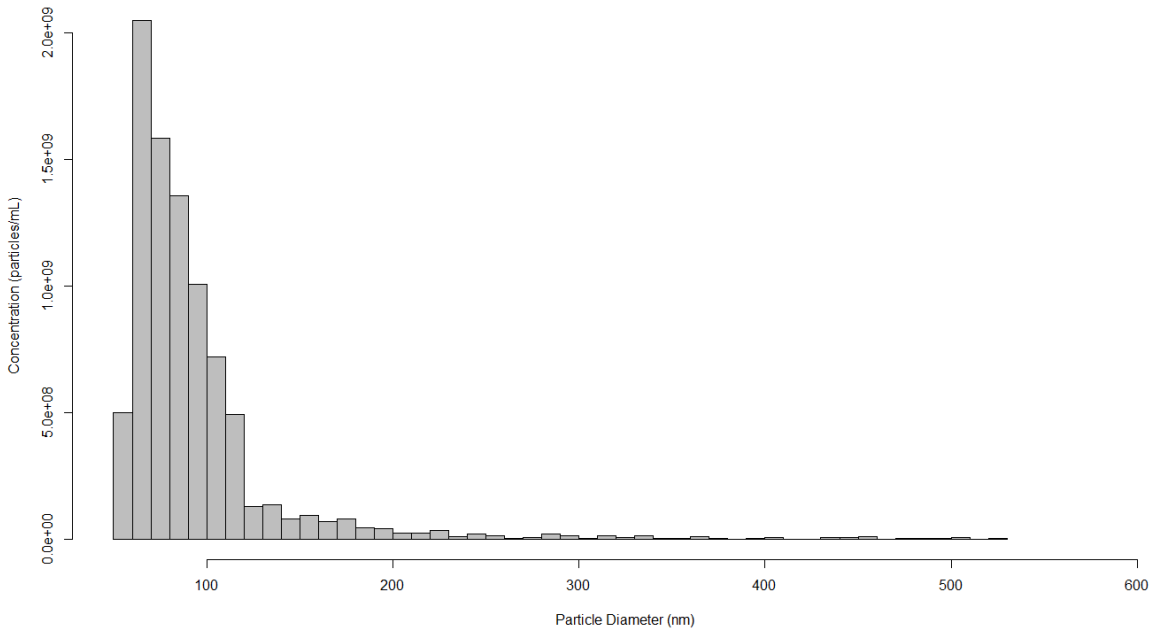

Figure xx, qEV8 from CCM CSDH

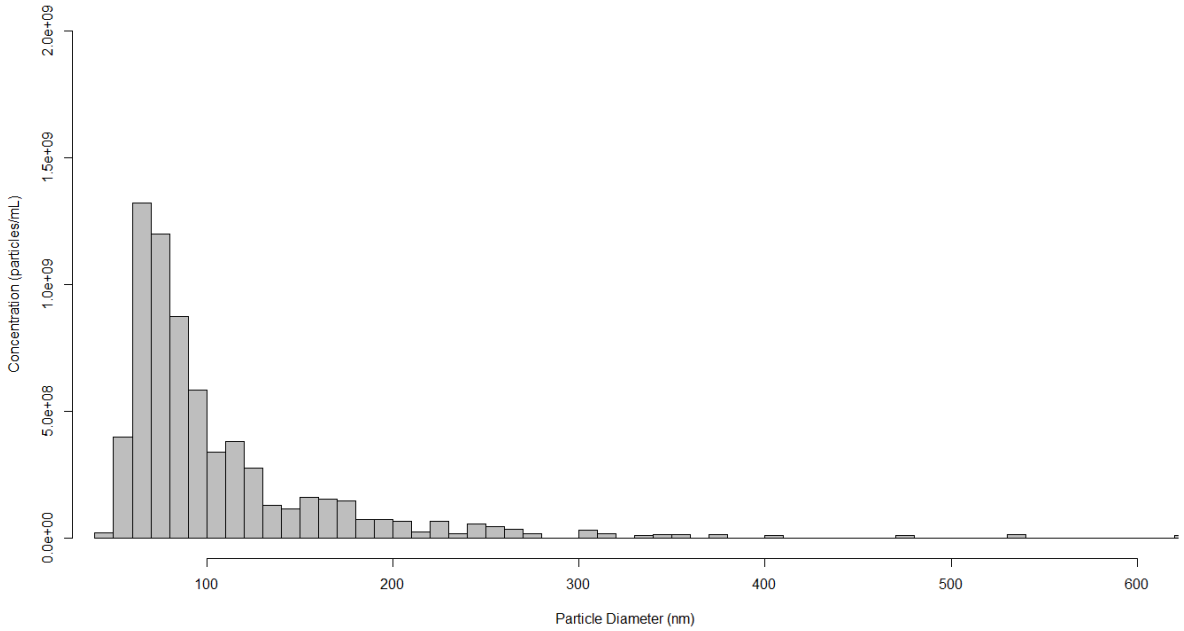

Figure xx, qEV9 from CCM CSDH

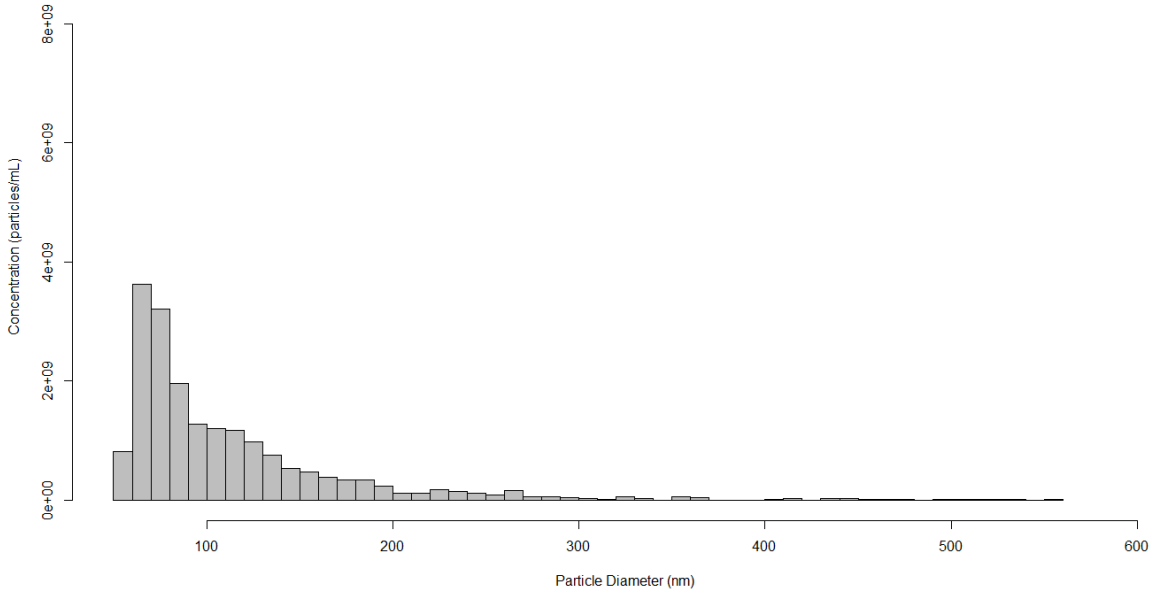

Figure xx, TEI from CCM CSDH

7.5.3. Combined Size Distribution Histograms (CSDH) from Plasma (No triton x-100)

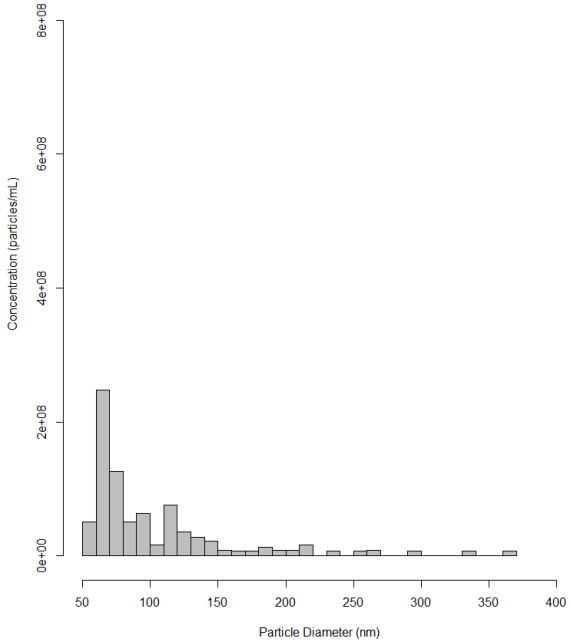

Figure xx, qEV7 from plasma (Control group donor) CSDH, No Triton x-100.

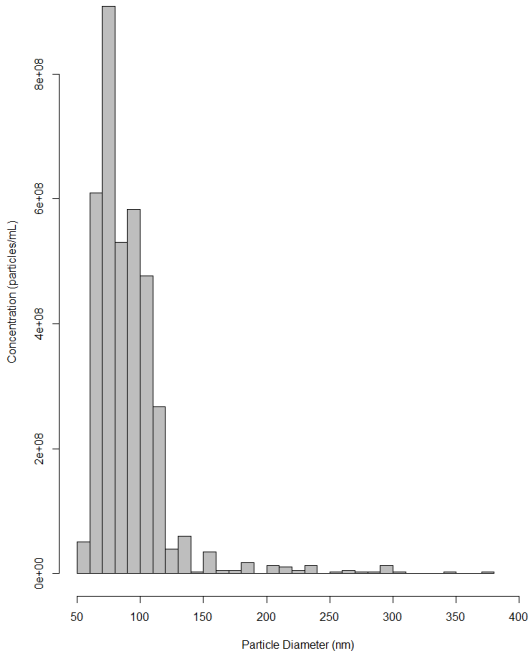

Figure xx, qEV7 from plasma (PC patient donor) CSDH, No Triton x-100.

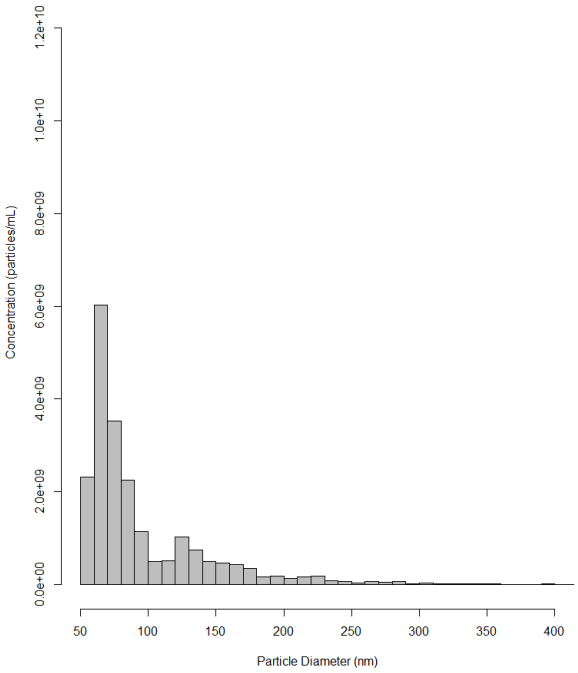

Figure xx, qEV8 from plasma (Control group donor) CSDH, No Triton x-100.

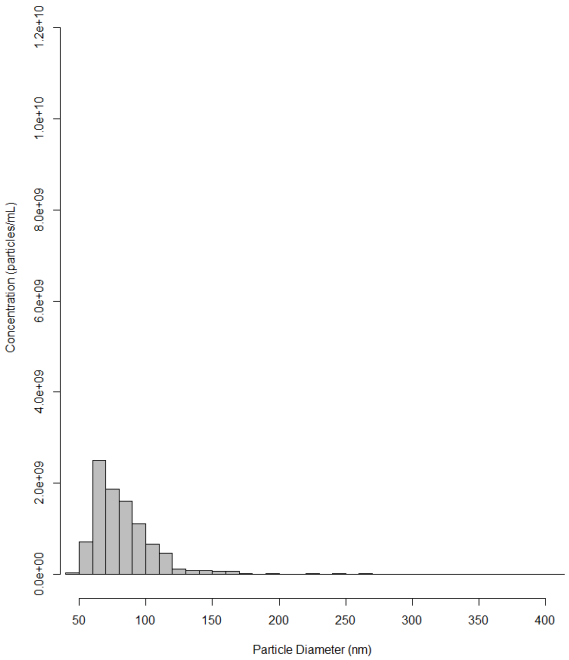

Figure xx, qEV8 from plasma (PC patient donor) CSDH, No Triton x-100.

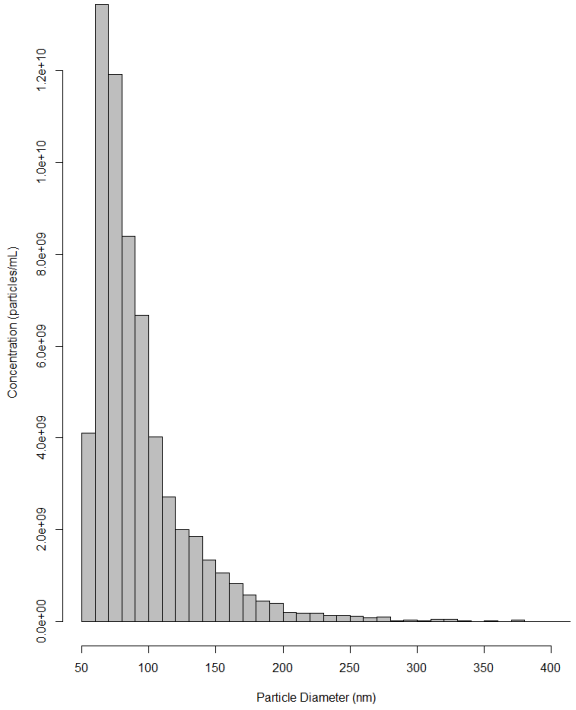

Figure xx, qEV9 from plasma (Control group donor) CSDH, No Triton x-100.

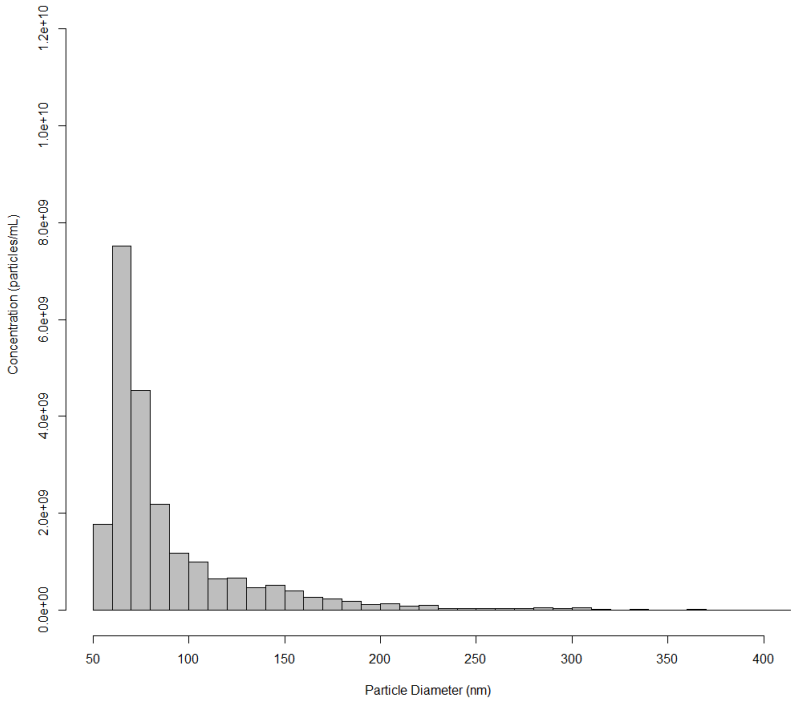

Figure xx, qEV9 from plasma (PC patient donor) CSDH, No Triton x-100.

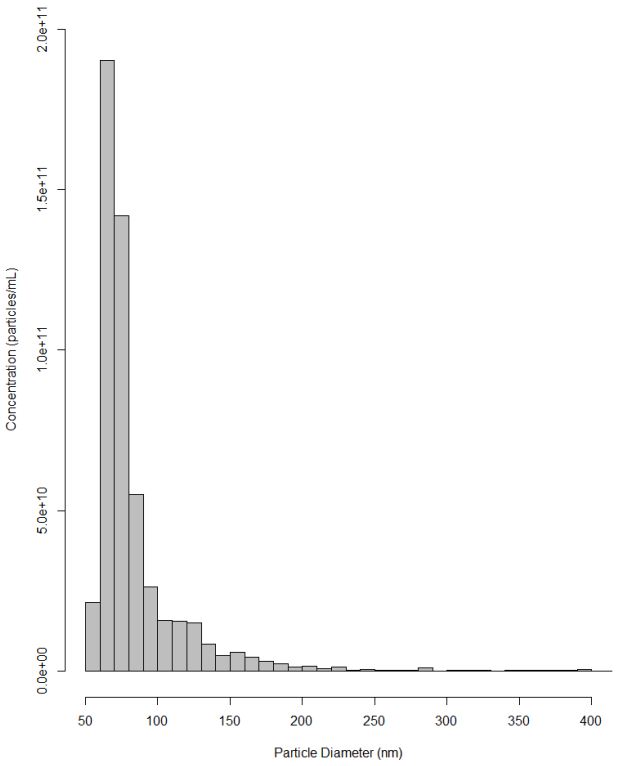

Figure xx, TEI from plasma (Control group donor) CSDH, No Triton x-100.

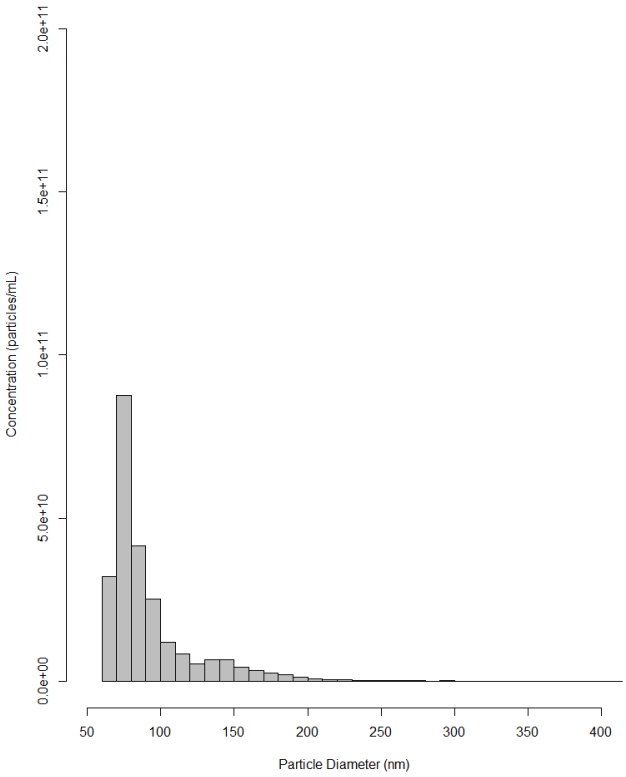

Figure xx, TEI from plasma (PC patient donor) CSDH, No Triton x-100.

7.5.4. Combined Size Distribution Histograms (CSDH) from Plasma (WITH triton x-100)

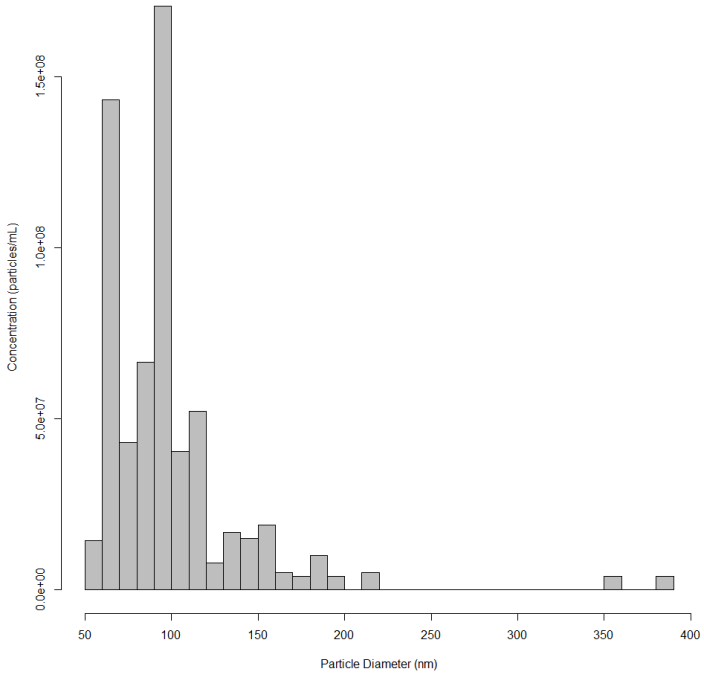

Figure xx, qEV7 from plasma (Control group donor) CSDH, With Triton x-100.

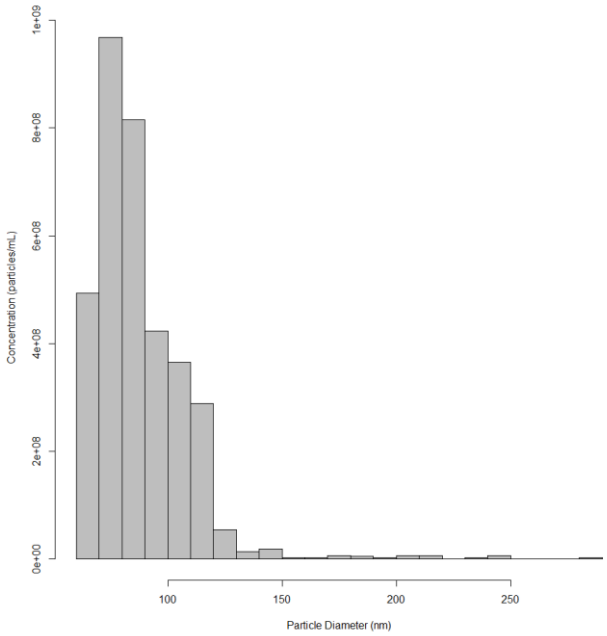

Figure xx, qEV7 from plasma (PC patient donor) CSDH, With Triton x-100.

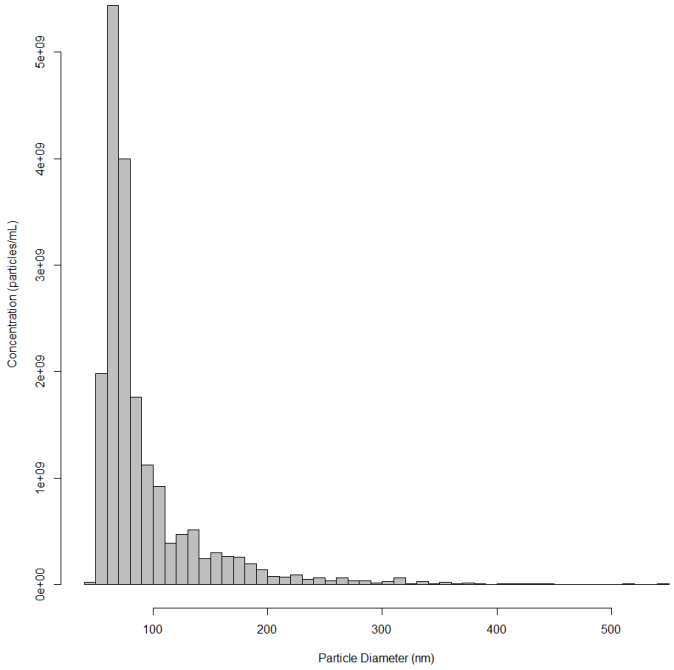

Figure xx, qEV8 from plasma (Control group donor) CSDH, With Triton x-100.

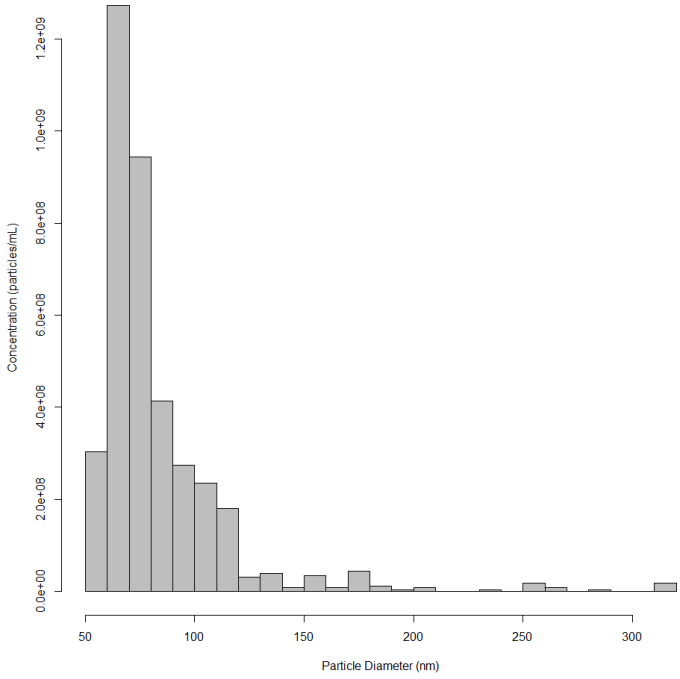

Figure xx, qEV8 from plasma (PC patient donor) CSDH, With Triton x-100.

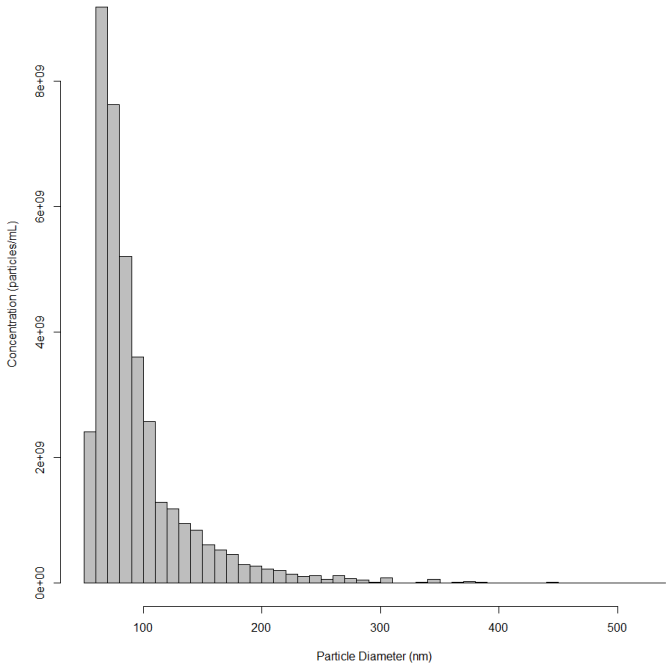

Figure xx, qEV9 from plasma (Control group donor) CSDH, With Triton x-100.

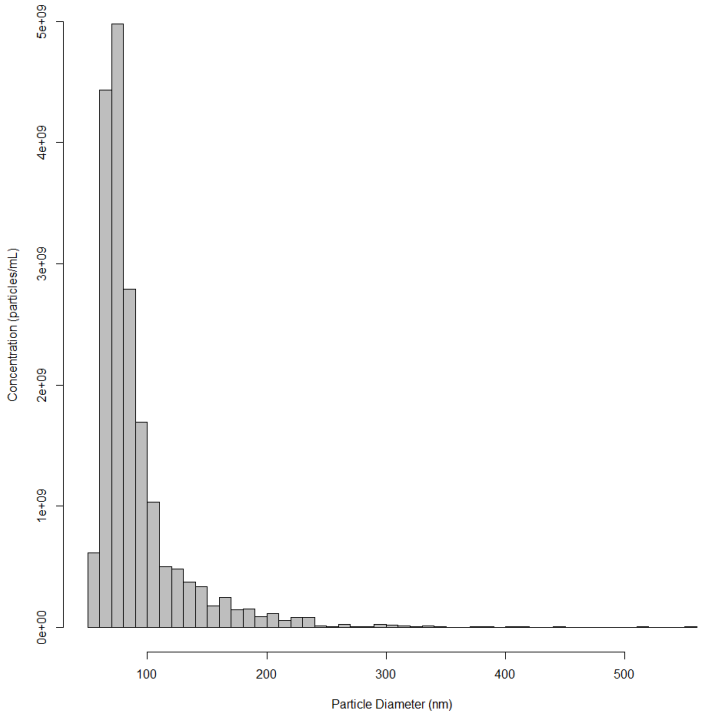

Figure xx, qEV9 from plasma (PC patient donor) CSDH, With Triton x-100.

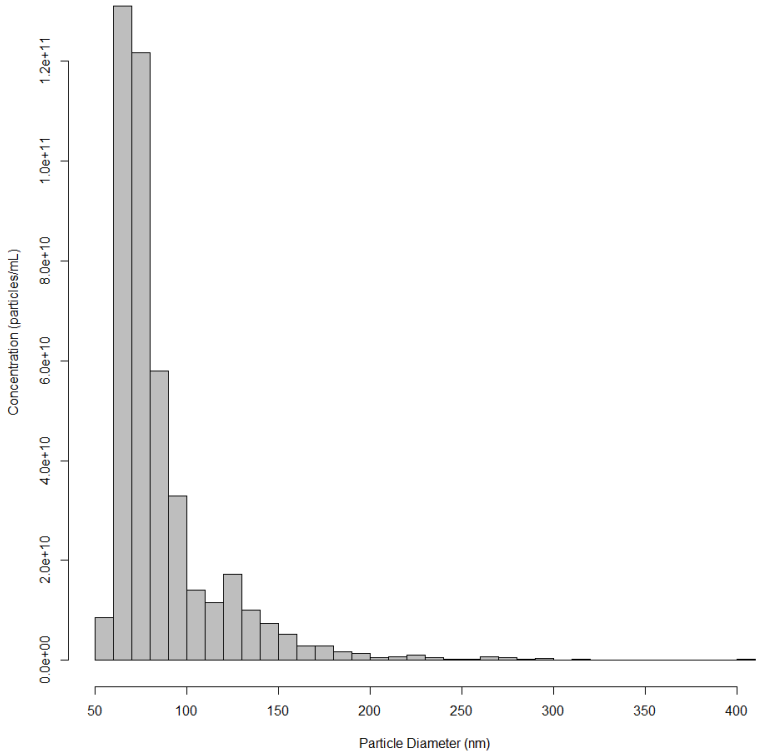

Figure xx, TEI from plasma (Control group donor) CSDH, With Triton x-100.

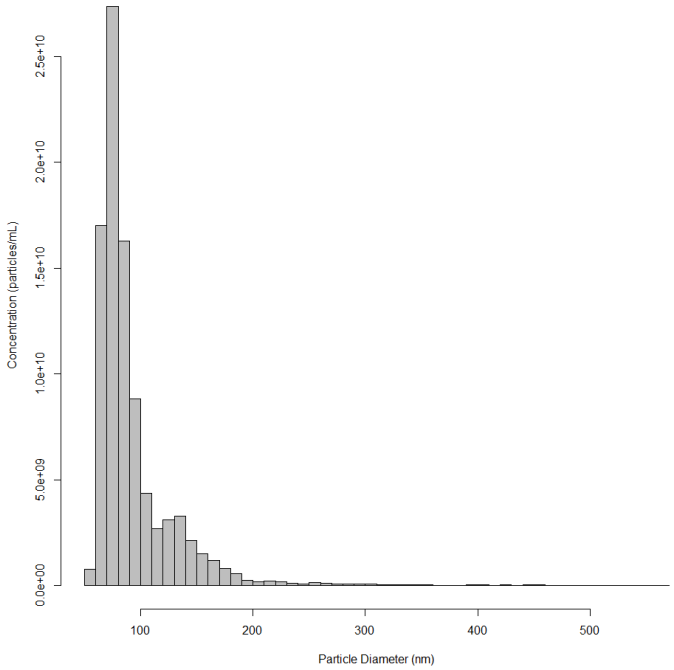

Figure xx, TEI from plasma (PC patient donor) CSDH, With Triton x-100.

7.6 Characterization of isolated EVs

BAFC

Table xx: measured MFI fold change as consequence of exosomal protein/ antibody interactions

	Beads	TEI	ExoEasy	ExoQuick	qEV7	qEV8	qEV9	UC
CD9	1,03	1,37	3,7	1,35	1,32	2,85	6,75	1,33
CD63	1,93	1,76	22,8	2,43	1,62	8,83	31,61	3,24
CD9	0,96	1,5	2,42	1,31	3,06	3,09	2,64	1,12
CD63	0,65	2,18	17,51	2,17	13,34	12,68	6,3	1,74
CD9	1	1,43	3,06	1,33	2,19	2,97	4,69	1,23
CD63	1,29	1,97	20,15	2,3	7,48	10,76	18,95	2,49
STDAV CD9	0,04	0,09	0,91	0,03	1,23	0,17	2,90	0,14
STDAV CD63	0,90	0,30	3,73	0,19	8,29	2,72	17,90	1,07

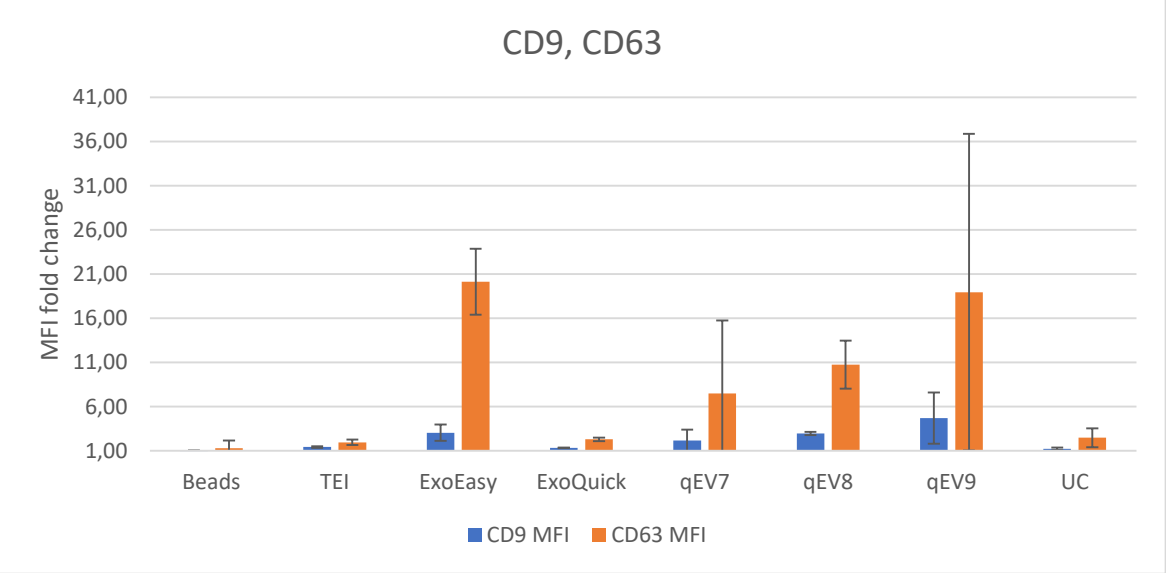

7.7 Manufacturer provided protocols and materials